Front. Mech. Eng. 2021, 16(4): 649–697
https://doi.org/10.1007/s11465-021-0654-2

REVIEW ARTICLE

Mingzheng LIU, Changhe LI, Yanbin ZHANG, Qinglong AN, Min YANG, Teng GAO, Cong MAO, Bo LIU, Huajun CAO, Xuefeng XU, Zafar SAID, Sujan DEBNATH, Muhammad JAMIL, Hafz Muhammad ALI, Shubham SHARMA

Cryogenic minimum quantity lubrication machining: from mechanism to application

Abstract Cutting fluid plays a cooling–lubrication role in the cutting of metal materials. However, the substantial usage of cutting fluid in traditional flood machining seriously pollutes the environment and threatens the health of workers. Environmental machining technologies, such as dry cutting, minimum quantity lubrication (MQL), and cryogenic cooling technology, have been used as substitute for flood machining. However, the insufficient cooling capacity of MQL with normal-temperature compressed gas and the lack of lubricating performance of cryogenic cooling technology limit their industrial application. The technical bottleneck of mechanical–thermal damage of difficult-to-cut materials in aerospace and other fields can be solved by combining cryogenic medium and MQL. The latest progress of cryogenic minimum quantity lubrication (CMQL) technology is reviewed in this paper, and the key scientific issues in the research achievements of CMQL are clarified. First, the application forms and process characteristics of CMQL devices in turning, milling, and grinding are systematically summarized from traditional settings to innovative design. Second, the cooling–lubrication mechanism of CMQL and its influence mechanism on material hardness, cutting force, tool wear, and workpiece surface quality in cutting are extensively revealed. The effects of CMQL are systematically analyzed based on its mechanism and application form. Results show that the application effect of CMQL is better than that of cryogenic technology or MQL alone. Finally, the prospect, which provides basis and support for engineering application and development of CMQL technology, is introduced considering the limitations of CMQL.

Keywords cryogenic minimum quantity lubrication (CMQL), cryogenic medium, processing mode, device application, mechanism, application effect

Received April 5, 2021; accepted July 27, 2021

Mingzheng LIU, Changhe LI (✉), Yanbin ZHANG, Min YANG, Teng GAO
School of Mechanical and Automotive Engineering, Qingdao University of Technology, Qingdao 266520, China
E-mail: sy_lichanghe@163.com

Qinglong AN
School of Mechanical Engineering, Shanghai Jiao Tong University, Shanghai 200240, China

Cong MAO
College of Automotive and Mechanical Engineering, Changsha University of Science and Technology, Changsha 410114, China

Bo LIU
Sichuan Future Aerospace Industry LLC, Shifang 618400, China

Huajun CAO
State Key Laboratory Mechanical Transmissions, Chongqing University, Chongqing 400044, China

Xuefeng XU
Key Laboratory of Special Purpose Equipment and Advanced Processing Technology (Ministry of Education and Zhejiang Province), Zhejiang University of Technology, Hangzhou 310032, China

Zafar SAID
Department of Sustainable and Renewable Energy Engineering, University of Sharjah, Sharjah 27272, the United Arab Emirates

Sujan DEBNATH
Mechanical Engineering Department, Curtin University, Miri 98009, Malaysia

Muhammad JAMIL
College of Mechanical and Electrical Engineering, Nanjing University of Aeronautics and Astronautics, Nanjing 210016, China

Hafz Muhammad ALI
Mechanical Engineering Department, King Fahd University of Petroleum and Minerals, Dhahran 31261, Saudi Arabia

Shubham SHARMA
Department of Mechanical Engineering, I.K. Gujral Punjab Technical University, Jalandhar 144603, India

1 Background

With the rapid development of the global manufacturing

industry, remarkably stringent requirements have been introduced for the mechanical properties of core components in the fields of aerospace, weapons, petrochemical industry, and medical equipment; high strength, toughness, high-temperature resistance, and other characteristics of new materials emerged to meet the usage requirements [1]. However, these new materials have poor processing performance; thus, they are also called difficult-to-cut materials. Typical examples include titanium alloy, nickel-based alloy, and high-strength steel.

At present, cutting is still the most important machining method for difficult-to-cut materials. Titanium alloy is often used in the manufacture of wing spar, frame, joint, compressor sheet, and other important parts for aircraft engines [2]. The thermal conductivity of titanium alloy is low, and the cutting heat is mostly concentrated in a small range near the cutting edge. A total of 78% of heat is left in tools, and only 12% is transferred to chips [3]. Titanium alloy can remain stable below 550 °C for a long time. However, the chemical reaction activity of titanium increases when the temperature reaches 600 °C, and the hardened layer is formed after oxidation. The softening effect is observed when the temperature exceeds 650 °C, and adhesion is strengthened. Titanium reacts with tool coating and diffuses when the temperature reaches 800 °C [4]. A nickel-based superalloy is developed in accordance with the strict requirements on raw materials of contemporary space shuttle engines. This superalloy is mainly used for four hot-end parts of the engine combustion chamber, guide vane, turbine vane, and supercharger disc, and the usage proportion reaches more than 50% [5]. However, the thermal conductivity of nickel-based alloy is low, and the surface energy density of the tool/workpiece is remarkably high in the cutting. The temperature can reach 900 °C and 1300 °C in low- and high-speed cutting, respectively, which leads to surface burn of the workpiece [6]. As a new rising material in recent years, high-strength steel is widely used in national defense, automobile, construction, and other fields [7]. High-strength steel has a low thermal conductivity and a high toughness. Cutting is unstable under high-temperature and high-pressure environment, which leads to serious workpiece surface deformation, large tool−chip contact length, complicated chip breaking, and easy winding [8].

The above difficult-to-cut materials are accompanied by elastic–plastic deformation and severe friction during cutting; this condition maintains the cutting zone in a high-temperature and high-stress state for a long time, resulting in tool wear and surface quality deterioration [9]. The most widely used flood technology has the advantages of cooling, lubrication, and chip removal, but several defects that cannot be ignored in the cutting remain [10]. High temperatures cause local boiling of the cutting fluid at the tool−workpiece interface, resulting in the continuous formation of oil vapor film by micro bubbles, which substantially increases thermal resistance and seriously reduces heat transfer efficiency [11]. In practical application, the amount of cutting fluid used is remarkably large, and its cost accounts for 18% of total production cost, which is considerably higher than 7% of tool cost [12]. Second, cutting fluid causes serious pollution to the environment, and the micro particles formed by heat volatilization easily harm the health of workers [13]. Therefore, flood technology cannot meet the requirements of clean production.

Reducing the environmental pollution caused by cutting fluid and realizing clean production according to the requirements of environmental protection and sustainable development is necessary [14]. Green cutting is an inevitable development trend in the field of mechanical manufacturing in the future [15]. In recent years, the development of green processing technology based on sustainable science and engineering principles has become a major research hotspot in the manufacturing industry [16].

1.1 Green machining technology

Current green machining technology mainly includes dry cutting [17], minimum quantity lubrication (MQL) cutting [18], and cryogenic cutting [19]. However, each technology still has defects despite its unique process performance advantages.

Dry cutting does not use cutting fluid and reduces the production cost. Moreover, this technology does not need waste-cutting liquid treatment, which is clean and pollution free. However, dry cutting, which has strong limitations, must be under special process conditions for easy-to-cut materials to show the ideal effect. A high temperature in the cutting zone easily aggravates tool wear and workpiece surface quality deterioration for difficult-to-cut materials [20].

Near-dry MQL technology sprays atomized micro droplets into the cutting zone by high-speed gas to reduce friction heat and cutting force between the tool and workpiece [21]. The requirements of green processing indicate that vegetable oil can replace traditional mineral oil as base oil, which not only has good lubrication performance but also prevents environmental pollution due to biodegradation [22]. However, the cooling performance of MQL is insufficient. A high temperature can easily lead to oil film rupture, desorption, and even oxidation failure. Consequently, continuous lubrication cannot be formed in the cutting zone [23].

Nanoparticle minimum quantity lubrication (NMQL) technology is a new cooling–lubrication method based on MQL. The addition of nanoparticles with a high thermal conductivity into lubricating oil not only enhances the heat transfer in the cutting zone but also improves the friction performance of the tool/workpiece interface [24]. The commonly used nanoparticles mainly include Al_2O_3

[25], hexagonal boron nitride (hBN) [26], and graphite [27]. However, the heat transfer capability of nanoparticles is still limited in the high-temperature environment (600 °C−800 °C) of the cutting zone. The temperature drop ratio is 15%−20% compared with MQL [28]. NMQL is mostly used in actual production for cutting easy-to-cut materials (such as aluminum alloy) and has achieved good results [29]. The cooling effect can still be improved despite the gain effect of NMQL for difficult-to-cut materials [30].

Cryogenic technology sprays a cryogenic medium into the cutting zone by utilizing large temperature differences and increasing the heat transfer zone to strengthen the convective heat transfer and then effectively reduce the cutting zone temperature. Thus far, the main cryogenic media for difficult-to-cut materials include liquid nitrogen (LN_2) [31], liquid carbon dioxide (LCO_2) [32], supercritical carbon dioxide ($scCO_2$) [33], and cryogenic air (CA) [34]. A low temperature can reduce the thermal softening degree of the workpiece and improve the cutting performance, which not only enhances the material removal rate of the workpiece but also effectively extends tool life [35]. The cost of cryogenic machining is lower than that of traditional machining methods considering high tool life and productivity [36–38]. However, cryogenic technology has insufficient lubrication performance, and the antiwear/antifriction capability must be improved.

1.2 Cryogenic minimum quantity lubrication technology

Cryogenic minimum quantity lubrication (CMQL) technology is introduced to realize green, high-quality machining of difficult-to-cut materials.

CMQL is the organic combination of cryogenic and MQL technologies; this technology not only markedly reduces the cutting zone temperature and maintains the effective lubricating capability of oil film but is also crucial in improving the quality of the workpiece and reducing tool wear, reflecting its unique advantages [39]. Moreover, CMQL is environmentally friendly and pollution free, thus meeting the requirements of green, clean processing.

1.2.1 LN_2 + MQL technology

LN_2 is the most widely used cryogenic medium in the world because of its wide source, low cost, cleanliness, and low chemical activity. Cutting can be introduced into the extremely cryogenic field when the boiling point of LN_2 is as low as −196 °C; this approach is called the ultra cryogenic process. LN_2 was first used in cryogenic cutting of low-carbon steel in the United States, which effectively inhibited hot plasticity and achieved an ideal machining effect. This approach is effective in improving cutting capability and obtaining a high machining quality to harden highly plastic metal materials (such as aluminum alloy [40] and magnesium alloy [41]) moderately through LN_2. However, cryogenic hard embrittlement may increase cutting force [42]. LN_2 lacks lubricating capability, especially for difficult-to-cut materials, despite its excellent cooling effect, which is not conducive to improving surface processing quality [43]. LN_2 + MQL technology is used to spray LN_2 and micro lubricating oil into the cutting zone in the form of a high-pressure jet. LN_2 sublimates and absorbs a large amount of heat to place the cutting zone in a low-temperature state. Simultaneously, lubricating oil forms a stable lubricating film on the tool/workpiece interface to enhance the antiwear/antifriction effect [44]. Table 1 compares LN_2 + MQL with other cooling strategies in cooling, lubrication, and sustainable development.

1.2.2 LCO_2 + MQL technology

In the early 20th century, Bartley first proposed using cryogenic CO_2 as a cutting coolant [46]. Hollis (1961) [47] used LCO_2 as a coolant in titanium alloy cutting, and the tool wear degree substantially decreased. The combination of LCO_2 and MQL realizes green, high-quality processing through the continuous progress of technology. The passage of a high-speed jet of LCO_2 into the cutting zone through the nozzle results in a rapid adiabatic expansion and a large amount of heat absorption; 60% of heat is converted into cryogenic CO_2 while 40% is rapidly cooled to form micron-sized dry ice

Table 1 Effectiveness and application of various cooling and lubricating strategies [45]

Effects of cooling and lubricating strategy	Flood (emulsion/oil)	Dry (compressed air)	MQL (oil)	Cryogenic (LN_2)	Hybrid (LN_2+MQL)
Cooling	Good	Poor	Marginal	Excellent	Excellent
Lubricating	Excellent	Poor	Excellent	Marginal	Excellent
Chip removal	Good	Good	Marginal	Good	Good
Machine cooling	Good	Poor	Poor	Marginal	Marginal
Workpiece cooling	Good	Poor	Poor	Good	Good
Dust/Particle control	Good	Poor	Marginal	Marginal	Good
Product quality	Good	Poor	Marginal	Excellent	Excellent
Sustainability	Water pollution, microbial infestation, and high cost	Poor surface integrity due to thermal damage	Harmful oil vapor	Initial cost	Initial cost, oil vapor

particles [48]. Micro oil mist plays a stable lubrication role. The surface hardening degree of processed materials is relatively light due to the lower cooling temperature of LCO_2 than that of LN_2, and cutting force and tool wear are relatively low [49].

$scCO_2$+MQL technology is a new cooling–lubrication technology that applies $scCO_2$ to the cutting field. Figure 1 shows the temperature–pressure relationship of CO_2. In the supercritical state, $scCO_2$ not only has a high diffusion coefficient and a low viscosity equivalent to gas but also a density similar to liquid and good solubility, with a surface tension close to zero [50]. Furthermore, $scCO_2$ is the most widely used supercritical fluid solvent in the industry thus far. Common industrial lubricants, such as vegetable and mineral oils, can be effectively dissolved in $scCO_2$ [51].

Micro lubricating oil is dissolved in $scCO_2$ to form a high-pressure $scCO_2$–oil fluid, which will rapidly expand after ejection from the nozzle, resulting in rapid lubricating oil precipitation due to supersaturation and the formation of micron-sized oil mist particles. Simultaneously, $scCO_2$ oil fluid forms gaseous CO_2/lubricating oil mist/dry ice particle three-phase jet under the Joule–Thomson effect, and the temperature can be as low as −78.5 °C, which substantially reduces the temperature of the cutting zone and plays a lubrication role [52]. $scCO_2$ + MQL technology is currently in the stage of laboratory research due to its complex production, complex storage, and high cost.

1.2.3 CA + MQL technology

In 1996, Professor Yokogawa from Japan first proposed the scheme of using CA to replace cutting fluid and verified its feasibility. However, meeting the requirements of high-quality cutting by using CA is difficult due to the diversity of cutting factors. Thus, scholars proposed the near-dry cooling–lubrication technology of CA + MQL, which is a combination of CA (−10 °C to −60 °C) and MQL. Micro lubricating oil is atomized into micron-sized particles by high pressure and cryogenic gas, and sprayed to the cutting area at a high speed [53]. The temperature difference between the CA and cutting zone can enhance heat transfer, and the high-speed airflow can lead the heat away from the cutting zone. The minimal effect of atomized particles results in strong permeability and lubricity, reduces tool wear, and improves workpiece surface quality. CA + MQL is environmentally friendly and does not affect the health of workers, thus meeting the requirements of clean production [54].

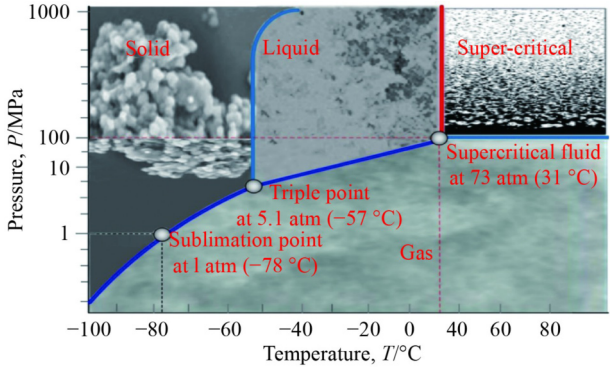

Fig. 1 Temperature–pressure diagram depicting phases of supercritical carbon dioxide. Reproduced from Ref. [48] with permission from Springer Nature.

The largest advantage of CA technology is its accurate control of the medium temperature to adapt to the cutting of different plastic metals. A reasonable low-temperature range for easy-to-cut materials, such as low carbon steel, can help maintain workpiece hardness that is conducive to cutting, prevent highly plastic workpiece and tool bonding due to high temperature, and reduce cutting performance [55]. The cutting temperature for difficult-to-cut materials, such as titanium and nickel-based alloys, is high. However, the CA temperature is limited, and the cooling performance is not ideal. CA combined with NMQL can provide a good cooling effect to improve the cooling range and the surface processing quality [56]. This combination also introduces a new way for cryogenic cutting of difficult-to-cut materials.

1.3 Article purpose

CMQL technology saves resources, minimizes pollution, and meets the requirements of green machining [45]. The cutting performance of the cooling–lubrication mechanism of CMQL changes due to its difference from that of cryogenic medium and MQL (or NMQL) used alone. This paper aims to summarize the application of CMQL technology in cutting difficult-to-cut materials in recent years. First, the mechanisms of LN_2 + MQL, LCO_2 + MQL, and CA + MQL technologies are introduced. Second, the application forms and process characteristics of CMQL devices in turning, milling, and grinding are presented. Third, the effects of the three CMQL technologies on cutting performance, tool life, and surface quality in turning, milling, and grinding progress are revealed. The conclusion is drawn based on the analysis, and the development prospect of CMQL manufacturing technology is investigated to provide a reference for further research and engineering application of CMQL. Figure 2 shows the overall structure of the paper.

2 Application form of CMQL device

The cryogenic medium in the cutting is generally sprayed into the cutting zone by different types of transport pipes and nozzles in the form of jets. At present, most of the academic research on cryogenic medium supply in

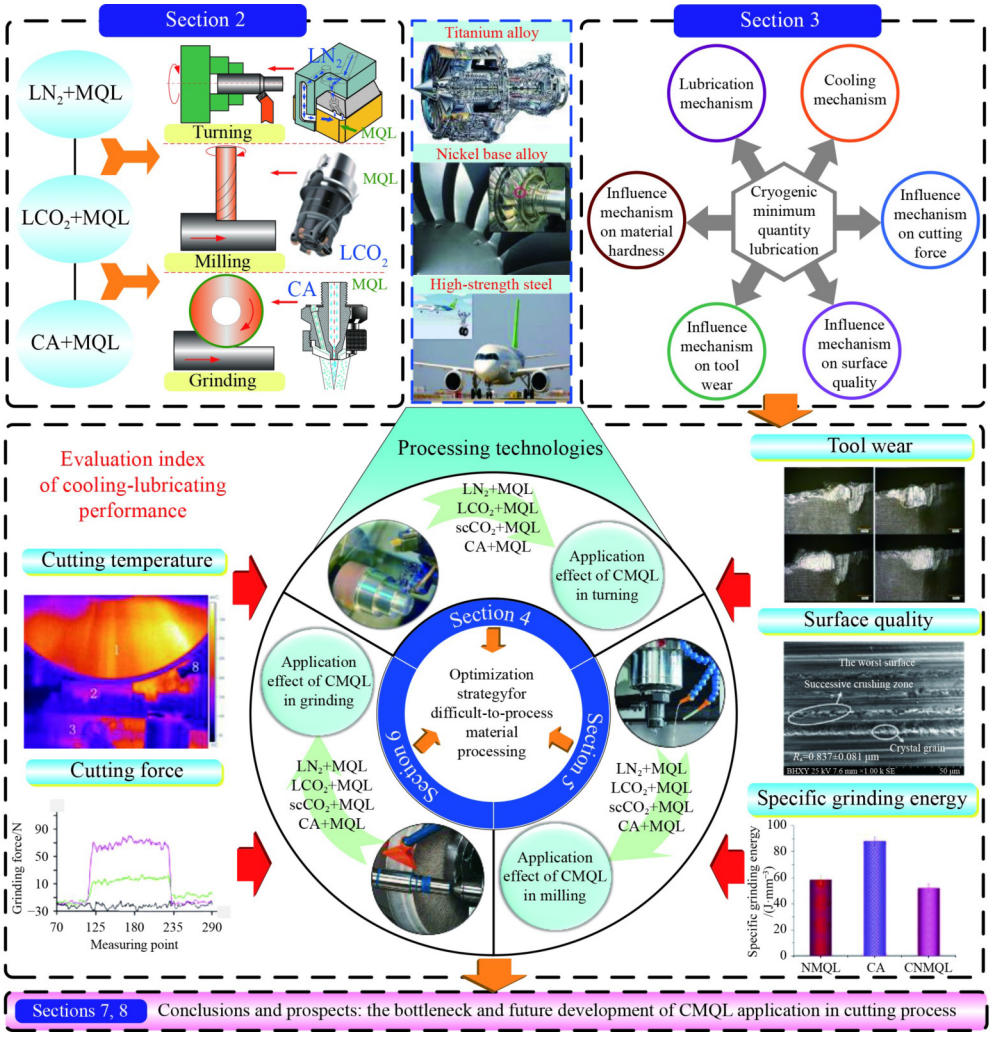

Fig. 2 Overall structure of this paper.

different processing methods (such as turning, milling, grinding, and drilling) focuses on the external jet because it can be realized without modifying the machine tool [57]. However, with the development of technology, the internal supply of cryogenic medium in the milling can be realized and accurately transported to the cutting area through the internal structure transformation of the machine tool spindle, tool holder, and milling cutter [58]. A channel for turning is set inside the turning tool to drain the cryogenic medium into the cutting zone to realize integrated processing [59].

The application forms, advantages, and disadvantages of CMQL device in turning, milling, and grinding are summarized in this paper according to the order of CMQL device from traditional configuration to innovative design.

2.1 Characteristics of LN_2 and LCO_2

LN_2 and LCO_2 are the most commonly used cryogenic media, but their refrigeration mechanisms are remarkably different. Therefore, different requirements must be considered in the storage and transportation of cryogenic medium.

CO_2 can only be stored in the tank in liquid form under the pressure of 5.7 MPa. CO_2 is supplied to the tool−workpiece interface through pressure pipes during use. The machine components and power supply lines will not be affected as long as the LCO_2 is at the specified pressure. However, considering completely different cryogenic characteristics is necessary when using LN_2. Moreover, LN_2 must be stored in an incubator because it begins to boil at −196 °C and absorbs a considerable amount of heat at ambient pressure. This characteristic introduces specific problems in practical engineering applications. First, all supply pipes, machine parts, and tool transport channels must be thermally insulated to avoid freezing hazards. Second, LN_2 rapidly evaporates to form a gas film, which reduces the cooling effect [60].

Only a small amount of phase change latent heat of LN_2 and LCO_2 is used in cutting cooling, whereas a part of latent heat is consumed in the environment [61].

Compared with LCO_2, the start-up time of LN_2 before system cooling is substantially long due to the drainage requirement of nitrogen from the cooling medium transportation pipeline. Figure 3 [45] shows that cutting can be conducted after approximately 60 s of starting the LCO_2. Afterward, the minimum cooling temperature can be maintained at −50 °C. However, cooling remains unstable even when LN_2 reaches the outlet temperature of −170 °C due to the generation of nitrogen in the supply system [60].

2.2 Turning machining

2.2.1 Application of LN_2 + MQL device

The common LN_2 sprayer comprises a storage tank and an insulated pipeline. Under the set pressure (usually 0.4 MPa), the LN_2 jet is sprayed into the cutting zone with a certain amount of flow through the nozzle to cool. MQL uses vegetable oils, such as castor oil [62], rapeseed oil [63], and soybean oil [64], to realize green processing. The high-speed airflow (0.6–0.8 MPa) atomizes the lubricating oil and plays a lubrication role. Lubricating oil is insoluble in LN_2 and condenses into solid at −196 °C, causing nozzle blockage. Therefore, mixing the cooling–lubrication medium and spraying it through one nozzle is impossible. The conventional setting method uses two nozzles to spray LN_2 and lubricating oil directly on the tool−workpiece interface, as shown in Fig. 4 [65,66]. However, completely covering the actual working face of the cutting tool may be difficult for the cooling–lubrication medium.

The conventional method uses a multinozzle-directional jet for different tool and workpiece positions [67] to solve the low coverage rate effectiveness of the cooling–lubrication medium, as shown in Fig. 5(a). LN_2 is sprayed into the workpiece cutting position through nozzle A in turning to cool the workpiece in advance. LN_2 and micro oil mist are simultaneously sprayed for the cutting tool. LN_2 enters the rake face through nozzle B, and oil mist enters the flank face through nozzle C, as shown in Fig. 5(b). The spraying positions of the cooling–lubrication medium then change.

The above method aims to change the number and

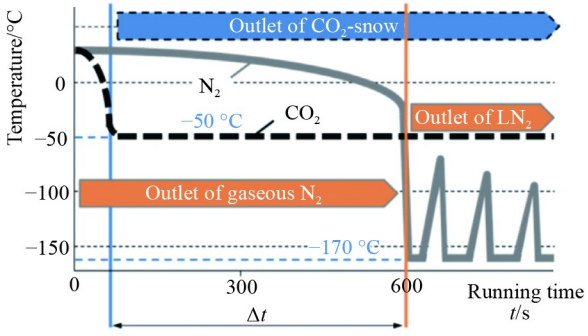

Fig. 3 Temperature profile of LN_2 and LCO_2 at coolant exit. Reproduced from Ref. [45] with permission from Elsevier.

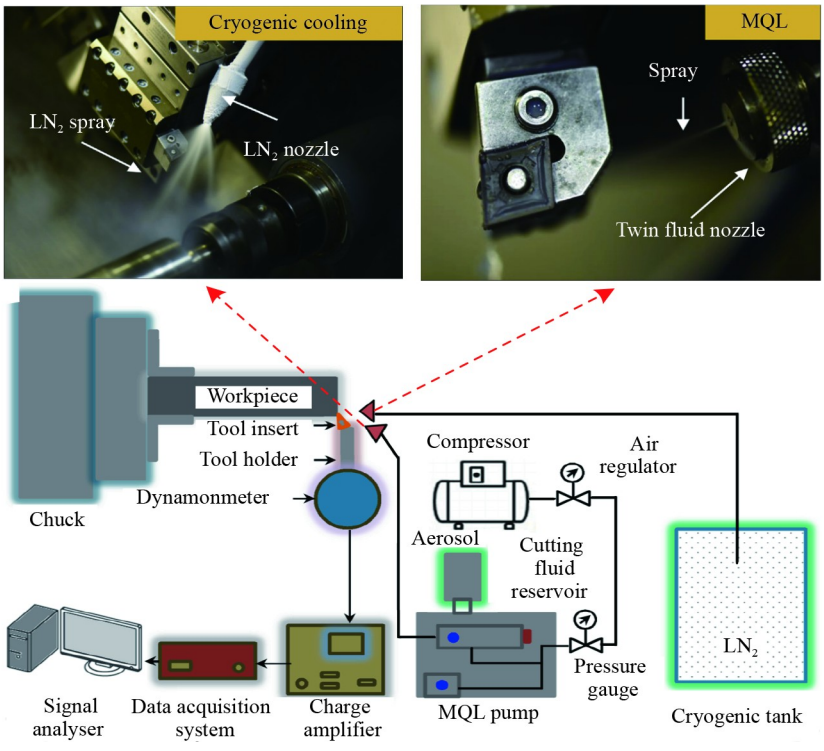

Fig. 4 Schematics and setups for LN_2 and MQL. Reproduced from Refs. [65,66] with permission from Elsevier.

position of nozzles to achieve the effective working face of cutting tools covered by the cooling–lubrication medium. The new supply device is currently realized by optimizing the structure of the tool holder. The cryogenic medium-conveying system with dual channels is integrated into the tool holder. LN_2 enters the storage pool in the tool holder and flows to the rake and flank faces through two internal channels in different directions [68]. Severe friction between rake face and chip is the main heat source in cutting. Therefore, the channel outlet aimed at the rake face can be further designed as a side-by-side dual channel [69], as shown in Fig. 6(a), and its cooling effect is better than that of a single channel [70]. In addition to rake and flank faces, tool life is further improved by setting a nozzle under the tooltip for cooling [71]. Different nozzle combinations and their cooling areas are shown in Fig. 6(b). The internal channel comprises stainless steel with a low thermal conductivity and is embedded in the high-vacuum device to prevent the influence of ultralow temperature on the tool holder. The above supply device is for LN_2, but MQL still needs to be supplied through the external pipeline.

2.2.2 Application of LCO_2 + MQL device

Two nozzles are used to spray LCO_2 and micro lubricating oil into the cutting zone in the conventional approach of LCO_2 + MQL [48], as shown in Fig. 7(a). However, the pressure drop after the release of LCO_2 from the storage tank forms a layer of dry ice around the nozzle, leading to a certain degree of blockage and reducing jet velocity. Pereira et al. [72] designed two new nozzle adapters to solve this problem effectively. The adapter is installed on the MQL nozzle, and four "plug and play" pipes are connected to the adapter to transport LCO_2. The principle of the two adapters is the same, but the type of LCO_2 nozzle is different. Figure 7(b) shows convergent nozzles on the left and right. The fluid velocity of divergent convergent nozzles is high, but their dispersibility is strong. Convergent nozzles have a relatively low flow velocity but realize substantial spray concentrations. The convergent nozzle adapter is suitable for practical machining operations.

A multipipe nesting device for conveying LCO_2 and micro lubricating oil can be installed on the tool holder [74], as shown in Fig. 8. The LCO_2 outlet is located at the

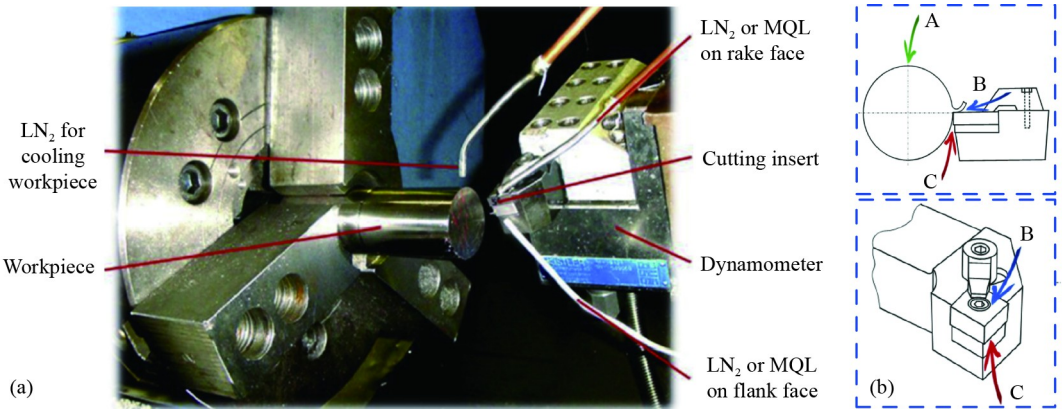

Fig. 5 Nozzle setup for simultaneous application of LN_2 and MQL: (a) experimental setup with workpiece and delivery nozzles, (b) LN_2 and MQL delivery through different combinations of three nozzles. Reproduced from Ref. [67] with permission from Elsevier.

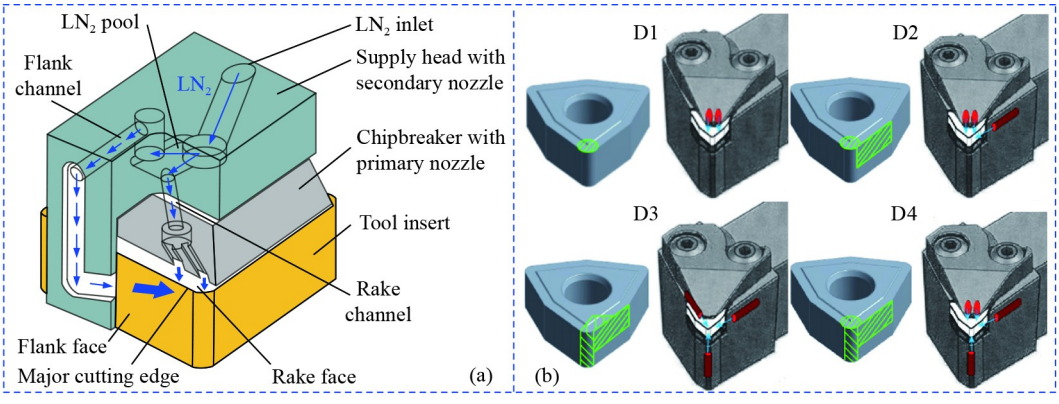

Fig. 6 Assembly of multiple nozzles for LN_2 delivery: (a) structure of turning tool for liquid internal supply, (b) four kinds of schematics for coolant delivery. Reproduced from Refs. [69,71] with permission from Elsevier.

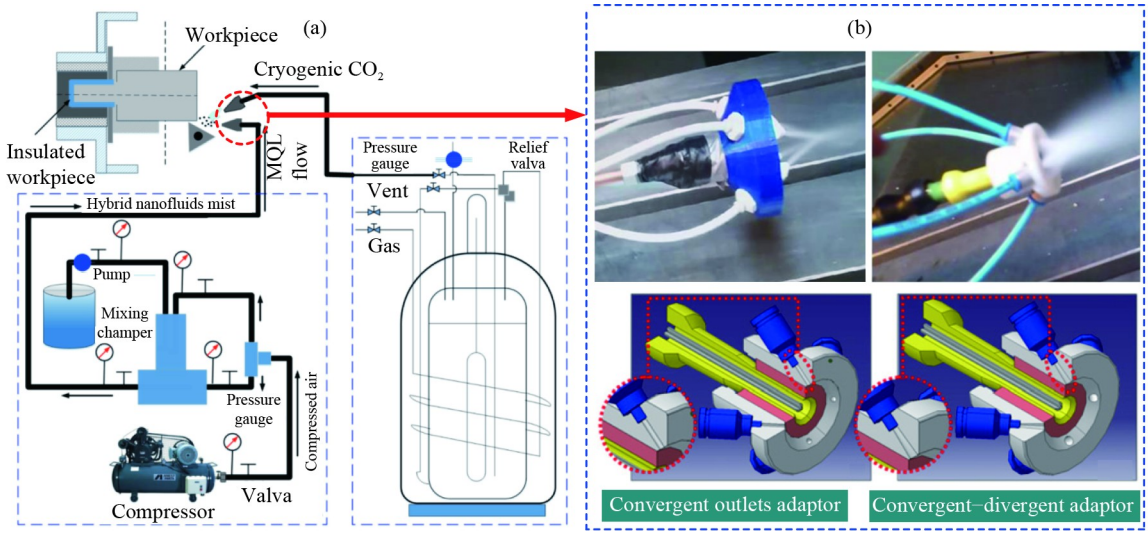

Fig. 7 LCO_2 + MQL system in turning: (a) schematic of MQL and cryogenic cooling-assisted turning system, (b) convergent outlet and convergent–divergent adapters. Reproduced from Refs. [48,73] with permission from Springer Nature.

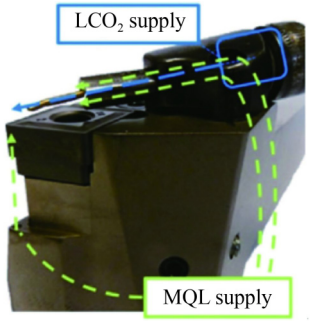

Fig. 8 Tool holder for the combination of LCO_2 + MQL. Reproduced from Ref. [74] with permission from Springer Nature.

nozzle tip (indicated by the dotted blue line), and the MQL outlet is located in the middle of the nozzle body (indicated by the dotted green line). The micro droplets are carried by the LCO_2 jet and mixed upon reaching the nozzle tip. The mixture temperature at the nozzle is approximately −78 °C and covers the rake face. However, this temperature cannot effectively cover the flank face.

2.2.3 Application of CA + MQL device

The conventional way is using two nozzles to spray CA and micro lubricating oil into the cutting zone. Another way is to cool the compressed air to −10 °C to −60 °C through the cooling system and mix it with the lubricating oil in the mixing chamber in front of the nozzle to form a gas–liquid two-phase flow. Low-temperature micro droplets are sprayed to the cutting zone at a certain speed and pressure after nozzle atomization, playing the role of cooling and lubrication, as shown in Fig. 9 [75,76]. The nozzle is usually designed as centralized type I or divergent type II to improve heat transfer efficiency. Centralization facilitates spraying of cooling–lubrication medium into the tool effective working face. The divergent type increases the heat transfer area of CA.

2.3 Milling machining

2.3.1 Application of LN_2 + MQL device

As in turning, conventional LN_2 + MQL is mixed at the tool−workpiece interface by spraying the cooling–lubrication medium separately. MQL is crucial to reducing the friction between rake face and chip and that between flank face and workpiece. LN_2 can reduce the chemical reaction between the special elements of the workpiece and material on the tool surface by lowering the temperature of the tool/workpiece, which helps improve tool life and surface quality [77].

End milling (cylindrical) and face milling (disc-shaped) cutters are common types in plane milling [78]. The dual-nozzle structure of LN_2 and MQL for the end milling cutter can realize full coverage of the cutting zone using the cooling–lubrication medium regardless of machining direction, as shown in Figs. 10(a) and 10(b). In milling, the specially designed nozzle outlet diameter is 2 mm, the divergence angle is 5°, and the distance from the periphery of the cylindrical milling cutter is 20 mm; these conditions restrict jet diffusion and reduce LN_2 evaporation [79]. The cutter head diameter is relatively large, and the coverage angle of LN_2 + MQL jet is limited. Thus, the cooling–lubrication medium for the face milling cutter can only cover part of the cutting zone in the milling, which may lead to increased wear of the milling cutter. Therefore, two groups of nozzles can be set to achieve full coverage of the entire cutting zone [80], as shown in Figs. 10(c) and 10(d).

LN_2 is generally sprayed into the cutting zone through

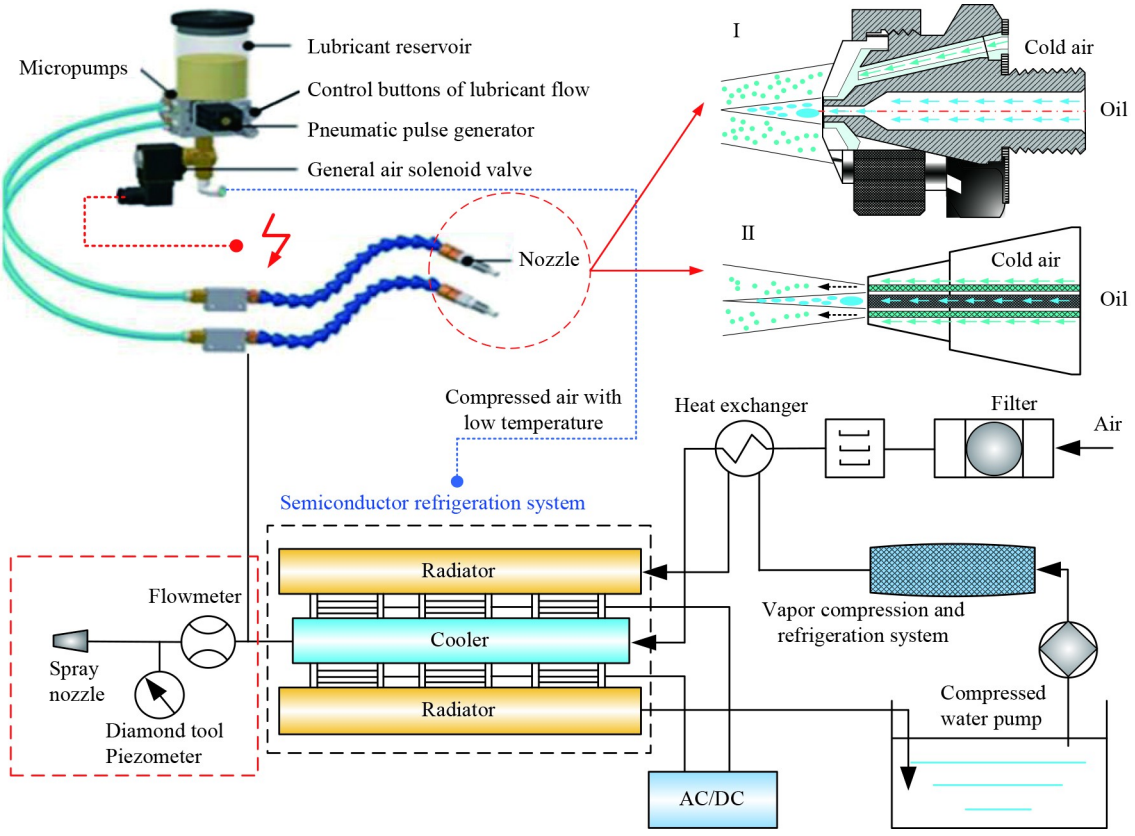

Fig. 9 Working principle diagram of developed CA + MQL system. Reproduced from Ref. [76] with permission from Elsevier.

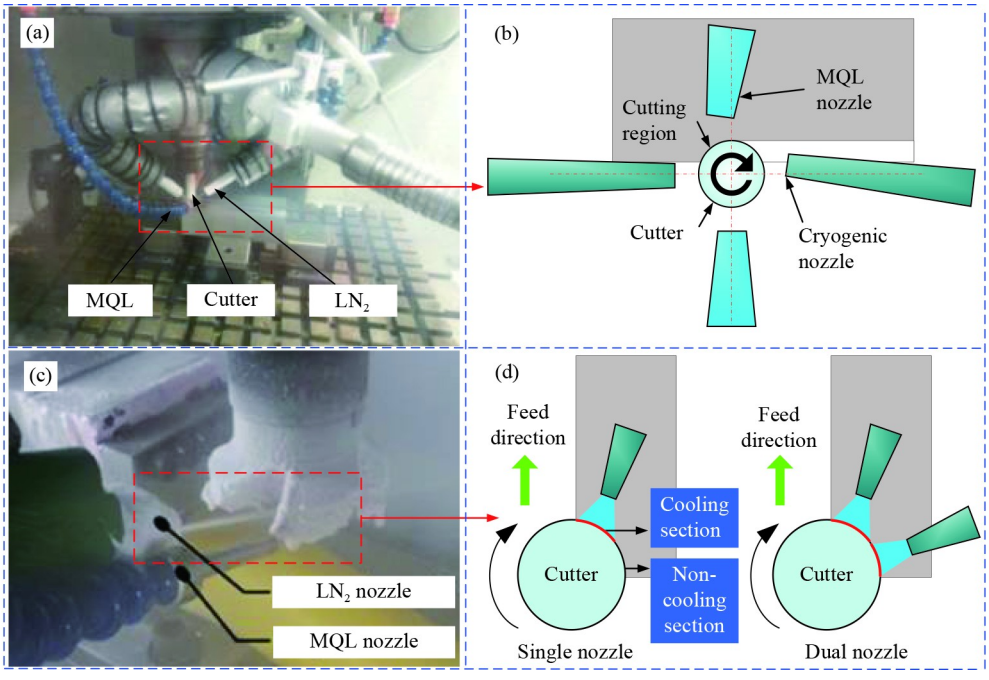

Fig. 10 CMQL application in end and facing milling: (a) pictorial view of hybrid cryogenic MQL system, (b) schematic of dual-nozzle MQL system, (c) position of cryogenic and MQL nozzles on experimental setup, and (d) LN_2 spray nozzle positions. Reproduced from Refs. [79,80] with permission from Elsevier and Springer Nature, respectively.

an external nozzle, but the high-speed rotation of the milling cutter produces a blocking airflow field [81]. This phenomenon leads to the decrease in the number of cooling–lubrication media effectively entering the

tool−workpiece interface and weakens the cooling effect. The internal jet tool holder device is introduced to improve effective permeability in milling. LN_2 internal spray tool holder device mainly comprises a tool holder body and an adapter, as shown in Fig. 11. The main body of the tool holder realizes the connection between machine tool spindle and milling cutter. The adapter is fixed on the spindle box, and the bearing realizes relative rotation between LN_2 channel and spindle. LN_2 flows into the annular cavity in the main body of the tool holder from the interface and ejects from the end or side through the internal channel of the milling cutter. Thus, transforming the machine tool for the internal jet-type tool holder device is no longer necessary, and the operation is convenient. However, this kind of form needs a peripheral MQL supply device.

2.3.2 Application of LCO_2 + MQL device

The inner channel supply has gradually become the main form of the cooling medium supply in the milling.

The channel is set inside the end milling cutter, which considers medium flow conditions, thermal resistance between cutting edge and channel, and mechanical structure strength of channel, as shown in Fig. 12(a). The exhaust vents can be set in various positions to adapt to different processing conditions. For example, the vent can guide the cryogenic medium away from the workpiece to prevent dimensional changes due to excessive cooling, as shown in Fig. 12(b). The vent can also guide the spraying of the cryogenic medium on the machined surface, reduce local thermal expansion, and improve the surface integrity of parts, as shown in Fig. 12(c). In addition to LN_2 using this form of supply [84], the same is true for LCO_2.

The new type of Cryo·tec^{TM} milling cutter with LCO_2 as a cooling medium has a disc structure, which has five inserts around the disc [58], as shown in Fig. 13. The tool holder has two concentric channels. The inner channel (green) conveys LCO_2, and the outer channel (red) conveys MQL, which realizes the separation of LCO_2 and lubrication medium. The concentric channel splits into several channels at the end of the spindle and points to each blade. The cooling–lubrication medium is sprayed from inside into the cutting zone during high-speed rotation of the spindle, which substantially improves permeability. However, modifying the structure of the machine tool to match the spindle is necessary and suitable for installing the tool holder.

Compared with LN_2, LCO_2 (especially $scCO_2$) has improved solubility in lubricating oil. Thus, spraying LCO_2 or $scCO_2$ into the cutting zone after mixing with micro lubricating oil is possible. Grguraš et al. [85] conducted a comparative study on the solubility of different polar lubricants in LCO_2, droplet size distribution after jet atomization, and tool life. The results show that the solubility of nonpolar lubricants is high, the particle size is uniform after atomization, and the tool life is long under the same cutting parameters, as shown in Fig. 14.

Using two separate channels for cooling–lubrication medium transport is the most common type, but the internal tool structure must be designed, and multiple channels (nozzles) need position calibration [86]. The single-channel cooling–lubrication medium transportation system is currently the most advanced because lubricating oil can be dissolved in LCO_2 or $scCO_2$ [85]. Compared with dual-channel systems, the geometry of single channels is markedly simplified, providing the milling cutter with a stable structural strength. Furthermore, no negative interaction is observed between LCO_2 and MQL [87]. Compared with $scCO_2$, LCO_2 is easy to process and obtain; thus, LCO_2 is widely used in the field of

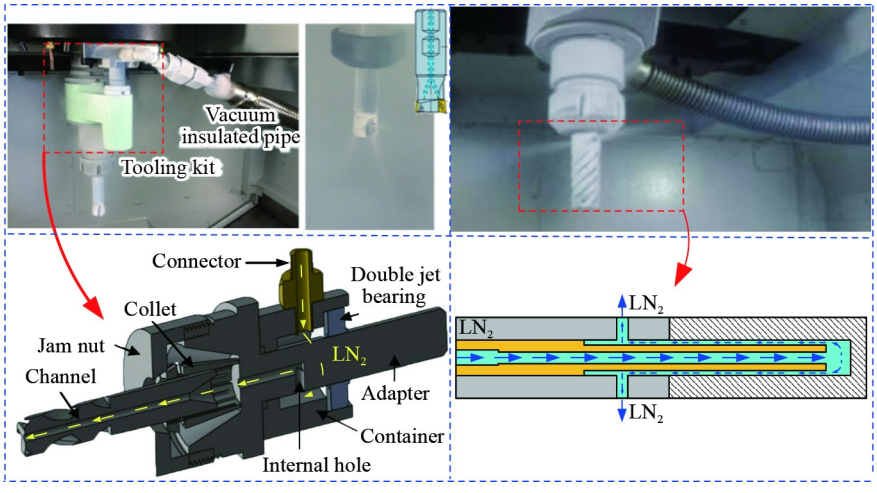

Fig. 11 LN_2 internal spray tool holder change device. Reproduced from Refs. [82,83] with permission from Springer Nature and Elsevier, respectively.

machining.

The new LCO_2 + MQL single-channel processing system is shown in Fig. 15(a). LCO_2 and lubricating oil simultaneously enter the mixing chamber through the precise control of flowmeter and needle valve, and then spray from the milling cutter to the cutting zone. The structure of the single-channel milling cutter is shown in Fig. 15(d). The traditional dual-channel cooling–lubrication medium supply mode is when LCO_2 is transported through the inner channel of the tool and MQL is transported through the external nozzle, as shown in Fig. 15(c). However, the LCO_2 ejected by high-speed rotation of the milling cutter prevents the micro lubricating oil from entering the cutting zone, which leads to unsatisfactory lubrication effects. Figure 15(b) compares milling cutter life under different transportation modes. The LCO_2 and micro lubricating oil of the single-channel transportation mode can effectively reach the cutting zone and considerably improve the milling cutter life.

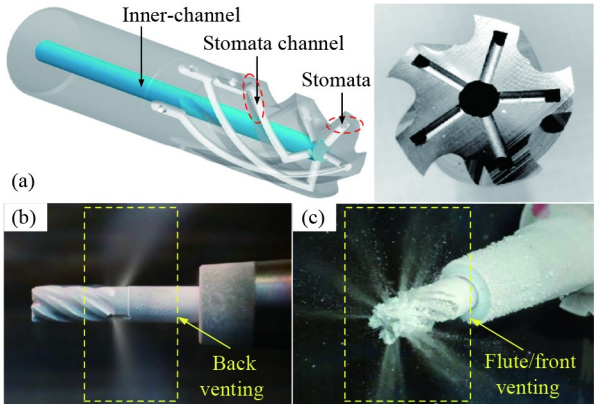

Fig. 12 Structure of inner passage end milling cutter and spraying direction of cooling medium: (a) internal structure of milling cutter, (b) back venting design, and (c) flute/front venting design. Reproduced from Ref. [84] with permission from Elsevier.

Fig. 13 New Cryo·tec™ milling cutter structure. Reproduced from Ref. [58] with permission from Elsevier.

2.3.3 Application of CA + MQL device

The type of CA + MQL can also be divided into internal and external jets. The external jet type is when compressed air is transported into MQL and refrigeration system, and then nozzles are arranged around the milling cutter at different angles. Micro lubricating oil and high-speed CA are sprayed into the cutting zone [88].

Song et al. [89] designed a new concept nozzle combining MQL and CA by using the Coanda effect, as shown in Fig. 16. CA (CO_2) enters the nozzle through inlet 2 and flows in two different directions. A part of the CA entering the nozzle flows rapidly to outlet 1 due to the Coanda effect and then along the airfoil structure to cool atomized droplets. Another part of CA flows rapidly to outlet 2 and ejects from the nozzle.

The internal jet type is when compressed air is treated by cryogenic equipment and multistage pressure regulation mixed with micro lubricating oil provided by MQL in the internal channel of the end milling cutter. Atomized droplets are then sprayed into the cutting zone under a high pressure [90]. The common internal channel

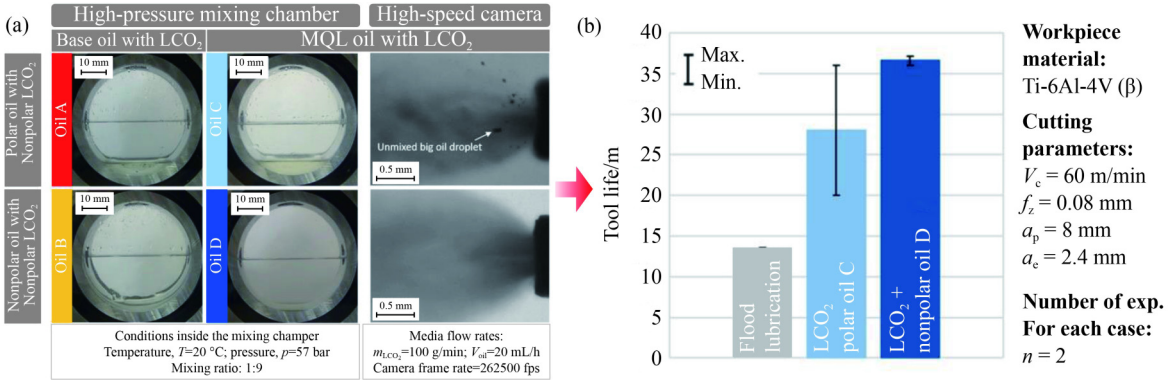

Fig. 14 Comparison of solubility and tool life of lubricating oil with different polarities: (a) investigation of oil polarity on the solubility of liquid oil in LCO_2, (b) influence of different cooling–lubrication on tool life [85].

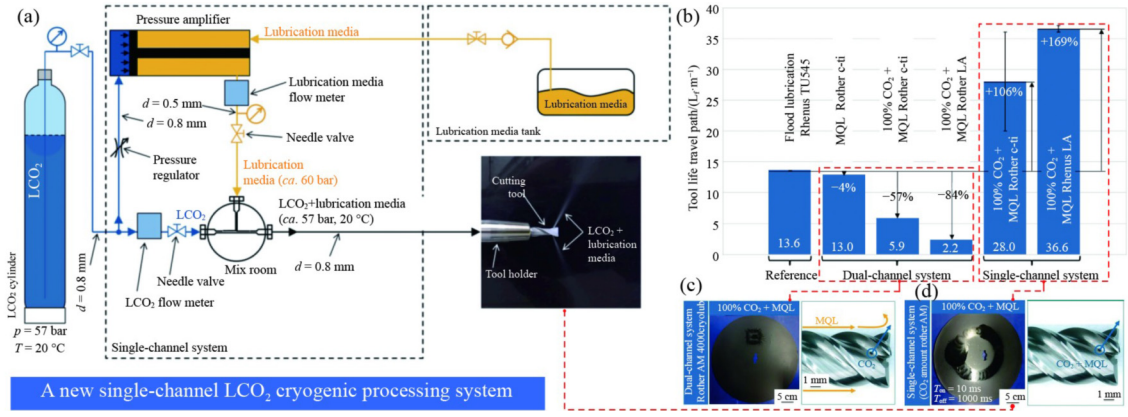

Fig. 15 Determination of spray pictures with dual- and single-channel systems: (a) schematic illustration of a novel cryogenic machining system based on single channels, (b) comparison between single- and dual-channel systems for CO_2 and MQL delivery, (c) MQL supplied out milling cutter, and (d) MQL supplied in milling cutter. Reproduced from Refs. [85,87] with permission from Elsevier (Ref. [87]).

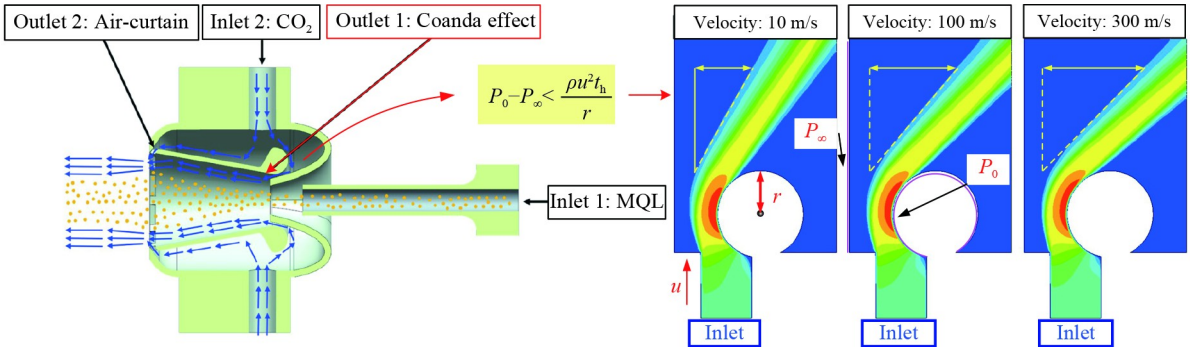

Fig. 16 New type nozzle with external spraying of CA + MQL. Reproduced from Ref. [89] with permission from Springer Nature.

structure of the internal jet end milling cutter has three forms, namely, double-helix channel (DHC), single straight channel (SSC), and double straight channel (DSC), as shown in Fig. 17. The inner channel structure has a remarkable effect on droplet size distribution. The number of small droplets obtained by DHC is the least (especially $R < 10$ μm) when spindle speed is 1500 r/min, whereas that by DSC is the most.

2.4 Grinding machining

Traditionally, grinding is a machining method that uses a high-speed rotating wheel to remove surplus material on the workpiece. Grinding can be divided into two types according to different grinding materials: plane and cylindrical grinding.

The wedge gap is formed between grinding wheel and workpiece in plane grinding, and the nozzle must be at a certain angle with the workpiece to spray the cooling–lubrication medium into the grinding area effectively. The conventional method sprays the cooling–lubrication medium into the grinding wheel–workpiece interface using an external spraying device [91–93]. However, an "air barrier layer" is formed in the wedge-shaped area due to the high-speed rotation of the grinding wheel, which prevents the cooling–lubrication medium from entering the grinding zone [94].

Therefore, Sanchez et al. [95] installed the LCO_2 + MQL system on the grinder to improve cooling–lubricating capability. First, the MQL nozzle sprays micro lubricating oil on the surface of the grinding wheel. Then, the LCO_2 nozzle is placed under the MQL nozzle along the rotation direction of the grinding wheel. The ejected LCO_2 not only cools down the grinding zone but also solidifies the lubricating oil on the surface of abrasive grains, forming a durable oil film, which can effectively enter the grinding wheel–workpiece interface and play a lubrication role. Figure 18 shows the formation of a frozen oil layer on the surface of abrasive particles.

The grinding wheel for cylindrical grinding is tangent to the cylindrical workpiece, which helps set nozzle position and angle. Therefore, the jet is parallel to the grinding wheel–workpiece interface and conducive to the cooling–lubrication medium entering the effective grinding zone. Ribeiro et al. [96] used CA generated by the vortex tube to atomize micro lubricating oil, and micro droplets directly enter the grinding zone, which has a good cooling–lubrication effect. However, the CA

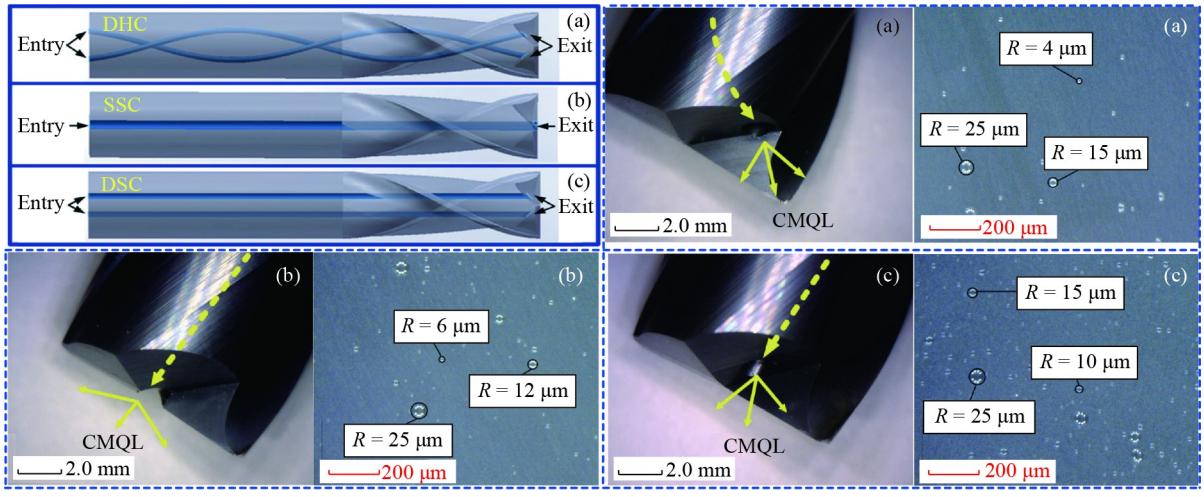

Fig. 17 Internal channel structures of three milling cutters: (a) DHC, (b) SSC, and (c) DSC. Reproduced from Ref. [90] with permission from Springer Nature.

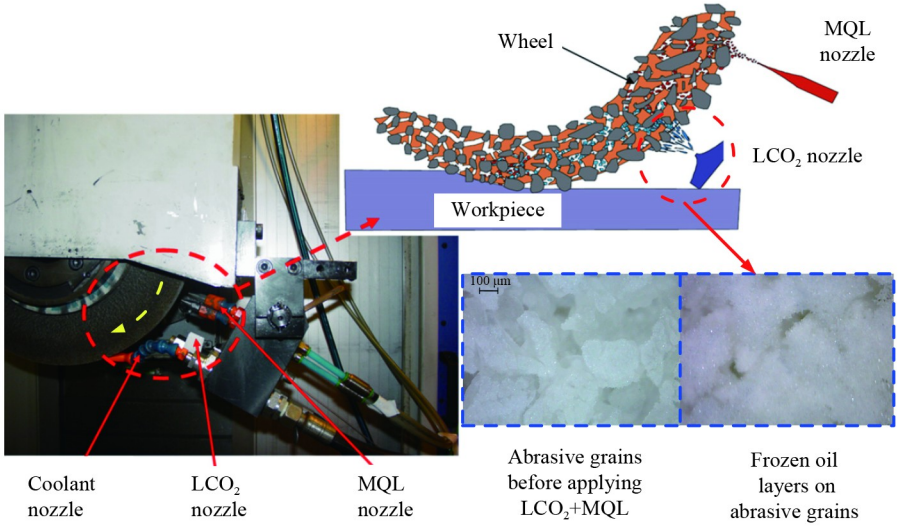

Fig. 18 Schematic of LCO_2 + MQL system in grinding. Reproduced from Ref. [95] with permission from Elsevier.

outlet must be sufficiently large to prevent backflow generated by high-speed rotation of the grinding wheel from blocking CA into the grinding zone, resulting in weakened cooling performance, as shown in Fig. 19.

2.5 Drilling machining

Different types of holes are important structural features for metal components to achieve specific functions. Many types of hole-forming methods are currently available, but drilling is the most extensive and practical for functional components of materials that are difficult to process, accounting for approximately 30%–40% of mechanical processing [98]. However, drilling machining of difficult-to-cut materials, such as titanium alloy, is characterized by low heat dissipation rate, large torque, difficult chip removal, serious bit bonding wear, and intermittent chip accumulation, which affect not only processing efficiency but also machining accuracy and workpiece surface quality [99]. Consequently, CMQL provides an excellent cooling and lubrication performance for difficult-to-cut materials, whereas traditional drilling techniques have considerable limitations.

The conventional external jet device is used to spray the cooling–lubrication medium directly into the drill bit. However, the blocking effect leads to a substantial decrease in the effective flow rate of the cooling–lubrication medium entering the drilling area due to the high-speed rotation of drill bits. In addition, the medium cannot enter and participate in cooling lubrication when the bit drills into the workpiece after a certain distance, especially deep hole machining, because the drilling space is semiclosed [100].

Mixed-medium spraying through the internal channel

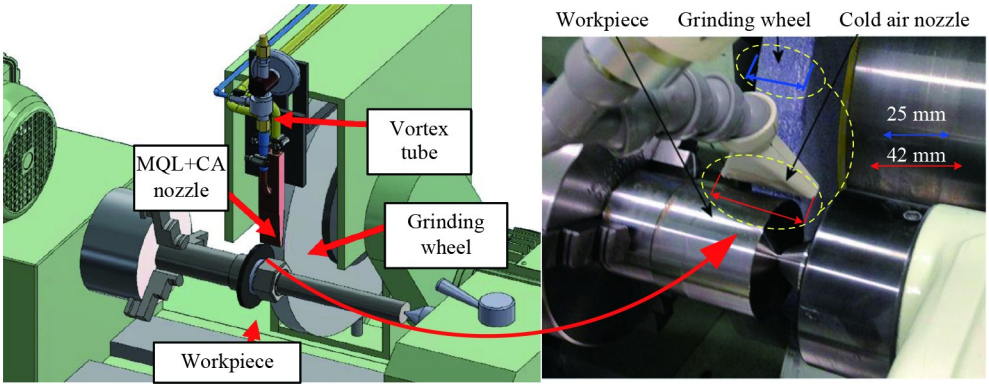

Fig. 19 Schematic of CA + MQL system in grinding. Reproduced from Refs. [96,97] with permission from Springer Nature.

drill bit is the best way to supply to improve cooling–lubrication capacity. However, lubricating oil cannot be dissolved in LN_2, and CA solidifies lubricating oil to block the channel. Therefore, LN_2 and CA, as the cooling media, are unsuitable for the mixed internal supply method. If only cooling without lubrication is considered, then LN_2 and CA are still the best cooling media available for the internal supply method [101]. In addition, LN_2 and CA need a high-pressure auxiliary supply, which plays a high-velocity carrying role in the narrow space of drilling holes and provides good chip removal effects. LCO_2 has good solubility for lubricating oil, which can effectively realize the inner channel supply after mixing of cooling–lubrication medium. Figure 20 shows the structure of the LCO_2 + MQL supply system [102]. The application of CMQL still has several limitations due to the geometric characteristics of drilling and the physical characteristics of the cooling medium.

2.6 Influence of CMQL machining on cooling–lubrication effect

2.6.1 CMQL supply mode

Two main ways to supply CMQL cooling–lubrication medium are currently available: external and internal jets.

External jets are the most commonly used supply mode. The cooling–lubrication medium supply system is designed separately, and modifying the cutting and machine tools is no longer necessary. The most suitable cooling medium for external jets based on the characteristics of the cooling medium and the processing method is LN_2, and the processing method involves turning and grinding.

Internal jets indicate the integration of the supply system into the machine tool, and the cooling–lubrication medium is accurately sprayed into the cutting zone through the inner channel of the tool holder and cutting tool. Therefore, transforming machine tools is necessary. The inner channel structure can be divided into two types: dual and single channels. The dual-channel system uses

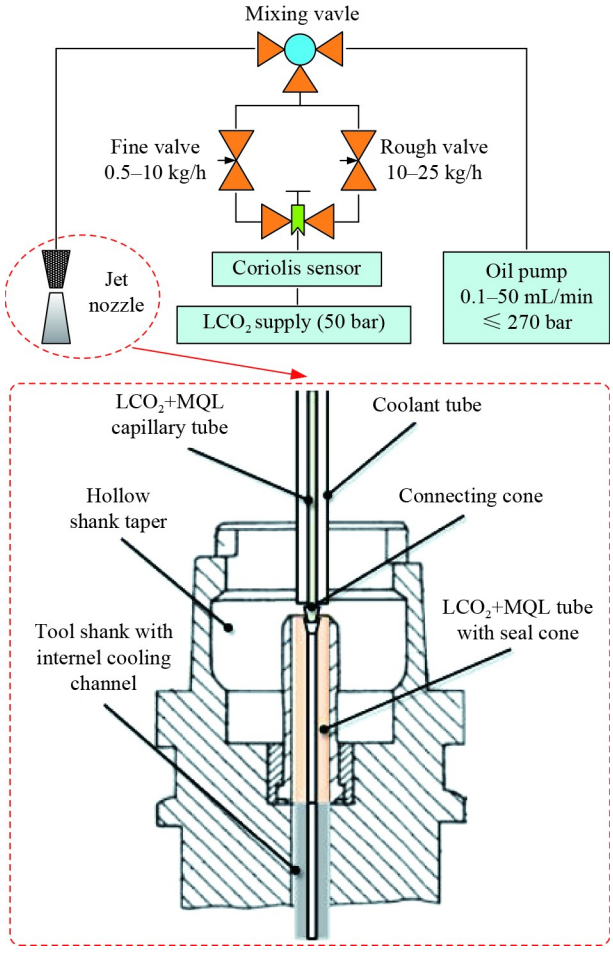

Fig. 20 Structure of LCO_2 + MQL supply system. Reproduced from Ref. [102] with permission from Elsevier.

two channels to transport cooling–lubrication media and perform mix atomization at the channel outlet. In single-channel systems, the cooling–lubrication medium is mixed in advance and atomized through a single channel. The most suitable cooling medium for internal jets is LCO_2 (or $scCO_2$) and CA, and the processing method is milling or drilling.

Compared with external jets, the internal jet effectively

penetrates the cooling–lubrication medium in the depth of the cutting deformation zone, which can effectively reduce friction between tool–chip and tool–workpiece interface. Under the condition of similar cooling medium, the effect of internal jet is better than that of external jet [103].

2.6.2 CMQL supply pressure

Supply pressure mainly affects the jet flow rate and velocity of the cooling–lubrication medium. Increasing pressure for the type of cooling–lubrication medium separately supplied to the cutting zone can effectively improve the jet flow and cooling capacity of the cooling medium [104]. Manimaran et al. [105] found that increasing LN_2 supply pressure can reduce tangential grinding force to a certain extent. Garcia et al. [106] indicated that the flow rate of LCO_2 has a considerable effect on G ratio during grinding, which gradually increases with flow rate.

However, different pressures have varying effects on MQL. Ejected speed is low when pressure is very small, and reaching the cutting zone is difficult for the mist due to the influence of air resistance around the rotating workpiece or cutting tool. Ejected speed is high when pressure is very large; this condition can easily lead to excessive impact and rebound of micro droplets, which cannot be effectively adsorbed on the tool–workpiece surface [107]. Therefore, appropriate pressure can effectively absorb and penetrate the cutting zone to form the lubricating film.

Different pressures produce varied cooling–lubrication effects for the type of micro lubricating oil dissolved in cryogenic media, such as $scCO_2$ + MQL [108]. The jet flow of $scCO_2$ dissolved with lubricating oil increases with input pressure, as shown in Fig. 21(a). The maximum cooling rate is 13.6 °C/s when pressure is 10.4 MPa. This phenomenon is attributed to droplet size reduction, increased number of droplets, and increased heat transfer due to high pressure. Cooling rate decreases with pressure, as shown in Fig. 21(b). Moreover, $scCO_2$ + MQL performs better than $scCO_2$ and MQL alone due to the effective superposition of cooling–lubrication effects.

2.6.3 CMQL jet distance

Jet distance mainly affects droplet spreading area for MQL [109]. Figure 22 shows that droplet coverage area decreases as jet distance increases. Coverage rate reaches the maximum when flow rate is 50 L/min and jet distance is 150 mm. Coverage decreases by 44.4% when jet distance increases from 150 to 290 mm. Therefore, a high droplet density is observed when close to the nozzle, and a considerable amount of droplets cover the tool–workpiece surface [110,111]. Furthermore, gas velocity rapidly decreases with increase in jet distance, resulting in a considerable reduction in the number of droplets effectively entering the cutting zone [112]. Therefore, shortening jet distance can improve lubrication effect.

A large jet distance indicates a large heat exchange capacity between the cryogenic medium and surrounding environment, which leads to a rapid rise in medium temperature. Heat exchange capacity decreases after entering the cutting zone, which affects cooling capacity. Figure 23 shows that the temperature of the measurement point increases with jet distance, indicating the reduction in cooling effect [45]. The milling cutter with d = 1.0 mm and d = 0.75 mm inner channel diameter when jet distance is 5 mm helps the cutting zone reach the lowest temperature, which is −10 °C and −15 °C, respectively. The cooling effect of LCO_2 can be improved by using the milling cutter with d = 0.75 mm because the cooling medium can be concentrated in the cutting zone using the

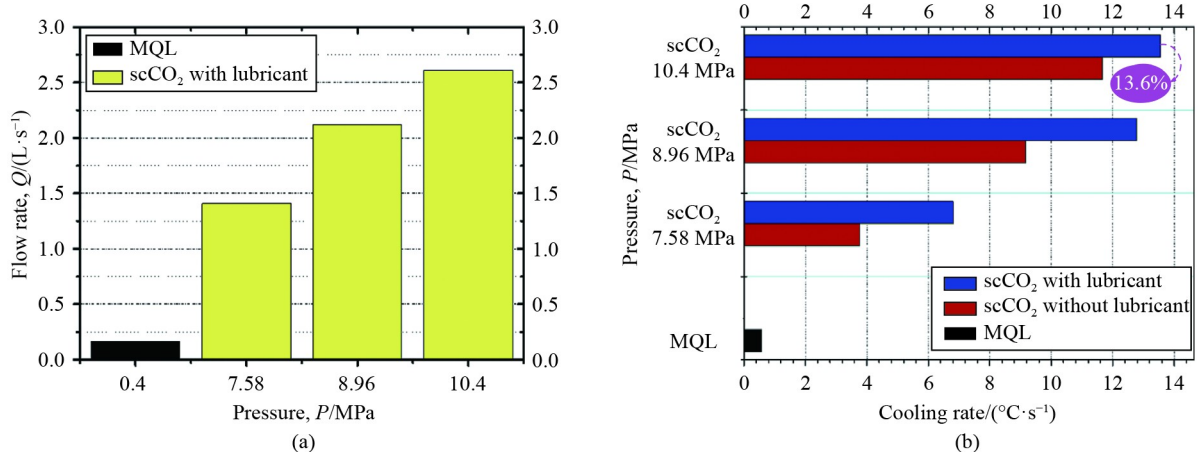

Fig. 21 Effect of CMQL supply pressure on jet flow rate: (a) value of flow rate for MQL at input pressure, (b) cooling rate value for each cooling technique. Reproduced from Ref. [33] with permission from Elsevier.

channel with a small diameter.

2.7 Applicability of CMQL device

The working characteristics of turning, milling, and grinding, such as tool structure and movement, are dissimilar. This difference leads to varying adaptability and cooling–lubrication effect of the CMQL device for several machining types. A systematic summary of the applicability of CMQL device is shown in Table 2.

3 Mechanism of CMQL

The working principles of cryogenic and MQL (or NMQL) are completely different, and the cooling–lubrication mechanism changes upon combination. The constitutive relation of workpiece material removal changes with varying thermal softening effects, which directly affects cutting temperature, cutting force, tool wear, and workpiece surface quality. However, no relevant mechanism is available to explain these changes, and no unified index system can be used to measure the performance of CMQL comprehensively. Therefore, this chapter contains the mechanism analysis of CMQL.

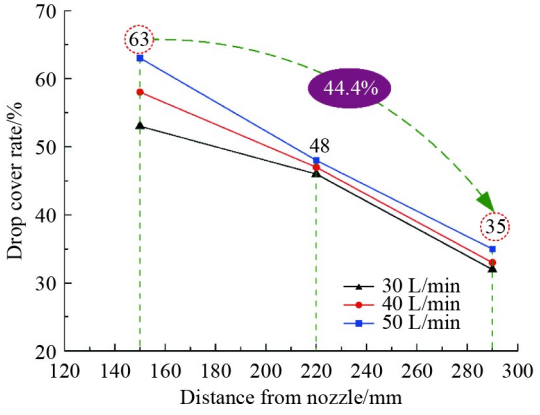

Fig. 22 Influence of CMQL jet distance on spread area and airflow velocity [112].

3.1 Lubrication mechanism of CMQL

Micro lubricating oil (vegetable oil) permeates the cutting zone in the form of gas mist under the carrying action of high-pressure and high-speed gas and forms a boundary lubricating film on the tool–chip and tool–workpiece surface through polar group adsorption. This phenomenon prevents direct dry friction between rake face–chip and tool–workpiece interface to a certain extent. However, the viscosity of lubricating oil decreases due to high speed/temperature/pressure in the cutting zone. The oil film becomes thin and breaks, which cannot completely cover the micro grooves on the workpiece surface. The lubricating film induces the desorption failure phenomenon when a critical temperature is exceeded. The decrease in lubrication performance leads to dry friction at tool–workpiece interface [113].

The viscosity of lubricating oil increases at a low temperature for CMQL, and the oil film thickness can maintain an effective state of completely separating the friction surface, in which bearing capacity is improved as shown in Fig. 24(a). The cryogenic medium maintains the

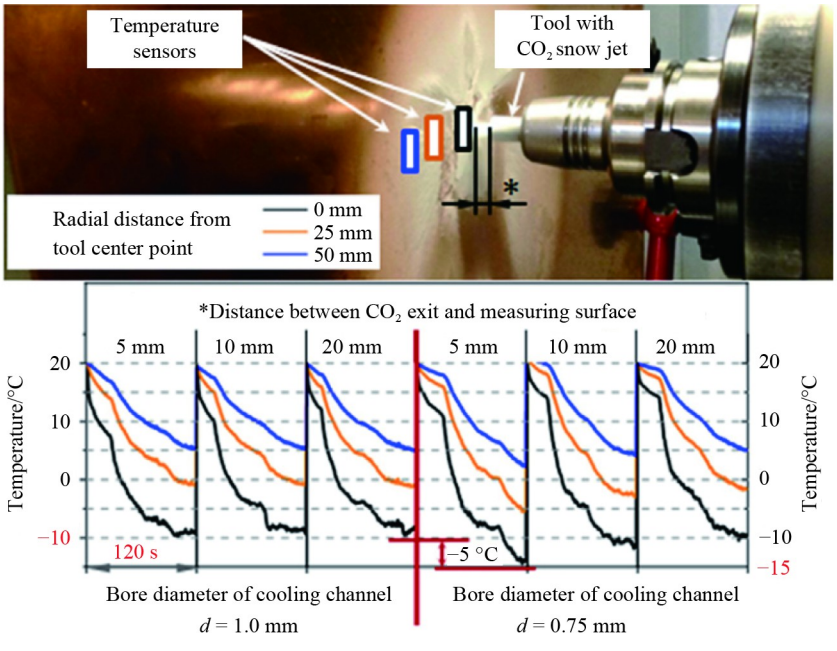

Fig. 23 Influence of distance between CO_2 jet exit and impact surface on measured temperature. Reproduced from Ref. [45] with permission from Elsevier.

Table 2 Adaptability and effect of CMQL device in different processing forms

Medium transport mode	Schematic	Medium	Application effect
External single nozzle	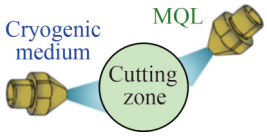	LN_2 + MQL LCO_2 + MQL CA + MQL	All three kinds of media are suitable for turning. Additional nozzles improve the coverage of the CMQL medium.
External multiple nozzles	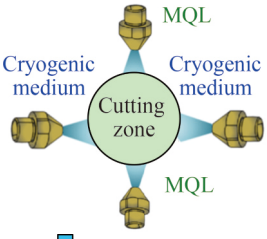	LN_2 + MQL LCO_2 + MQL CA + MQL	Spacing cutting edges of the milling cutter with high-speed revolution and preventing the medium from entering the cutting zone effectively.
External single or multiple nozzles	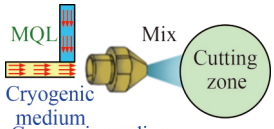	LCO_2 + MQL CA + MQL	LN_2 and LCO_2 may cause severe icing on the surface of the grinding wheel, thus blocking abrasive clearance and hindering the lubrication effect. CA is suitable for grinding.
Cryogenic medium by inner channel of tool handle and MQL by external nozzle	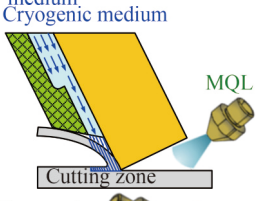	LN_2 + MQL LCO_2 + MQL	Effectively penetrating the contacted tool–workpiece interface and increasing the coverage is beneficial for the cryogenic medium.
Cryogenic medium by inner tool channel and MQL by external nozzle	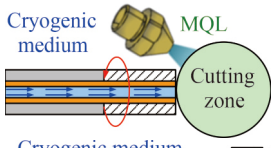	LN_2 + MQL LCO_2 + MQL	Suitable for end milling cutter, considerably improving the penetration effect. However, the permeability of oil is still affected by the high speed of milling cutter rotation.
Cryogenic medium and oil not mixed by the inner tool channel	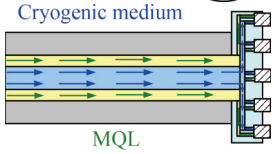	LCO_2 + MQL CA + MQL	Suitable for disc milling cutter, markedly improving the penetration effect of the cooling–lubrication medium.
Cryogenic medium and oil mixed by inner tool channel		LCO_2 + MQL $scCO_2$ + MQL	Suitable for end milling cutter, substantially improving the penetration effect of the cooling–lubrication medium.

temperature in the cutting zone at a relatively low level, which not only sustains the high absorption of the lubricating film but also avoids oil film oxidation failure caused by high temperature, as shown in Fig. 24(b). However, a low temperature increases the surface tension and contact angle of micro droplets to a certain extent [114]. This phenomenon results in a decrease in lubricating oil permeability to the capillary channel on the tool/workpiece surface, which harms lubricating capability, as shown in Fig. 24(c).

3.2 Cooling mechanism of CMQL

In cutting, the heat transfer between cooling medium and tool−workpiece follows Newton's convection heat transfer formula [115]:

$$q = h \cdot A \cdot \Delta T, \tag{1}$$

where q is the heat flux (W/m), h is the surface heat transfer coefficient (W/(m^2·K)), A is the heat transfer area (m^2), and ΔT is temperature difference (°C). The formula indicates that heat flux is proportional to the temperature difference in the cutting zone. A considerable amount of heat is exchanged when the temperature difference is large, and the cooling effect is evident.

The temperature for LN_2 is −196 °C, which forms a considerable difference with the cutting zone and plays a remarkable role in high-speed cutting with high-temperature environments. The temperature for LCO_2/$scCO_2$ is −78.5 °C, which is suitable for medium-speed cutting. The temperature range for CA is usually from −10 °C to −60 °C and can be controlled. Temperature can be adjusted in accordance with the actual situation to control the temperature of the cutting zone. Moreover, CA with a high speed increases the convection area and further enhances heat transfer capability [116].

Improving the survival capability of the lubricating film at low temperatures is beneficial. Such an improvement can effectively reduce friction between tool−workpiece

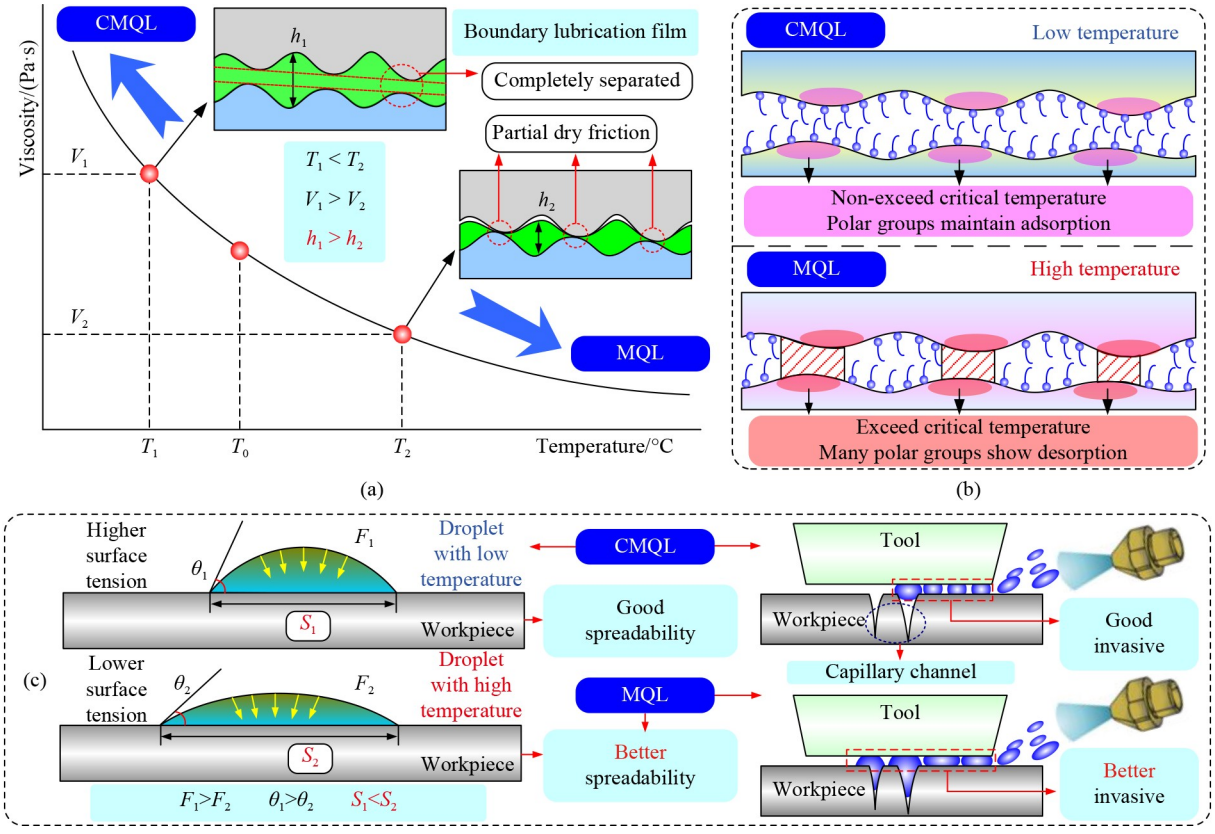

Fig. 24 Comparison of lubricating oil in viscosity, activity, and wettability between CMQL and MQL: (a) influence on viscosity of CMQL and MQL, (b) influence on oil film activity of CMQL and MQL, and (c) influence on droplet wettability of CMQL and MQL.

and restrain the thermal effect of machining. Furthermore, cryogenic medium may cause oil solidification. The phase transition of lubricating oil from solid to liquid in the cutting zone occurs at the friction interface, which can absorb some heat. The cooling superposition mechanism of CMQL is shown in Fig. 25(a). The spraying position of the cooling–lubrication medium in the cutting affects the cooling effect. Taking LN_2 + MQL as an example, the cooling–lubrication medium should be simultaneously sprayed on the rake and flank face to achieve the best cooling effect [68]. LN_2 is realized by direct jet to the tool−workpiece interface, which leads to a large consumption of cryogenic medium and increases the production cost in practical processing. Deep cooling of tools through LN_2 circulation in the inner channel of the turning tool is also feasible, as shown in Fig. 25(b). The turning tool can always remain in a low-temperature state, indirectly cooling the cutting zone and reducing the use of LN_2, which meets the requirements of green machining [117].

3.3 Influence mechanism of CMQL on material hardness

High temperature and pressure changes the surface and subsurface micro structure of metal materials and induce thermal softening, which leads to an increase in friction, cutting heat, and adhesion of the chip to the tool. Surface processing quality is also seriously affected. Therefore, a reasonable cooling–lubrication method helps restrain thermal softening and improve cutting performance.

The surface hardness of the workpiece is mainly affected by work hardening and temperature in the cutting. Work hardening always exists regardless of process conditions, and temperature can be controlled by cooling. CMQL not only cools the cutting zone but also changes the properties of workpiece materials. However, the mechanism of cryogenic and MQL is different.

MQL (or NMQL) aims to reduce the friction heat between tool and workpiece by lubrication effect and slow down the degree of thermal softening. The workpiece will not be over hardened [118]. Cryogenic technology can also inhibit thermal softening but produce refined and dense grains of workpiece materials, substantially improving the hardness and even over hardening [119–122]. The improvement degree of workpiece hardness by cryogenic technology is higher than that of MQL (or NMQL) [123,124] because the cooling capability of the cryogenic medium (especially LN_2 and LCO_2) is considerably higher than that of MQL (or NMQL).

MQL can provide a reasonable hardness range by slowing down the thermal softening degree of materials, which is conducive to improving cutting performance. A low temperature can also improve material hardness.

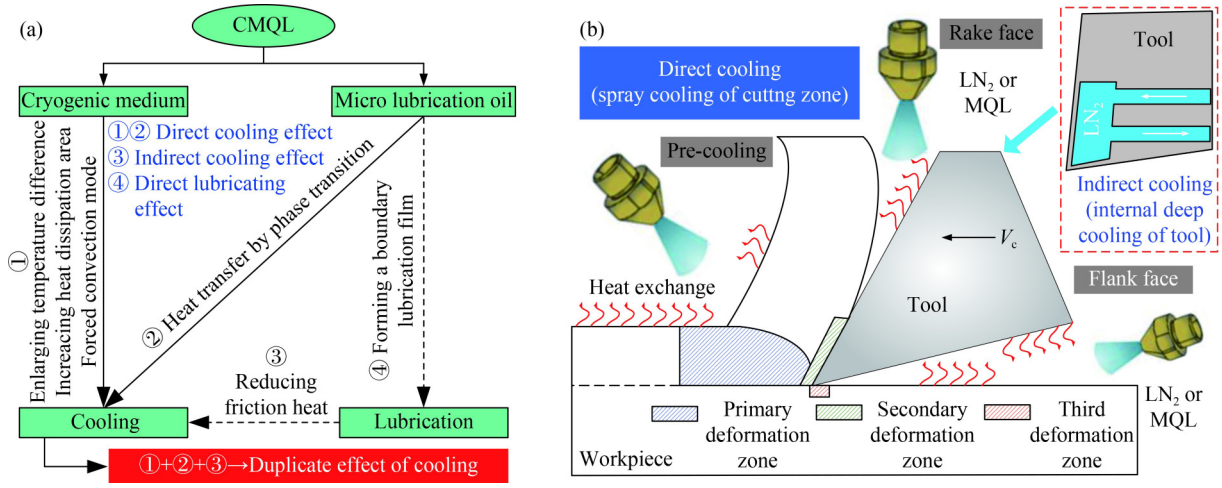

Fig. 25 Superimposed cooling mechanism of CMQL and measures to improve cooling effect: (a) four kinds of influence modes on cutting temperature, (b) combination of different jet positions. Reproduced from Ref. [67,75] with permission from Elsevier and Taylor & Francis, respectively.

However, the toughness and ductility of difficult-to-cut materials, such as titanium alloy, nickel-based alloy, and high-strength steel, have no changes. Consequently, material removal is difficult when cutting force and tool wear increase [125–127]. Combining cryogenic technology with MQL, the increase in material hardness is theoretically higher than that of cryogenic technology used alone. However, this phenomenon is indirectly explained by the cooling superposition effect of CMQL.

Huang et al. [128] compared and studied the influence of CA, MQL, and CA + MQL on workpiece hardness when turning Ti-6Al-4V. Figure 26 shows that the surface hardness of the workpiece under the CA + MQL condition is considerably higher than that of MQL but lower than that of CA because the application of CA alone can lead to a high degree of material hardening. Nevertheless, the lubrication effect of cryogenic oil film of CA + MQL can reduce the adhesion power of workpiece materials to the cutter, and the relaxed adhesion can considerably inhibit plastic deformation of the workpiece, which reduces processing hardness [129]. Therefore, CMQL can reduce the surface hardness of the workpiece to a certain extent and prevent excessive cutting force.

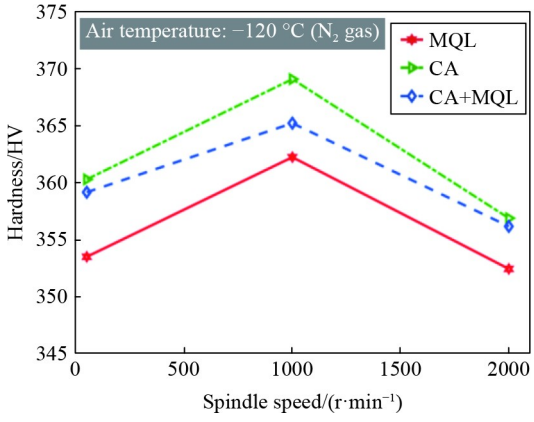

Fig. 26 Measurements of surface hardness generated under various cooling conditions. Reproduced from Ref. [128] with permission from Elsevier.

3.4 Influence mechanism of CMQL on cutting force

Using MQL (or NMQL) in cutting can substantially reduce cutting force [130–132]. This reduction is due to the absorption of polar oil mist particles on the tool–workpiece surface to form a physical film, which is crucial in lubrication and load bearing. Moreover, nanoparticles, such as MoS_2, carbon nanotubes, and Al_2O_3, are added to lubricating oil to facilitate the entrance of the tool–workpiece interface and play the role of "roll ball," replacing original sliding friction with rolling friction and effectively reducing cutting force [133].

The cooling temperature of different cryogenic media (LN_2, LCO_2, and CA) and spraying positions have different effects on the change trend of the main cutting force (tangential force), thrust force (axial force), and feed force (radial force) [134,135].

The cryogenic medium is usually sprayed on the rake or flank face or both. LN_2 cooling in the turning is taken as an example. Spraying on the rake face can prevent thermal softening and reduce adhesion between tool and chip, which is conducive to reducing friction force [136]. However, the cryogenic effect of LN_2 over hardens the workpiece and increases the difficulty in overcoming material deformation, resulting in an increased cutting force [137]. The competitive relationship between material hardening and friction reduction affects the changing trend of cutting force during cryogenic machining, which is directly related to the cooling degree

of workpiece.

Different structures of tool holder affect the jet depth of LN_2 in the gap between rake face and chip and then influence the cooling degree of the workpiece [138].

The main cutting force for mode A (Fig. 27) is higher than that of dry cutting regardless of the combination of LN_2 jet positions because the chip breaker lifts the chip away from the nozzle. LN_2 is directly sprayed on the chip root, and the cooling degree is high, which increases the hardness of the workpiece material [139]. LN_2 can reduce friction force, but the reduction is less than the increase in cutting force after cryogenic hardening; therefore, the main cutting force increases. The feed force when LN_2 is sprayed on the flank or rake face decreases by 2.3% and 9.5% compared with dry cutting, which indicates that the reduction in friction force is larger than the increase in cutting force [140]. However, the difficulty in cryogenic action on material removal is increased when LN_2 is sprayed on the flank and rake faces. The increase in cutting force is larger than that of friction reduction. Therefore, feed force increases, but the amplitude is unremarkable at only 1.7%. Thrust force increases because LN_2 raises the local hardness of the workpiece. Hardening degree is high when temperature is low, and thrust force is large [140].

The position of LN_2 jet on the rake face is relatively far from the chip root for mode B (Fig. 27), and the surface hardening degree of the workpiece is low. Therefore, the influence of material removal on cutting force is small [141]. The effect of LN_2 jet position on friction force of the workpiece–tool interface directly determines the change in cutting force [142]. The main cutting force is taken as an example. Compared with dry cutting, the main cutting force decreases with a maximum amplitude of 8.1% when rake and flank faces are sprayed simultaneously under different cutting parameters. However, the maximum increase in main cutting force is 8.8% when only rake face is sprayed, which is even higher than that of dry cutting. This result reveals the decreasing capability to reduce friction.

As mentioned above, the difference in cooling degree of workpiece surface caused by the cryogenic effect of LN_2 leads to different changing trends of cutting force, which is also suitable for milling and grinding [143,144]. The cooling temperature for LCO_2 and CA is considerably lower than that of LN_2. Thus, the hardening degree of the workpiece material is substantially low. The inhibition effect on chip adhesion also decreases [145].

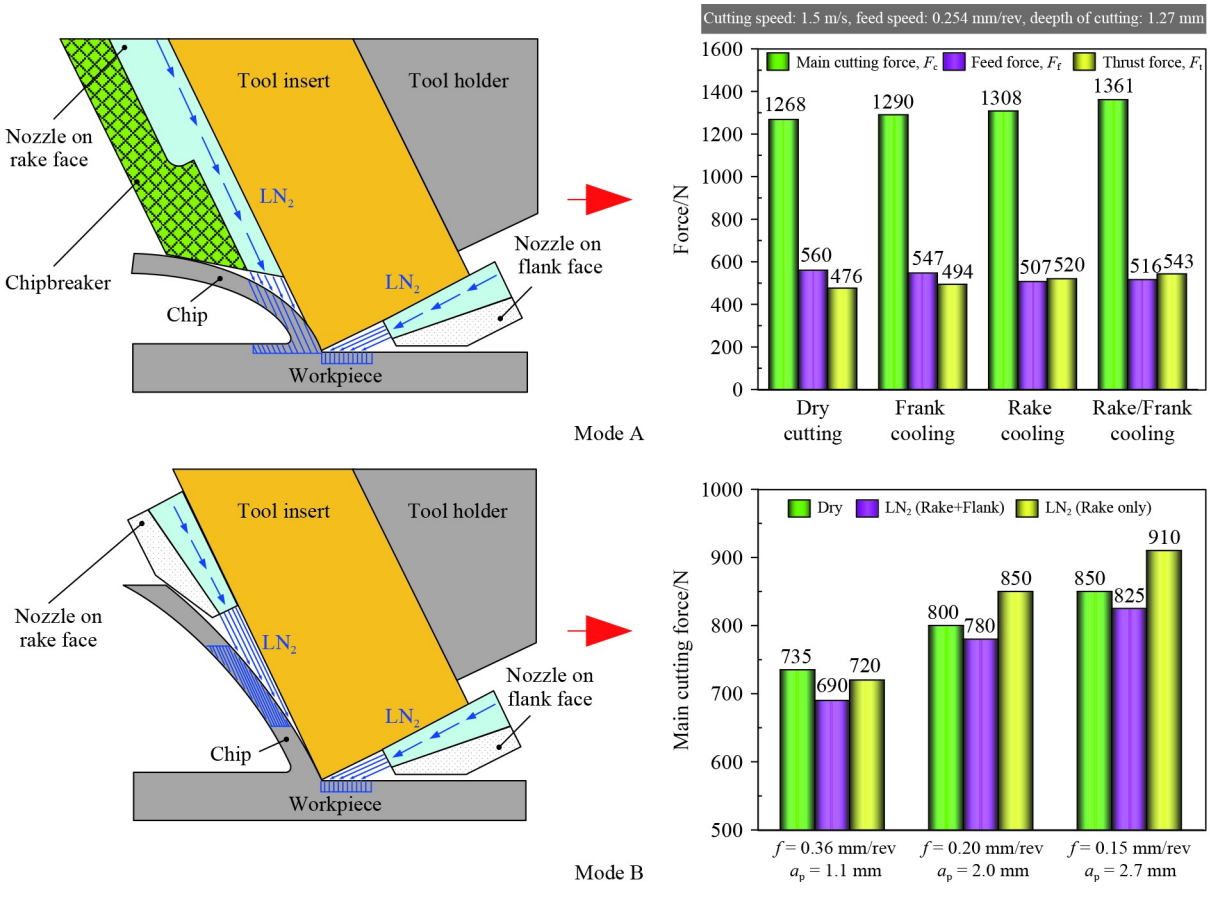

Fig. 27 Influence of different tool holder structures on workpiece cooling degree and cutting force. Reproduced from Ref. [140,142] with permission from Elsevier.

Elanchezhian and Kumar [146] found that LCO_2 effectively inhibits thermal softening in the grinding of Ti-6Al-4V, and the workpiece surface is not over hardened. The tangential and normal forces decrease by 21% and 9%, respectively. The main cutting and feed forces of CA (cooled by LN_2 at −110 °C to −130 °C) when Sun et al. [147] turned Ti-6Al-4V are higher than those of normal-temperature compressed air. However, Rahman et al. [148] used CA in −10 °C for cooling when turning ASSAB 718HH and observed the effective reduction of three cutting force components. Therefore, concluding that cryogenic medium can increase or decrease cutting force is still impossible [5].

Under the action of reducing adhesion of cryogenic technology and MQL (or NMQL), the reduction in friction force in the tool/workpiece interface is larger than the increase in cutting force caused by hardening. Cutting force decreases as a whole with increase in competitive power.

3.5 Influence mechanism of CMQL on tool wear

Coating a layer of special material on the tool surface is mainly used to improve the cutting performance of tools considering material technology innovation. The usage amount of coated tools in cutting accounts for approximately 68% of all types of tools [91]. Tool life, which is closely related to tool wear mechanism, is an important index to determine machining performance. Cutting of difficult-to-cut materials is accompanied by mechanical load impact and a harsh environment of high temperature/pressure/speed. Severe friction and complex physical and chemical reactions occur at the tool–workpiece interface, resulting in different wear types of tool matrix. The common tool wear types are crater, coating, adhesive, and diffusion wear. The wear pattern is shown in Fig. 28.

The micro protrusion on the chip surface sliding on the rake face causes peeling of the coating layer. The nonuniform temperature distribution of tools results in thermal cracks on the surface and then damages the tool matrix [151]. The continuous action of chips on the rake face leads to the formation of craters [152], as shown in Fig. 28(a). The crater expands with the increase in wear, and the strength of the cutting edge gradually weakens, leading to edge collapse as shown in Figs. 28(d) and 28(f). The phenomenon of spot welding occurs at convex points on the surface when the tool and the workpiece are in contact. The solder joint breaks under the action of relative sliding and dynamic load, and the melted workpiece material adheres to the tool surface to form build-up-edge (BUE) and build-up-layer (BUL), as shown in Figs. 28(b)–28(e). Turning Ti-6Al-4V is taken as an example. The coating on the rake face is worn due to high temperature and pressure, and the titanium element in the workpiece reacts with O, S, Cl, and other elements to form a layer of low-hardness compound. This phenomenon results in difference between tool surface and matrix, which weakens tool wear resistance and reduces tool life. Figure 28(g) shows the green dotted area, which indicates the diffusion of titanium element to the tool.

Tool wear is inevitable in cutting. However, reasonable measures can be taken to slow down wear. The said different wear mechanisms reveal that reducing tool temperature and improving the lubrication effect of the tool–workpiece interface are important measures to improve tool life. CMQL can satisfy the two conditions simultaneously. The superimposed cooling effect of CMQL maintains the tool at a low-temperature state, and the surface coating layer can maintain high hardness, thus improving wear resistance and prolonging the service time of the coating layer. Simultaneously, a low temperature can markedly reduce the thermal softening degree of the workpiece and inhibit the high-temperature adhesion of the tool–workpiece at the contact interface.

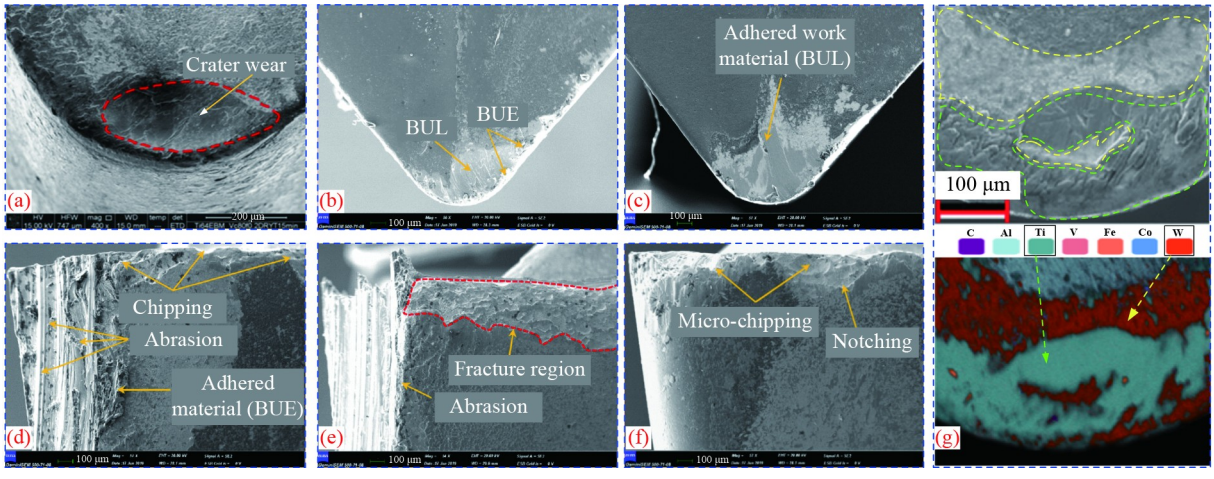

Fig. 28 Different types of cutter wear patterns. (a) Crater wear, (b) build-up-edge and build-up-layer, (c) build-up-layer, (d) abrasion and chipping, (e) abrasion, (f) chipping, and (g) diffusion. Reproduced from Refs. [149,150] with permission from Elsevier.

This temperature can also effectively prevent BUE or BUL.

Nevertheless, Sartori et al. [153] indicated that the adhesion phenomenon cannot be eliminated but only slowed down. By contrast, a low temperature helps inhibit the chemical reaction activity of special elements in difficult-to-cut alloy and markedly slows down diffusion wear rate. Bordin et al. [150], Sivalingam et al. [154], and Gajrani [66] found that compared with dry cutting, the diffusion amounts of titanium decreased by 33.7%, 43.9%, and 64.5%, respectively, when cutting Ti-6Al-4V, which considerably inhibited titanium diffusion. Tool coating wear is mainly due to the severe friction between rake face and chip. The high-viscosity oil film produced by MQL (or NMQL) at cryogenic conditions can effectively separate the rake face from the chip and substantially reduce coating layer wear. Furthermore, the cooling–lubrication effect of CMQL can effectively prevent the appearance of craters on the rake face and the phenomenon of chipping. Sartori et al. [153] did not find craters on the rake face of Ti-6Al-4V with tungsten carbide coating coated tool under the conditions of LN_2 + MQL and LCO_2 + MQL. By contrast, craters with different depths were observed on the rake face when using cryogenic technology or MQL alone.

3.6 Influence mechanism of CMQL on surface quality

Surface quality is the most important index of cutting performance. The formation of uneven micro gap and micro peak valleys on the machined surface is due to chip separation, severe tool–workpiece friction, and machine tool vibration. The feed motion of the tooltip forms regular overlapping tracks on the workpiece surface. The residual area height Ra of the uncut part is an important parameter to characterize surface roughness.

A high temperature in the tool–workpiece contact zone increases cutting force and tool wear and then directly affects surface roughness. Therefore, effectively reducing the cutting zone temperature and strengthening lubrication of the tool–workpiece interface are fundamental measures to reduce surface roughness [155]. The lubricant film produced by MQL can effectively reduce tool–workpiece interface friction and improve surface quality. The cryogenic medium lacks lubrication function despite its excellent cooling capability, and the tool–workpiece is still dry friction, which is not conducive to improving the surface quality. Particularly, the cryogenic effect of LN_2 substantially increases workpiece hardness and decreases cutting performance. This effect is even higher than the Ra value of MQL under the same cutting parameters [156–158]. The heat transfer coefficient and cooling capability of oil film remarkably increase after adding nanoparticles in MQL. Nanoparticles can fill and repair the micro grooves on the workpiece surface [159]; therefore, the Ra value of NMQL is lower than that of LN_2 [160] under most cutting conditions. The temperature for LCO_2 and CA is considerably lower than that of LN_2, which can effectively reduce cutting heat and avoid excessive hardening. Thus, the Ra value is usually less than MQL (or NMQL) [161,162].

As mentioned in Sections 3.1–3.5, the coupling effect of cooling and lubrication of CMQL provides a reasonable workpiece hardness range. Cutting heat, cutting force, and tool wear are considerably reduced. Therefore, CMQL also plays a remarkable role in improving surface quality.

4 Turning performance of CMQL

Turning is the most basic and common machining method. The workpiece is rotated relative to the tool to remove material continuously. Turning is also crucial in production. The ultimate goal of turning is to obtain a highly smooth surface. However, especially for difficult-to-cut materials, a high temperature caused by severe friction between turning tool and workpiece facilitates chip adherence to the cutting edge, which affects cutting performance. Workpiece surface and cutting quality worsen. In addition to the reasonable selection of cutting tools and the setting of cutting parameters, effective cooling–lubrication measures can reduce cutting heat and force. Improving tool life and surface processing quality is an important measure. As a new green processing method, CMQL shows an excellent cooling–lubrication superposition effect.

4.1 Cutting temperature

Cutting heat is an inevitable physical phenomenon in turning [163]. The main source of cutting heat is friction between rake face and chip, and the second is the friction between flank face and workpiece. Overcoming workpiece deformation is also an important factor [164]. The sharp temperature change in the tool–workpiece interface is only limited to the area of 1–2 mm on the surface [165]. Reasonable selection of cooling–lubrication method not only reduces usage but also sufficiently cools the cutting zone.

The influence of MQL, NMQL, LN_2, and LN_2 + MQL (or NMQL) on the turning temperature of Inconel 625 was studied by Yıldırım [166]. Figure 29 shows that the temperature of the tool–workpiece interface is the lowest at approximately 135 °C under the combined action of LN_2 + NMQL (0.5 vol% hBN). This value is 10% lower than that of LN_2 + MQL, 18.2% lower than that of LN_2, 28.9% lower than that of NMQL 1 vol% (hBN + Al_2O_3), and 40.4% lower than that of MQL. The effect of LN_2 + NMQL is better than that of LN_2 and NMQL alone. Figure 29 also shows the superior cooling effect of MQL

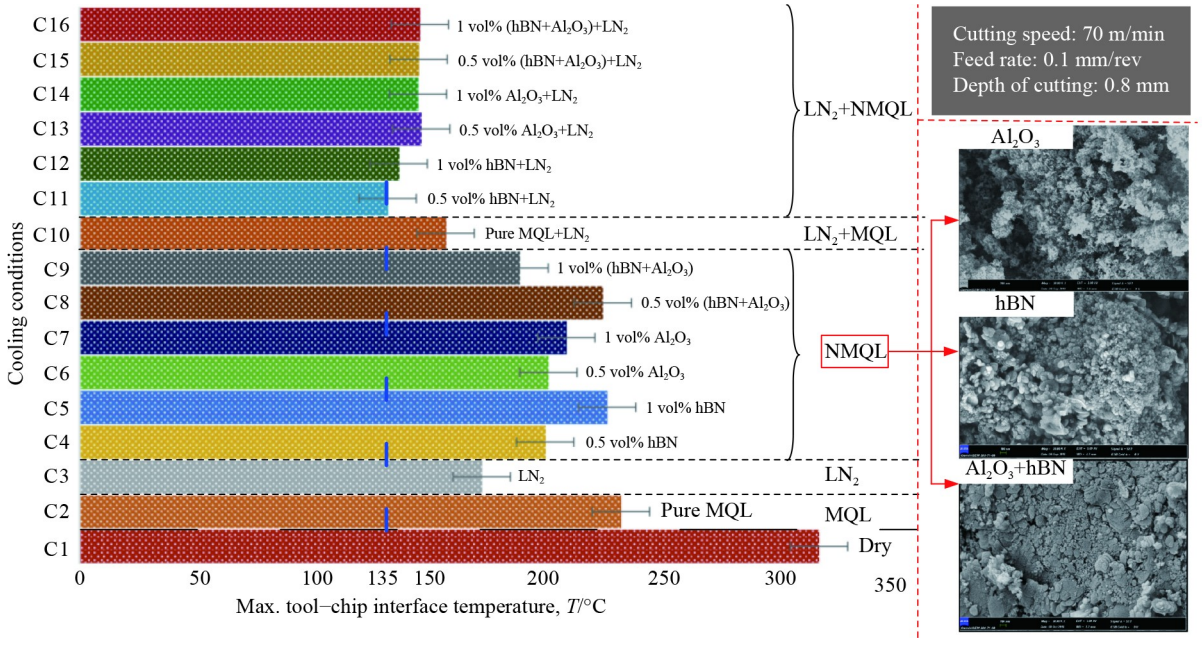

Fig. 29 Tool–chip interface temperature under different cooling conditions [166].

with nanoparticles due to the excellent thermal conductivity [167,168]. Moreover, hBN is better than Al_2O_3 in improving the performance of antiwear/anti-friction; therefore, the cooling effect of hBN is enhanced [169].

Bagherzadeh and Budak [170] studied the influence of spraying different tool faces with LCO_2 + MQL on the cutting temperature in turning Ti-6Al-4V. The combined spraying form of cooling–lubrication medium is shown in Fig. 30. In turning, the cutting zone temperature with (LCO_2 + MQL) (rake) strategy is the lowest, which is 43.7% and 18.2% lower than that of LCO_2 (rake) and LCO_2 (rake) + MQL (flank), respectively. The cooling effect of LCO_2 is the same. However, the micro lubricating oil entering the cutting zone condenses into a solid under low temperature for (LCO_2 + MQL) (rake). The phase transition from solid to liquid occurs after cutting, which can absorb extra heat.

Supekar et al. [171] studied the heat removal potential (HRP) and heat removal efficiency (HRE) of $scCO_2$ + MQL when turning Ti-6Al-4V. Figure 31(a) shows that flood technology has the highest HRP, which increases heat conduction capacity due to the high flow rate of coolant. However, the degree of environmental pollution is high, which does not meet the requirements of clean production. The HRE of MQL (vegetable oil) is the lowest because oxidizing micro lubricating oil at high temperatures is easy. Figure 31(b) shows that $scCO_2$-XL (lubricant expanded with $scCO_2$) spray has a long distance and a high oil content. However, a low pressure leads to the expansion of vegetable oil with $scCO_2$. The increase in condensate droplets and dry ice particles is not conducive to cooling and lubrication. The HRP and HRE of $scCO_2$-DL (dissolved lubricant in $scCO_2$) are the highest. This result indicates that high pressure and low oil content afford the cooling–lubrication medium with improved permeability and cooling effect.

Zou et al. [75] studied the influence of cooling–lubrication methods of CA, MQL, and CA + MQL on the turning temperature of turning 3Cr2NiMo. Figure 32(a) shows that the cooling effect of CA+ MQL is better than that of CA and MQL alone, which are 46.8% and 12.2% lower than that of CA and MQL, respectively. MQL can reduce the friction heat between the tool and workpiece, and the cooling effect is more prominent than that of CA. Zou further explored the influence of different kinds of lubricants on the cooling effect of CA + MQL. Figure 32(b) shows that synthetic ester and emulsion markedly enhance the cooling effect compared with castor oil. The CA + MQL of castor oil base with carbon group nanoparticles has the best cooling effect, which is 34.6% lower than that of pure castor oil. This finding is due to the high thermal conductivity of carbon nanoparticles, which can substantially improve heat transfer capability [172,173]. Therefore, adding appropriate nanoparticles in lubricating oil is an effective way to improve cooling capability.

4.2 Cutting force

Cutting force mainly comes from overcoming the elastic–plastic deformation of the workpiece material, the friction between the chip and rake face, and the friction between the machined surface and flank face [174]. Cutting force is an important index affecting tool wear, surface integrity, and power consumption of machine

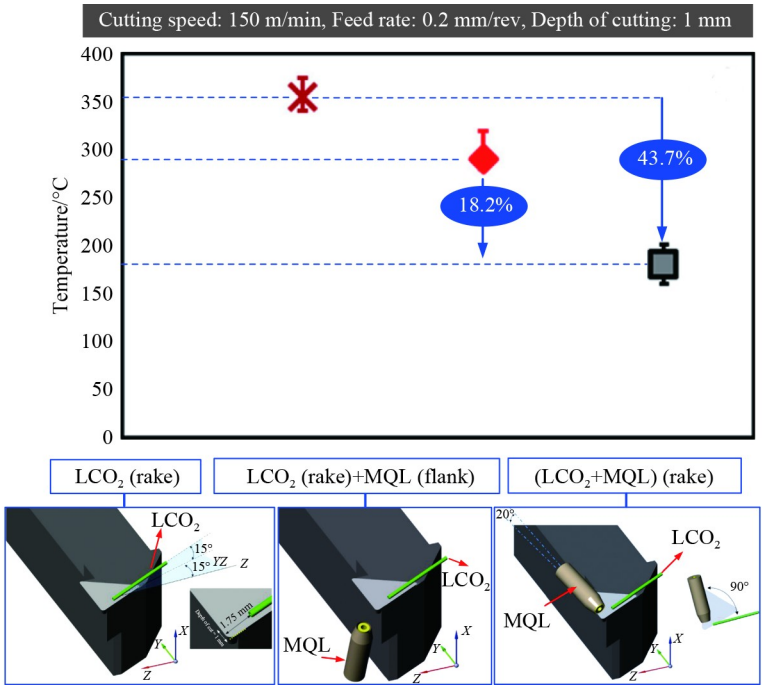

Fig. 30 Influence of LCO_2 + MQL spraying position on turning temperature. Reproduced from Ref. [170] with permission from Elsevier.

$scCO_2$-metalworking fluids form	Abbreviation	Oil fraction	CO_2 pressure/MPa
No dissolved lubricant	NDL	None	13
Dissolved lubricant in $scCO_2$	DL	Up to 2%	13
Lubricant expanded with $scCO_2$	XL	15% or greater	6 or 9

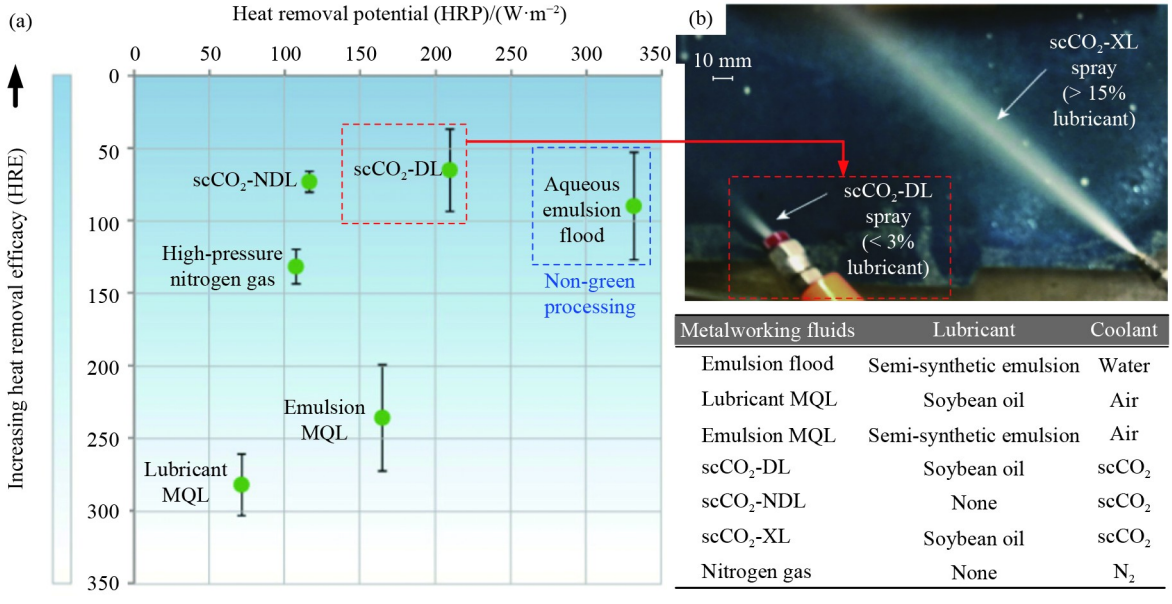

Metalworking fluids	Lubricant	Coolant
Emulsion flood	Semi-synthetic emulsion	Water
Lubricant MQL	Soybean oil	Air
Emulsion MQL	Semi-synthetic emulsion	Air
$scCO_2$-DL	Soybean oil	$scCO_2$
$scCO_2$-NDL	None	$scCO_2$
$scCO_2$-XL	Soybean oil	$scCO_2$
Nitrogen gas	None	N_2

Fig. 31 Comparison of HRP and HRE of $scCO_2$ + MQL: (a) influence of different technologies on cutting heat, (b) atomization effect of different nozzles. Reproduced from Ref. [171] with permission from Elsevier.

tools [175]. Cutting force is affected by many factors, such as material properties, cutting parameters, tool geometry, and cutting environment. The cutting environment mainly includes cooling and lubrication, which has a direct effect on the changing trend of cutting force [176].

The research results of Damir et al. [39] showed that the main cutting and feed forces of LN_2 + MQL are

decreased compared with LN_2 alone, as shown in Fig. 33(a). The main cutting and feed forces of LN_2 (flank) + MQL (rake) decrease with the largest amplitude at 11.1% and 3.8%, respectively. LN_2 is sprayed on the flank face after optimization of the tool holder structure, whereas MQL is still sprayed on the rake face, as shown in Fig. 33(b). Compared with LN_2, the main cutting and feed forces increased by 24.3% and 11.5%, respectively. LN_2 can enter the depth of the cutting zone to improve the cooling effect. Cutting force can be effectively reduced with the lubrication of MQL.

Bagherzadeh and Budak [170] studied the influence of different LCO_2 + MQL supply forms on cutting force when turning Inconel 718. Figure 34 shows that the main cutting force slightly decreases by 0.7%, but feed and thrust force increase by 21.4% and 7.8% after nozzle optimization for LCO_2 alone, respectively. The effect of using LCO_2 + MQL to reduce the main cutting force is better than that of using LCO_2 alone. Compared with single-nozzle outlet, LCO_2 + MQL (rake) and LCO_2 (rake) + MQL (flank) decrease by 4.3% and 6.5%, respectively.

Mehta et al. [177] conducted a comparative study on cutting forces of turning Inconel 718 under the processing environment of LN_2, MQL, LN_2 + MQL, and CA+MQL, as shown in Fig. 35. LN_2 + MQL and CA + MQL can effectively reduce cutting force, and the effect is better than that of cooling or lubrication medium alone. The cutting force reduction of CA + MQL is larger than that of LN_2 + MQL under the same cutting parameters. The main cutting and feed forces decrease by 10% and 30.2%, respectively. This decrease may be due to the considerably higher CA temperature than that of LN_2 and the low hardening degree of material, which is helpful to material removal.

4.3 Tool wear

The effect of cryogenic technology on tool life has been widely studied for more than 10 years. Cryogenic

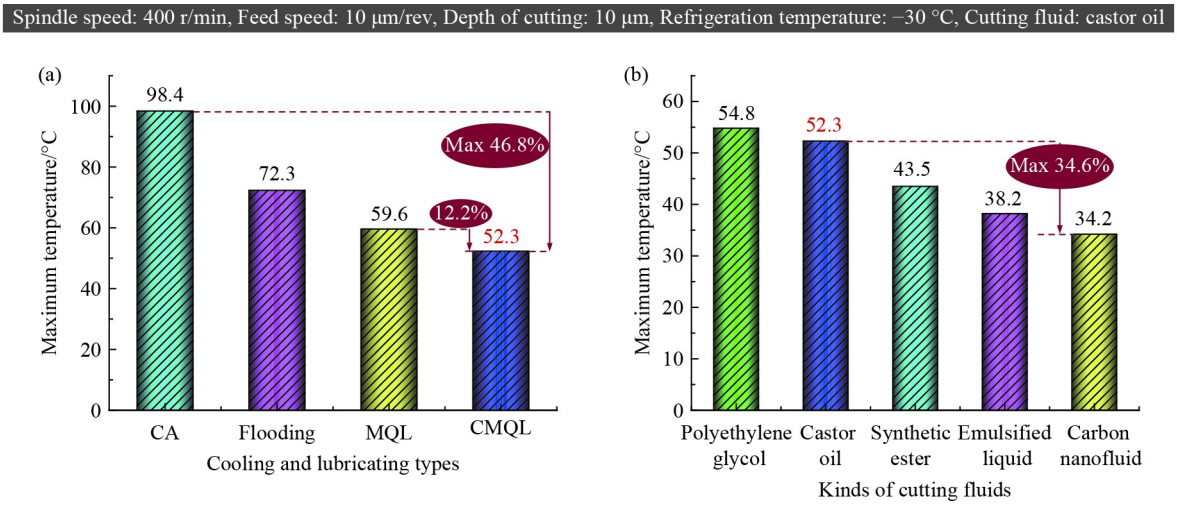

Fig. 32 Effect of CA + MQL with different base oils on cutting temperature: (a) change regulation temperature under different technologies, and (b) change regulation temperature under different kinds of cutting fluids. Reproduced from Ref. [75] with permission from Taylor & Francis.

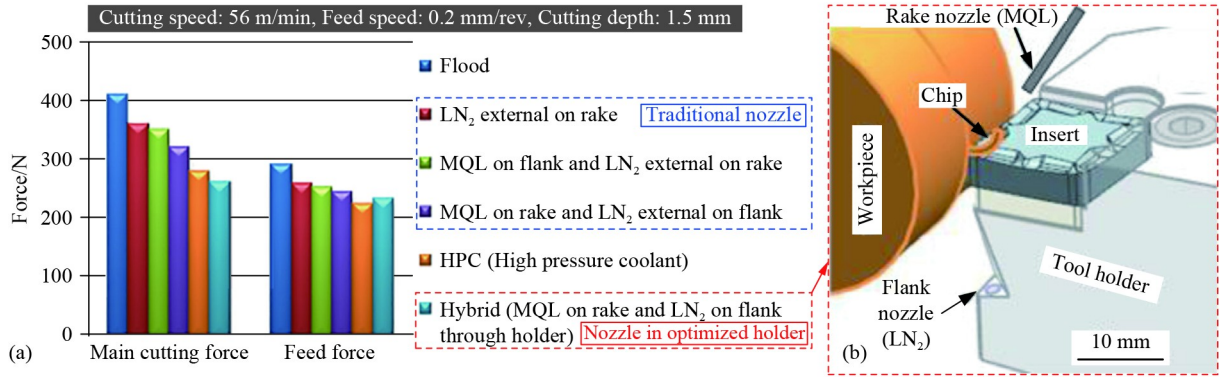

Fig. 33 Influence of LN_2 + MQL spraying position and tool holder structure on cutting force: (a) main cutting forces for different tested cooling methods, and (b) turning setup. Reproduced from Ref. [39] with permission from Elsevier.

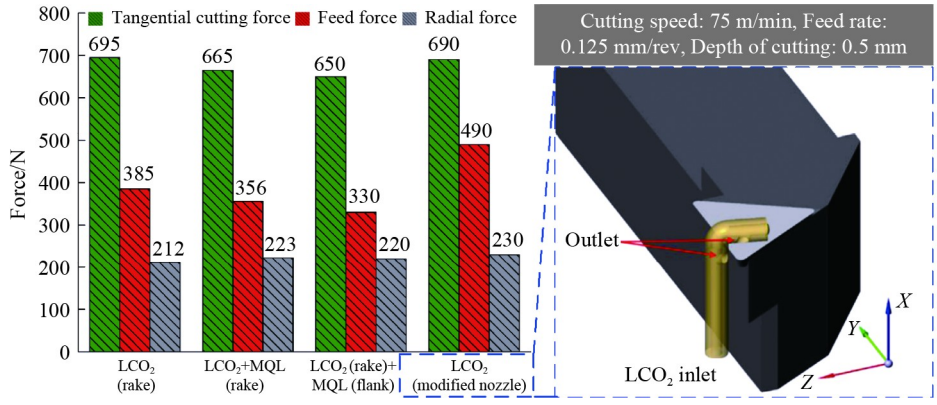

Fig. 34 Influence of LCO_2 + MQL supply form on cutting force. Reproduced from Ref. [170] with permission from Elsevier.

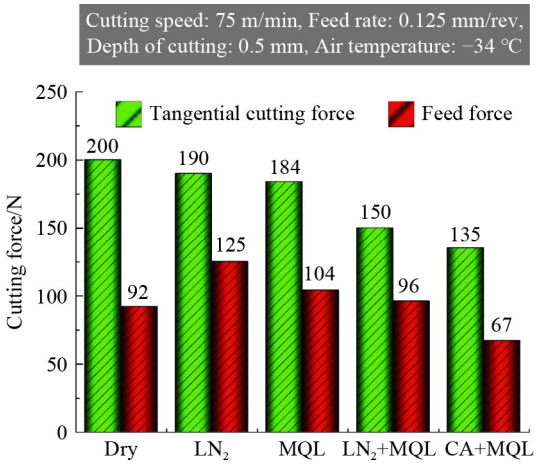

Fig. 35 Comparison of cutting forces under different cooling and lubricating conditions. Reproduced from Ref. [177] with permission from Elsevier.

machining can generally remarkably reduce tool wear [178]. Cryogenic medium can reduce friction coefficient of tool/workpiece interface and inhibit heat transfer [179]. Figures 36(a)–36(c) show that MQL and cryogenic medium (LN_2, LCO_2, and CA, respectively) can effectively reduce tool wear [180,181]. Notably, the effect of LN_2 on reducing tool wear is better than that of LCO_2 when the cutting parameters are the same, as shown in Fig. 36(d). Compared with dry cutting, LN_2 and LCO_2 can reduce the VB value by 22% and 59%, respectively, when the cutting speed is 200 m/min because LN_2 has a stronger capability to inhibit thermal effect than LCO_2. Therefore, a low temperature in the cutting zone is conducive to improving tool life under the same cutting parameters [182,183].

Using CMQL to reduce tool wear is better than using cryogenic medium and MQL alone. Pusavec et al. [67] studied the influence of MQL, LN_2, and LN_2 + MQL on VB value under different cutting parameters. Figure 37 shows that the increase in cutting speed v_c and feed speed v_f results in increased wear. However, tool wear decreases with the increase in a_p. The VB value of LN_2 + MQL is the lowest under different cutting parameters, which proves that LN_2 + MQL can effectively reduce the temperature of the cutting zone and inhibit tool wear.

Compared with pure MQL, the effect of reducing temperature and cutting force is better when MQL with nanoparticles and cryogenic medium are simultaneously used. Figure 38 shows that the wear degree of the flank face under the condition of LN_2 + NMQL (0.5 vol% hBN) is the lowest, VB = 0.12 mm, which is 14.2% lower than LN_2 + MQL, and the effect is better than LN_2, MQL, and NMQL. Furthermore, scanning electron microscope (SEM) reveals that the wear degree of the rake face is the lowest under the condition of LN_2 + NMQL. Only slight BUE and BUL occur, which maintain a good integrity. Serious BUE, BUL, and workpiece material adhesion are observed on the rake face when LN_2, MQL, and NMQL are used individually. A phenomenon of cutting-edge burst crack may even emerge.

Iqbal et al. [186] compared and studied the effects of LN_2 + MQL, LCO_2 + MQL, LN_2, LCO_2, and MQL on tool wear when turning Ti-6Al-4V. Figure 39 shows that the tool wear inhibition at low temperature is considerably stronger than that at MQL. The effect of cryogenic medium combined with MQL can be further improved. The VB value of LN_2 + MQL is the lowest, which is 54.5% lower than that of LCO_2 + MQL, under the same cutting parameters. This finding is due to the substantially lower temperature of LN_2 + MQL than that of LCO_2 + MQL. Therefore, the capability to inhibit thermal softening and chemical reaction of active elements is strong. Tool wear is markedly reduced with the help of MQL lubrication, which also proves the superiority of CMQL.

4.4 Surface quality

CMQL can effectively reduce temperature, cutting force, and tool wear, and then improve the surface quality of the workpiece [121]. Yıldırım et al. [149] studied the influence of MQL, LN_2, and LN_2 + MQL on surface roughness when turning Inconel 625. Figure 40 shows

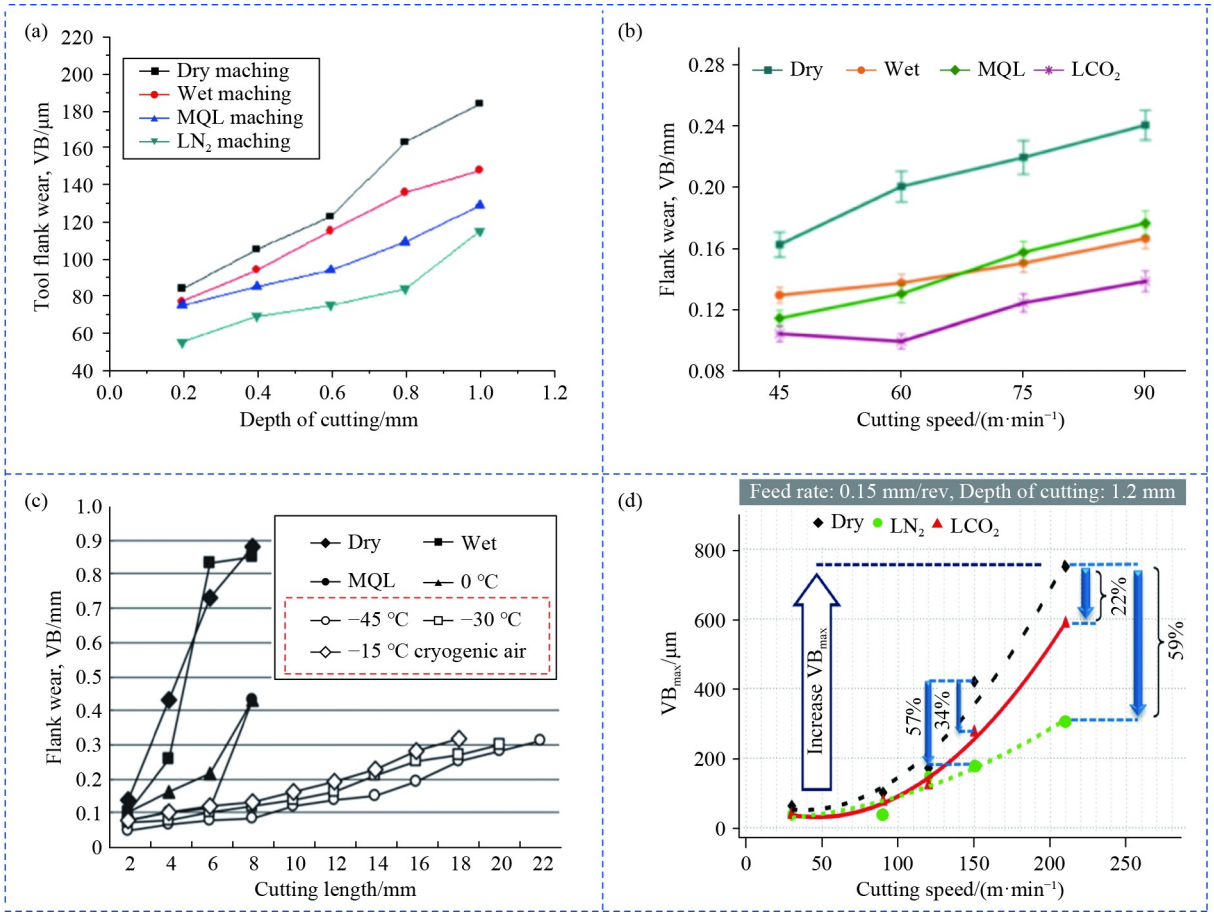

Fig. 36 Effect of cryogenic and MQL on VB value of tool wear: (a) influence on flank wear of LN_2, (b) influence on flank wear of LCO_2, (c) influence on flank wear of CA, and (d) comparison on flank wear between LN_2 and LCO_2. Reproduced from Refs. [88,123,184,185] with permission from Elsevier and Springer Nature.

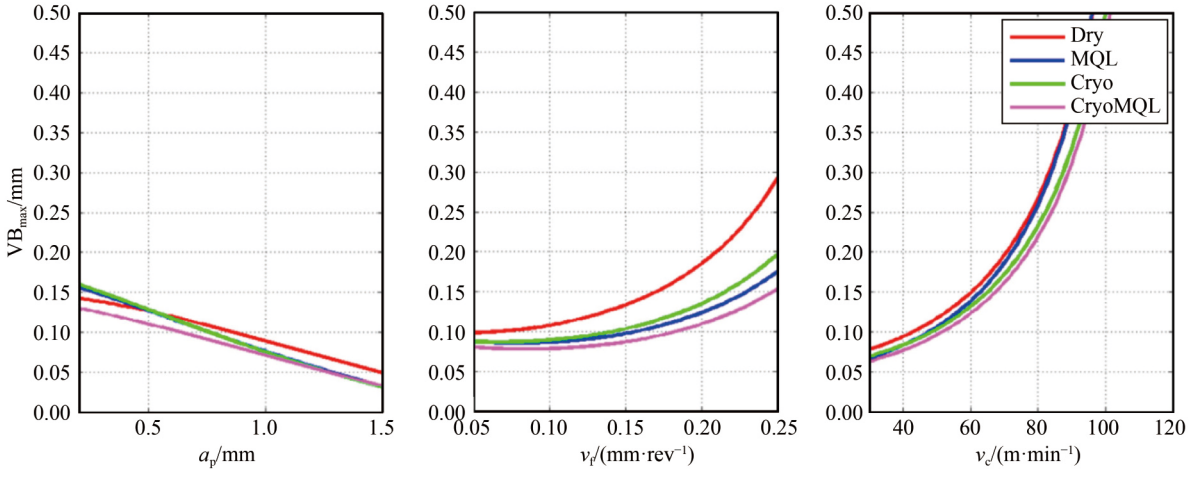

Fig. 37 Influence of cutting process inputs and cooling–lubrication condition on tool wear. Reproduced from Ref. [67] with permission from Elsevier.

that LN_2 + MQL has the best effect of reducing the Ra value under different cutting speeds. Compared with MQL and LN_2, the Ra value of LN_2 + MQL decreases by 22.2% and 28.6% at a cutting speed of 50 m/min, respectively. LN_2 + MQL can also obtain the best surface quality at other cutting speeds. Yıldırım [166] also obtained the same rule when turning Inconel 625 using the same cooling–lubrication method. Furthermore, the

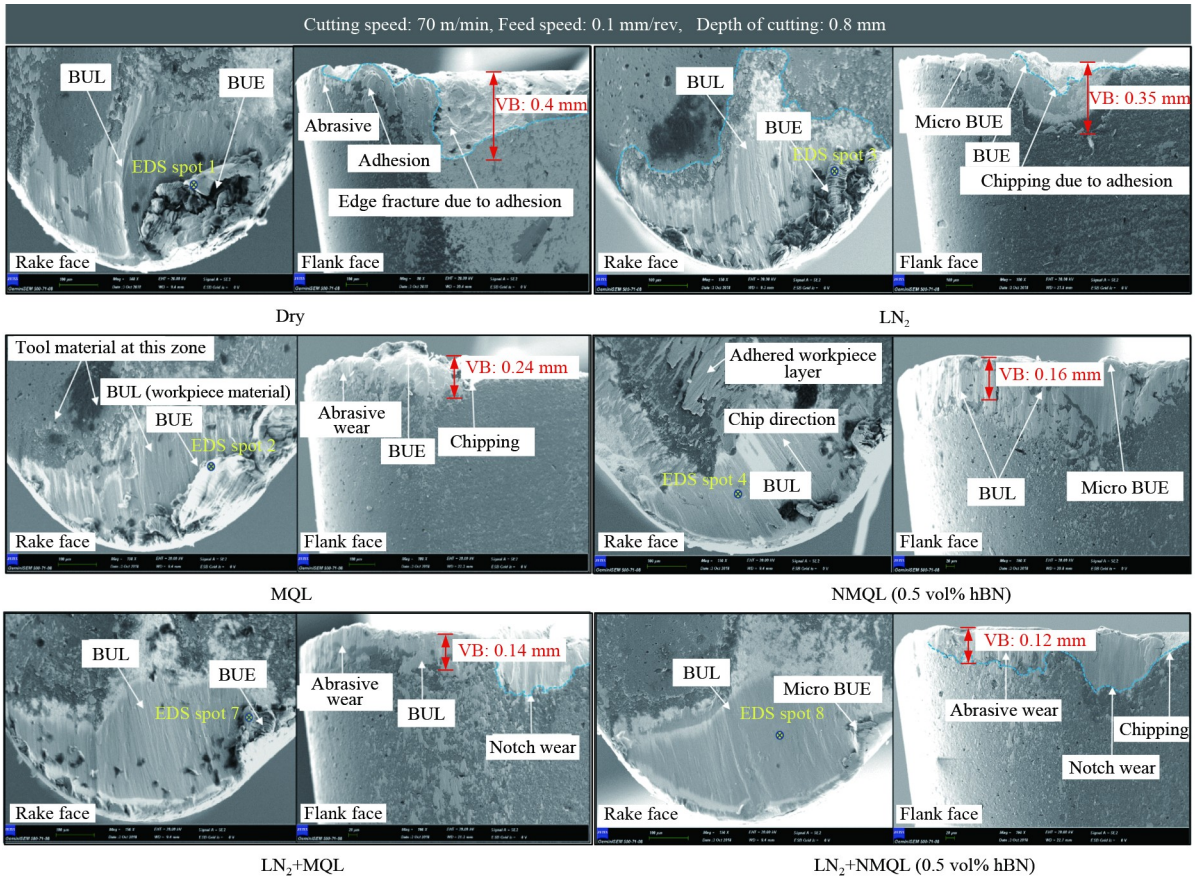

Fig. 38 SEM image of tool wear under different cooling and lubrication conditions. Reproduced from Ref. [166] with permission from Elsevier.

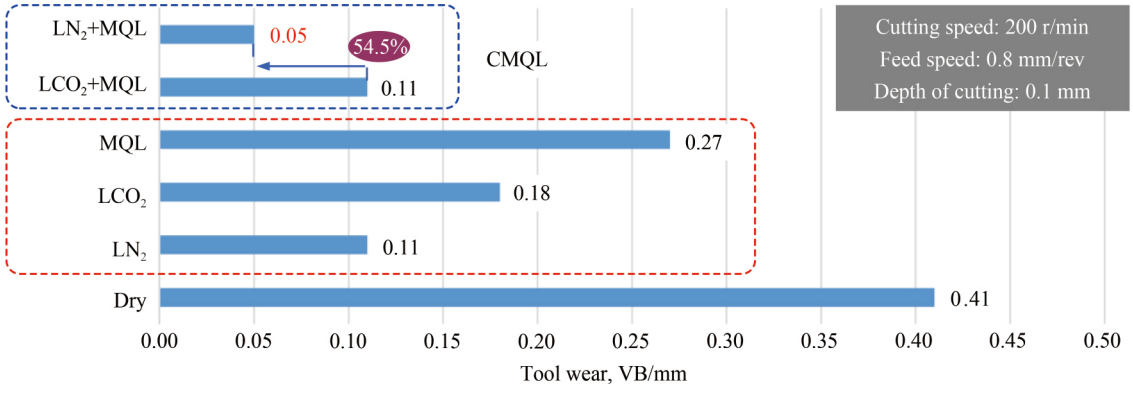

Fig. 39 Comparison of tool wear with different cooling–lubrication regimes [186].

gain effect of LN_2 + MQL (0.5 vol% hBN) on improving surface quality was further explored. Thus, the effect of LN_2 + NMQL is better than that of LN_2 + MQL.

Figure 41 shows that surface quality produced by LCO_2 + MQL is the best, which is 32.8% lower than that produced by LN_2 + MQL [186]. This finding shows that the mechanism of high-efficiency heat dissipation and cutting force reduction of cryogenic medium assisted by micro lubricating oil helps obtain the best surface roughness. However, LN_2 + MQL does not produce a good surface quality possibly due to the limited heat generated by low-speed cutting, and LN_2 produces an excessively low cutting zone temperature, resulting in excessive hardening of workpiece surface.

Su et al. [187] explored the influence of CA and CA + MQL on workpiece surface quality when turning Inconel 718. The Ra value of CA + MQL is the lowest in the entire cutting, which is 26.7% lower than that of CA. Surface quality depends on the cutting accuracy of the tool tip to a large extent. CA + MQL can effectively

reduce the wear of tool tip and improve machining accuracy.

4.5 Application effect of CMQL

Previous research revealed that cryogenic medium or MQL has different effects on turning performance, but CMQL shows advantageous effects, such as superposition through the synergy of two technologies. However, the influence degree of four evaluation parameters has advantages and disadvantages due to different characteristics of different cryogenic media, as shown in Table 3 where CNMQL represents cryogenic nanoparticle minimum quantity lubrication.

Overall, the application of CMQL in turning achieves the ideal cutting performance, and the final effect is better than the single application of cryogenic medium and MQL. However, the application of CMQL can still be further improved.

First, the matching problem between the selection of cryogenic medium and cutting parameters should be addressed. The performance of the lathe reveals the presence of a certain range of temperature, cutting force, and tool wear under specific cutting parameters. For example, a high cutting speed produces additional heat, resulting in large cutting force and tool wear. In this case, cryogenic media with strong cooling capability, such as LN_2, should be selected to reduce the above evaluation index effectively and then obtain the ideal surface quality of the workpiece. On the contrary, if LN_2 is selected for low-speed cutting, then it may cause excessive hardening of the workpiece and increase cutting force and tool wear despite the sharp drop in temperature. Thus, the surface quality will decrease. Therefore, the establishment of the quantitative corresponding relationship through the selection of a reasonable cooling medium and its flow parameters will improve machining quality according to the corresponding evaluation index level of cutting parameters.

Second, the application of nanoparticles should be further investigated. Undoubtedly, adding nanoparticles into micro lubricating oil can effectively improve cutting performance and demonstrates a gain effect. However, if CMQL can obtain the surface quality of workpiece that meets engineering application, then adding nanoparticles will cause waste of resources and increase cost.

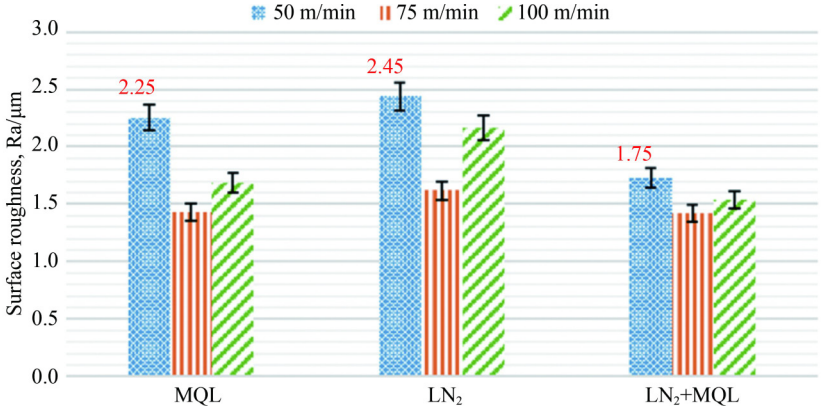

Fig. 40 Effect of cooling–lubrication regimes on surface roughness. Reproduced from Ref. [149] with permission from Elsevier.

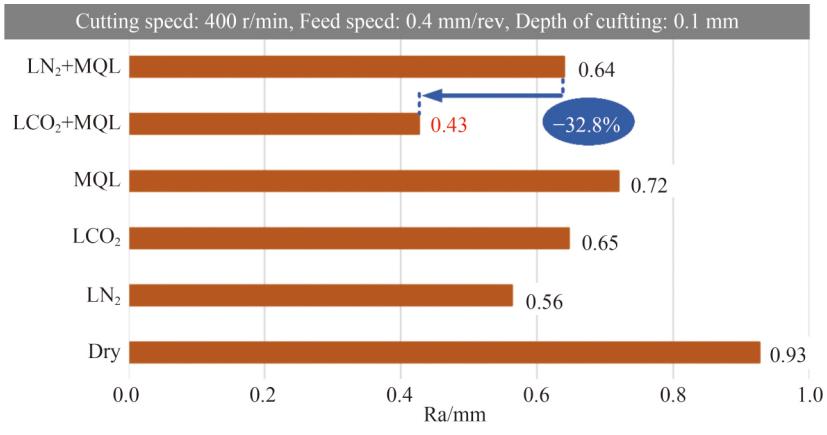

Fig. 41 Comparison of surface quality with different cooling–lubrication regimes [186].

Table 3 Conclusion of processing properties in turning

Evaluation index	Style of CMQL	Conclusions	References
Cutting temperature	LN_2 + MQL (NMQL) LCO_2 + MQL	1) Order of decreasing degree each style: MQL or cryogenic < CMQL < CNMQL; 2) Better effect of application: LN_2 + NMQL (LN_2 with the lowest temperature and NMQL with the best antifriction and antiwear capability).	[156,158]
Cutting force	LN_2 + MQL LCO_2 + MQL CA + MQL	1) Order of decreasing degree each style: MQL or cryogenic < CMQL; 2) Better effect of application in the same cutting parameters: CA + MQL (avoid excessive hardening of material).	[175,188,189]
Tool wear (VB)	LN_2 + MQL (NMQL) LCO_2 + MQL CA + MQL	1) Order of decreasing degree: MQL or cryogenic < CMQL < CNMQL; 2) Better effect of application in the same cutting parameters: (LCO_2 + MQL) < (LN_2 + MQL) (avoid excessive hardening of material).	[74,147,153,166]
Surface integrity (Ra or Rz)	LN_2 + MQL LCO_2 + MQL	1) Order of decreasing degree: MQL or cryogenic < CMQL < CNMQL; 2) Better effect of application: LCO_2 + MQL (with suitable material hardness).	[162,190–192]

Therefore, nanoparticles should be used reasonably in CMQL-assisted processing.

5 Milling performance of CMQL

Milling is a common method of plane machining, which is different from turning because the milling cutter rotates at high speed under the spindle drive while the workpiece remains in a static state. Different from the continuous machining of the single cutting edge of a turning tool, the milling cutter has multiple teeth, and each cutting edge is processed intermittently during high-speed rotation. In addition, the contact length between the cutting edge of the milling cutter and the workpiece is larger than that of the turning tool. The above differences lead to various thermal force changes and tool wear between milling and turning. The effect on the surface quality of the workpiece is also different. CMQL is crucial in milling. However, the supply mode of the cooling–lubrication medium is also different due to the difference between the structure and motion of the milling cutter and turning tool. Such a difference has an influence on milling performance.

5.1 Cutting temperature

Cryogenic medium and MQL alone can effectively reduce the cutting zone temperature in milling, and the mechanism is similar to turning. Correspondingly, CMQL can further improve cooling capability.

In milling high-thermal-conductivity steel, Mulyana et al. [33] found that compared with MQL and $scCO_2$, the cooling effect of $scCO_2$ + MQL is the best, which decreased by 37% and 5% when the pressure was 10.4 MPa, respectively. This finding shows that the cooling capability of $scCO_2$ is effectively combined with the lubricating capability of MQL, which plays a superimposed cooling role. Beyond that, a high pressure can increase jet velocity, which can facilitate penetration of the cooling–lubrication medium in the cutting area and improve cooling capability, as shown in Fig. 42.

An et al. [193] studied the influence of different cooling–lubrication conditions on the temperature of tooltip and workpiece when milling Ti-6Al-4V. Figure 43 shows that the temperature of tooltip and workpiece is positively correlated with cutting speed. The temperature of the tooltip is 50%–60% higher than that of the workpiece under the same milling conditions due to the low thermal conductivity of Ti-6Al-4V. Compared with dry milling, CA, MQL, and CA + MQL can effectively reduce temperature, but the effect is different. Different from Fig. 43, which shows that $scCO_2$ has a better cooling capability than MQL, CA has a worse cooling effect than MQL due to the substantially lower temperature of CA than that of $scCO_2$. Therefore, heat transfer capability is poor, and the cooling range is lower than that of MQL. However, the cooling effect of CA + MQL on tooltip/workpiece is better than that of CA and MQL, which not only reduces tool wear but also ensures the surface quality of the workpiece.

5.2 Cutting force

Park et al. [80] studied the influence of MQL, LN_2, and LN_2 + MQL on milling force in milling Ti-6Al-4V. LN_2 and MQL adopt single-channel external jets. Figure 44 shows that the cutting force of LN_2 is higher than that of MQL when milling speed is 47.7 m/min. This finding is due to the relatively less heat generated by low-speed milling and the excessive hardening of the workpiece due to the ultralow temperature of LN_2, thus complicating material removal. In high-speed milling (76.4 m/min), the penetration of MQL oil mist decreases and the lubrication effect weakens due to the obstruction of high-speed airflow. Moreover, LN_2 can effectively reduce a large amount of heat generated by high-speed milling, providing suitable workpiece hardness for processing [194]. Therefore, the cutting force of LN_2 is lower than that of MQL. LN_2 + MQL obtains the best cutting force

reduction effect under the synergistic effect of cooling and lubrication under high- or low-speed milling, and its performance is better than that of LN_2 and MQL alone.

Pereira et al. [195] studied the influence of MQL, internal or external LCO_2, and LCO_2 (internal) + MQL on tool life when milling Inconel 718. Figure 45 shows that cutting force is remarkably sensitive to the wear degree of milling cutter edge in all cooling strategies and has a positive correlation. The cutting force of flood technology is the smallest but does not meet the requirements of clean production. VB = 0.2 mm is taken as an example. The cutting force of MQL is the largest, which may be due to the failure of lubricating oil film caused by a high temperature, thus causing serious tool wear. Internal or external LCO_2 can effectively cool the cutting zone, which inhibits the adhesion effect of the tool−workpiece interface and reduces tool wear. However, the cutting force of internal LCO_2 is slightly higher than that of external LCO_2 due to the high degree of hardening caused by internal spray. The cutting force of LCO_2 (internal) + MQL is the lowest, which decreased by 2.5% and 7.8% compared with internal LCO_2 and MQL, respectively. This finding is not only due to the effective temperature reduction of LCO_2 but also its maintenance of the normal lubrication effect of the oil film formed by MQL.

Yuan et al. [88] compared and analyzed the influence of CA + MQL at different temperatures on cutting force when milling Ti-6Al-4V. The results show that the cutting force of CA + MQL is lower than that of MQL

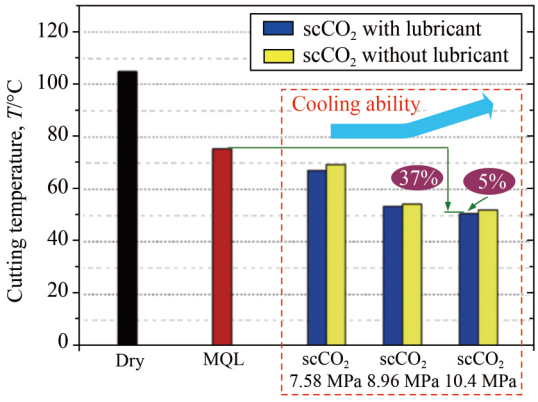

Fig. 42 Result of temperature under various cooling conditions. Reproduced from Ref. [33] with permission from Elsevier.

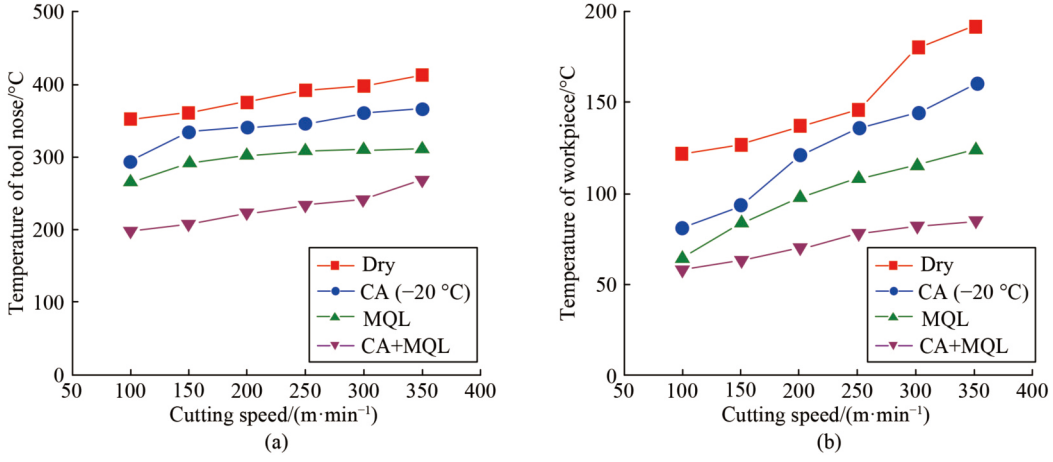

Fig. 43 Variation of milling temperatures with cutting speed under different cooling environments: (a) temperature of tool nose under different methods, (b) temperature of the workpiece under different methods [193].

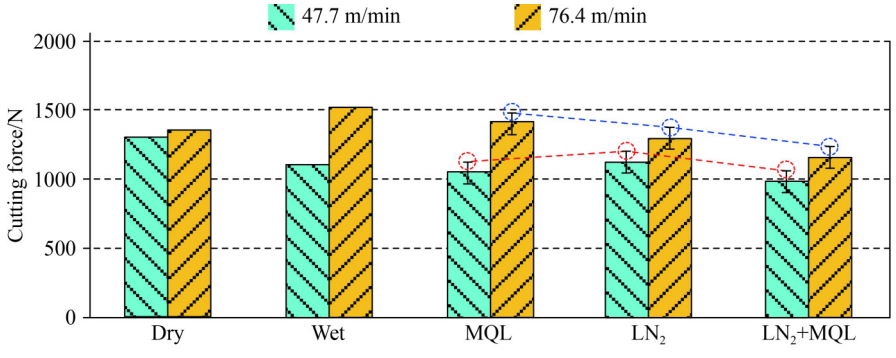

Fig. 44 Effect of cooling–lubrication regimes on cutting force at different cutting velocities. Reproduced from Ref. [80] with permission from Springer Nature.

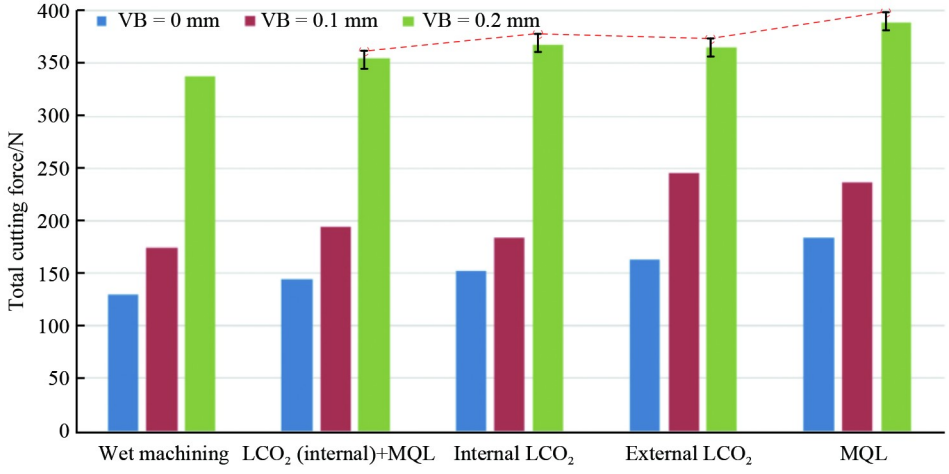

Fig. 45 Total cutting force evolution for different cooling–lubrication techniques at different wear stages. Reproduced from Ref. [195] with permission from Elsevier.

because low temperatures can continuously retain the lubricating oil film in an effective continuous state, which plays a load-bearing role. Moreover, the results reveal that the cutting force of CA + MQL is the lowest when temperature is −15 °C. Compared with MQL, the main cutting, feed, and thrust forces decreased by 13.6%, 10.4%, and 37.5%, respectively. However, cutting force has an upward trend with the decrease in CA + MQL temperature (−30 °C, −45 °C). This trend may be due to the relatively low temperature of low-speed milling and the best cutting hardness of the material at −15 °C. The decrease in temperature leads to an increase in hardening degree and a decrease in cutting performance.

5.3 Tool wear

All types of tools will be worn in cutting regardless of machining environment. The basic law of milling cutter wear is similar to that of turning tool. Severe friction between tool and workpiece during milling causes the wear of tool surface coating layer and exposes the tool matrix. A high temperature induces the chemical reaction of the workpiece material and facilitates welding to the rake face, thus forming chip accumulation. The combination of wear, adhesion, and diffusion wear can lead to tool failure.

The cutting thickness of a high-speed steel milling cutter is smaller than that of a cemented carbide milling cutter, especially in upmilling. The tool teeth squeeze and slide seriously on the workpiece surface; thus, wear mainly occurs on the flank face. The chip sliding speed along the rake face is high due to the high cutting speed of cemented carbide milling cutter. Hence, the rake face is also worn. In addition, the cutter teeth are subjected to repeated mechanical and thermal impacts when cemented carbide milling cutter is used for high-speed milling, resulting in cracks and fatigue damage of cutter teeth. Therefore, in addition to the reasonable selection of milling cutter type and the setting of milling parameters, effective cooling and lubrication to reduce cutting heat and force are crucial.

Shokrani and Newman [196] studied the influence of MQL, LN_2, and LN_2 + MQL on tool life and wear degree in milling Inconel 718. Figure 46(a) shows that the tool life of LN_2 is 30.3% lower than that of MQL. High temperature is not the only reason for tool failure. Although LN_2 can effectively reduce the temperature, its cryogenic hardening and lack of lubrication lead to high cutting force and changes in cutting edge geometry. Figure 46(b) shows the supply form of LN_2 and MQL. The high-speed rotating airflow field of the milling cutter hinders the LN_2 jet and influences the cooling effect. Two groups of MQL can improve the effective permeability of droplets and enhance lubricating capability. The combination of LN_2 and MQL plays a role of superposition and promotion, effectively inhibiting tool−workpiece interface adhesion and friction. Compared with MQL and LN_2, tool life is increased by 44.8% and 61.5%, respectively. Figure 46(c) shows that all cooling–lubrication strategies have different degrees of tool wear, but LN_2 + MQL has the strongest inhibition effect. This finding is also similar to that of Kaynak [155]. Using LN_2 + MQL will not change the mechanism of tool failure but can slow down wear [197].

The structure of the milling cutter and its tool holder is completely different from that of the turning tool. The milling cutter rotates at a high speed in machining; thus, spraying the cooling–lubrication medium on each tool face as in turning is impossible [198]. Therefore, in addition to the conventional external nozzle, the internal jet mode of the milling cutter has become the mainstream to improve the effective permeability and coverage of the cooling–lubrication medium to the tool−workpiece.

Pereira et al. [195] studied the influence of MQL, internal or external LCO_2, and LCO_2 + MQL on tool life in milling Inconel 718 (based on the criterion of tool wear

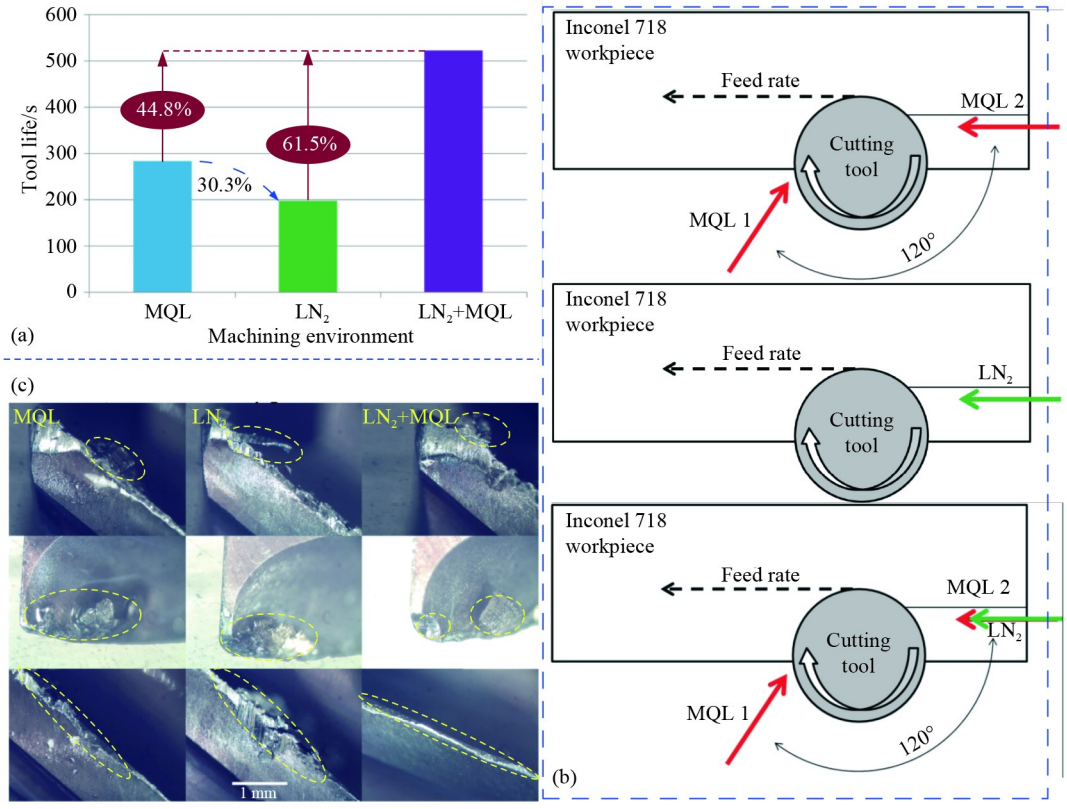

Fig. 46 Influence of different cooling–lubrication strategies and feeding modes on tool wear and life: (a) tool life graph for each machining environment, (b) arrangement of nozzles with different combinations, and (c) micro graphs of cutting tools. Reproduced from Ref. [196] with permission from Elsevier.

VB = 0.2 mm). Figure 47(a) shows that the tool life of external LCO_2 is the shortest because of the difficulty of LCO_2 in penetrating the cutting zone effectively due to intermittent high-speed milling. Internal LCO_2 can effectively penetrate; hence, tool life is increased by 16.2%. The mechanical effect remains serious despite the effective reduction of thermal effect by internal/external LCO_2. MQL has a limited cooling capability but can substantially reduce the severe friction between tool and workpiece; thus, tool life is 26.8% higher than that of internal LCO_2. Compared with internal LCO_2 and MQL, the tool life of LCO_2 (internal) + MQL is increased by 36.3% and 52.9%, respectively, due to the superposition effect of LCO_2 cooling and MQL lubrication. The wear evolution of cutting edge under different cooling–lubrication strategies (1–4) in Fig. 47(b) also effectively verifies the above conclusion.

5.4 Surface quality

Shokrani and Newman [196] studied the effects of LN_2, MQL, and LN_2 +MQL on the surface quality of Inconel 718 in end-milling. The machining surface produced in end-milling is divided into two parts: bottom and wall faces. Figure 48 shows that the Ra value of the wall face is considerably higher than that of the bottom face under different cooling–lubrication strategies. This phenomenon is due to the substantially larger contact area between the milling cutter and wall faces than that of the bottom face. Consequently, the friction range is large, and additional heat is generated. A high temperature may lead to the failure of micro lubricating oil, and LN_2 can effectively reduce the temperature, which can inhibit the adhesion. Therefore, an improved surface roughness can be obtained. However, LN_2 + MQL does not produce the optimal machined surface possibly due to the decrease in flow rate of the coolant supply. Minimal heat is generated for the bottom face. MQL satisfies the requirements of effective cooling and lubrication. However, the ultralow temperature of LN_2 may cause excessive workpiece hardening and decrease cutting performance; thus, the Ra value is higher than that of MQL. The Ra value of LN_2 + MQL is the smallest due to the effective superposition of LN_2 cooling and MQL lubrication. This result also proves that CMQL helps milling obtain the best surface quality.

Yuan et al. [199] studied the influence of oil-on-water (Oow), $scCO_2$, $scCO_2$ + MQL, and $scCO_2$ + Oow on surface quality when end-milling 316L stainless steel. Oil molecules are adsorbed on the interface of water molecules due to expansion after the mixture of oil- and water-based cutting fluid, and then Oow droplets are formed. The surface roughness of $scCO_2$ + MQL and

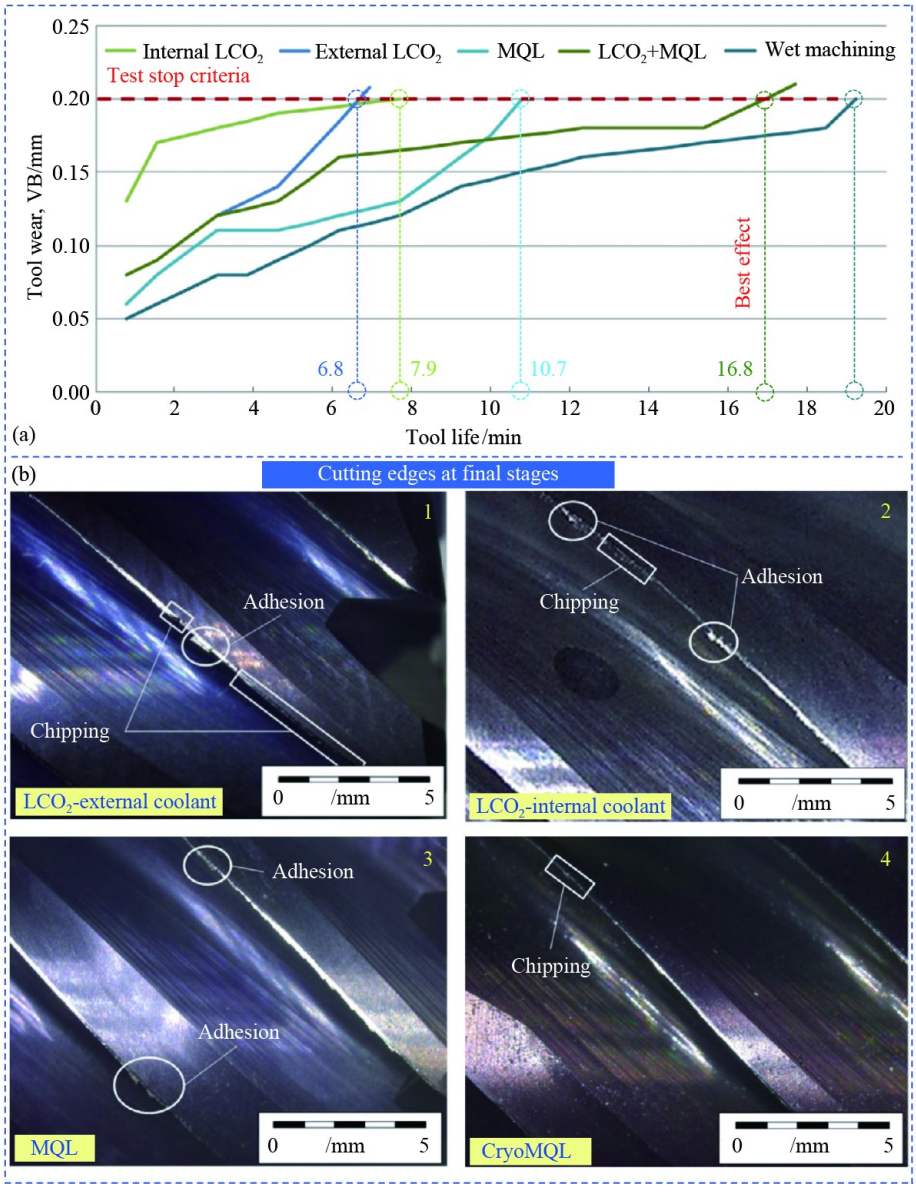

Fig. 47 Tool wear and life evolution rule under different cooling–lubrication strategies: (a) tool wear evolution, and (b) cutting edges at final stages. Reproduced from Ref. [195] with permission from Elsevier.

$scCO_2$ + Oow at different cutting speeds is lower than that of Oow and $scCO_2$ alone. In addition, Yuan found that $scCO_2$ + MQL and $scCO_2$ + Oow are suitable for low- and high-speed milling, respectively, and Ra value decreased substantially.

Pušavec et al. [200] studied the influence of LCO_2 (internal), LCO_2 + MQL, and LCO_2 + NMQL on the surface quality of 42CrMo4 workpiece in end-milling under different cutting parameters. Figure 49 shows a negative correlation between the friction coefficient of the workpiece surface and milling speed in different processing environments. Compared with dry cutting, friction coefficient increases when LCO_2 is used alone because LCO_2 has no lubrication effect. However, friction coefficient substantially decreases when LCO_2 is combined with MQL (or NMQL). This reduction is due to the formation of a solid oil film by lubricating oil under a low temperature, which blocks friction between tool and workpiece. LCO_2 can harden the workpiece to a certain extent and restrain the plastic accumulation and thermal damage of surface materials. In addition, the effect of LCO_2 + NMQL on improving the surface quality of the workpiece is better than that of LCO_2 + MQL, which benefits from the excellent properties of antiwear/antifriction of MoS_2 nanoparticles. Sterle et al. [201] reached the same conclusion through research.

5.5 Application effect of CMQL

The above discussion reveals that CMQL also obtains a

better cutting performance than cryogenic medium and MQL alone under different milling conditions. This finding is the same as the law obtained by turning. The influence of CMQL characteristics (such as temperature and supply mode) on the evaluation indices is shown in Table 4.

Overall, CMQL application in milling also achieves an ideal cutting performance. Similar to turning, milling has the problems of cryogenic medium matching and nanoparticle selectivity. Internal jet supply has gradually become the mainstream based on the particularity of milling equipment, such as the structure and movement form of cutter and tool holder. However, the current situation is that the cryogenic medium is directly sprayed into the cutting zone, which cannot be recycled. This phenomenon undoubtedly increases energy consumption and production costs for engineering applications. Cryogenic milling by internal circulation tool with cryogenic medium may solve the problem of energy and resource consumption, but this method is mainly suitable

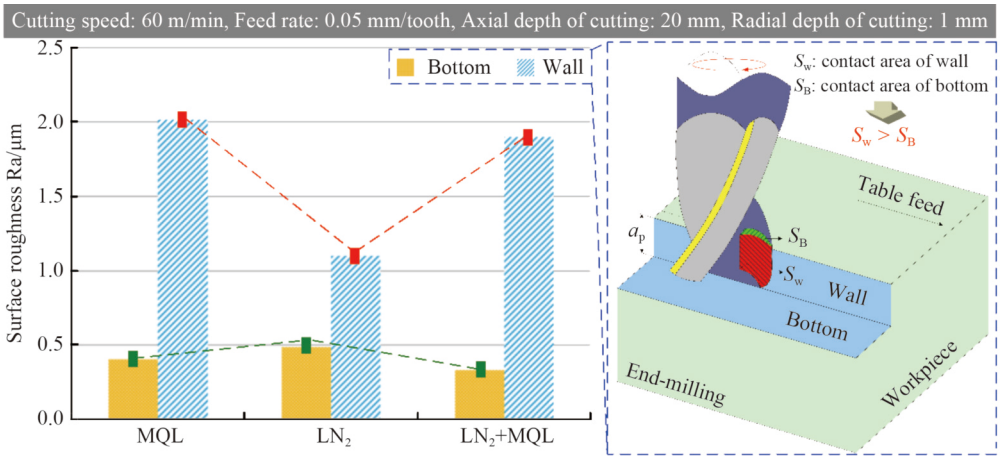

Fig. 48 Average surface roughness results for each machining environment. Reproduced from Ref. [196] with permission from Elsevier.

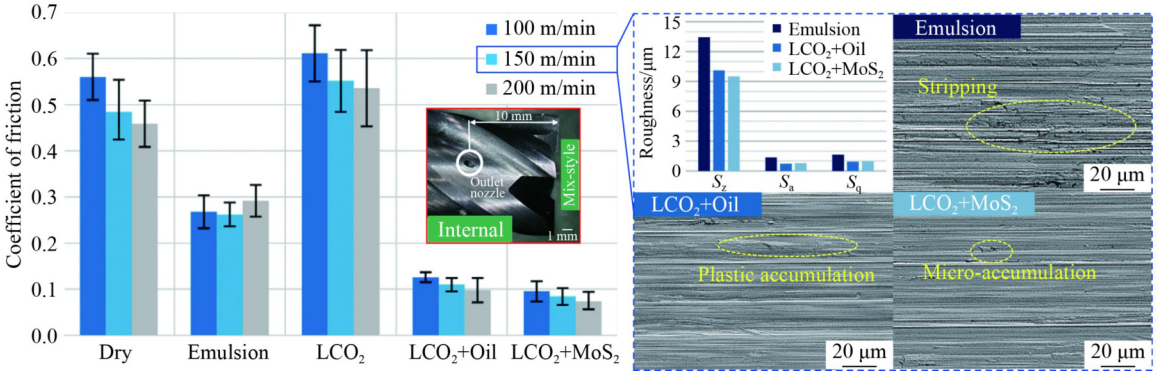

Fig. 49 Surface topography and average surface roughness. MoS_2: molybdenum disulfide. Reproduced from Ref. [200] with permission from Elsevier.

Table 4 Conclusion of processing properties in milling

Evaluation index	Style of CMQL	Conclusions	References
Cutting temperature	LN_2 + MQL $scCO_2$ + MQL	1) Order of decreasing degree for each style: MQL or cryogenic < CMQL; 2) Low temperature of cryogenic medium results in an enhanced cooling effect.	[33,202,203]
Cutting force	LN_2 + MQL LCO_2 + MQL CA + MQL	1) Order of decreasing degree for each style: MQL or cryogenic < CMQL; 2) Low temperature of cryogenic medium is suitable for high cutting speed.	[194,202,204]
Tool wear (VB)	LN_2 + MQL LCO_2 + MQL CA + MQL	1) Order of decreasing degree: MQL or cryogenic < CMQL; 2) Improved effect of cryogenic medium supplying form: external < internal (with enhanced permeability).	[58,83,205,206]
Surface integrity (Ra or Rz)	LN_2 + MQL LCO_2 + MQL (NMQL) $scCO_2$ + MQL	Order of decreasing degree: MQL or cryogenic < CMQL < CNMQL (NMQL with the best antifriction and antiwear capabilities)	[52,201,206,207]

for end-mills. LN_2 is used to circulate in the internal spiral channel of a certain diameter milling cutter, and the milling cutter is maintained in the cryogenic range of −100 °C to −140 °C by phase change heat absorption to transfer the heat in the cutting zone quickly and reduce workpiece temperature. The internal circulation cryogenic technology introduces remarkably high requirements for the milling cutter manufacturing, tool holder thermal insulation technology, and pressure supply system.

6 Grinding performance of CMQL

Grinding is an important part of modern precision machining. The contact area of the grinding wheel and workpiece is substantially larger than that of turning and milling, and is mainly characterized by its abrasive cutting with negative rake angle, severe friction, and high specific energy. Thus, a high temperature is observed in the grinding zone, and most of the heat flows into the workpiece [208]. Therefore, avoiding thermal damage of workpiece materials through effective cooling and lubrication is crucial to ensure machining accuracy [209]. MQL (or NMQL) has been used in grinding, especially for aluminum alloy, which has played a good role in reducing wear and cooling [210]. However, the cooling effect of MQL (or NMQL) is limited to difficult-to-cut materials. Cryogenic medium has also been used in grinding to reduce grinding heat effectively [211,212].

Paul et al. [213] analyzed the surface cracks of high-carbon steel in different grinding environments. The uneven distribution of temperature field in dry grinding results in stress gradient and cracks. The tendency of crack formation decreases in wet grinding, and the crack disappears when LN_2 cools. This phenomenon is mainly due to LN_2, which can effectively cool down and reduce the stress gradient. In addition, burning the surface of difficult-to-cut materials is easy during dry grinding, which can be effectively avoided by LN_2. The grinding of AISI304 revealed that LN_2 cooling is beneficial to reducing residual tensile stress and surface roughness [214,215]. Manimaran et al. [105] found that LN_2 can effectively reduce grinding force and specific energy, which decreased by 37% and 50%, respectively, compared with dry grinding. This reduction is due to the low temperature, which can effectively reduce the adhesion of debris to abrasive particles. The mechanical strength of the abrasive grains is improved, and the abrasive grains are kept intact and sharp. However, LN_2 lacks lubrication, and the improvement of surface quality is limited. Reddy and Ghosh [216] showed that the Ra value of MQL decreased by 39.8% compared with LN_2 when grinding AISI 51200 with the same machining parameters. The application effect of LCO_2 [106,146] and CA [217] in grinding also conforms to the above rules. However, several shortcomings are still observed in the separate application of cryogenic medium and MQL. The combination of the two technologies can achieve complementary advantages and provide a superimposed cooling–lubrication effect.

6.1 Grinding temperature

An et al. [218] studied the effect of CA and CA + MQL on grinding temperature of Ti-6Al-4V with different cutting depths. The temperature of the grinding zone increases to more than 400 °C with the increase in cutting depth, resulting in film boiling of cutting fluid and loss of heat transfer capability. The oil mist of CA + MQL penetrates the air barrier layer near the grinding wheel at high speed and forms lubricating oil film on the surface of the grinding wheel and workpiece, which reduces the generation of grinding heat. CA can further reduce the grinding temperature by strengthening heat transfer. The cooling amplitude of CA + MQL is 23.2% higher than that of CA with a prominent cooling effect.

Zhang et al. [219] added Al_2O_3 nanoparticles into the basis of MQL and analyzed the influence of NMQL, CA, and CA + NMQL on the surface temperature of the workpiece during grinding Ti-6Al-4V by numerical simulation. CA and MQL are supplied into the grinding zone through their respective pipelines. Figure 50(a) shows the evolution of the heat source temperature field in the grinding zone. Heat is concentrated in the grinding wheel/workpiece contact area due to the low thermal conductivity of Ti-6Al-4V. Figure 50(b) shows that grinding zone temperature is the lowest under CA + MQL, which is 26.8% and 20.5% lower than CA and NMQL, respectively. In addition, Zhang et al. [56] found that increasing the flow rate of CA can accelerate heat transfer and reduce grinding heat.

6.2 Specific grinding force

In grinding, the force between the grinding wheel and workpiece is characterized by unit grinding force, which is called specific grinding force.

Zhang et al. [219] compared and analyzed the effects of NMQL, CA, and CA + NMQL on the grinding force during grinding of Ti-6Al-4V. Figure 51(a) shows that the grinding force of CA is higher than that of NMQL. CA can restrain the thermal softening of the workpiece and reduce grinding force to a certain extent. However, the Al_2O_3 nanoparticles added in micro lubricating oil can easily enter the grinding wheel−workpiece interface due to their micro size effect and high surface energy. These nanoparticles can fill the furrow on the workpiece surface, as shown in Fig. 51(b), and provide an excellent antiwear effect [220]. The cooling–lubrication effect can be effectively superimposed after the combination of CA and NMQL, which has a gain effect on reducing specific grinding force. Therefore, the minimum specific

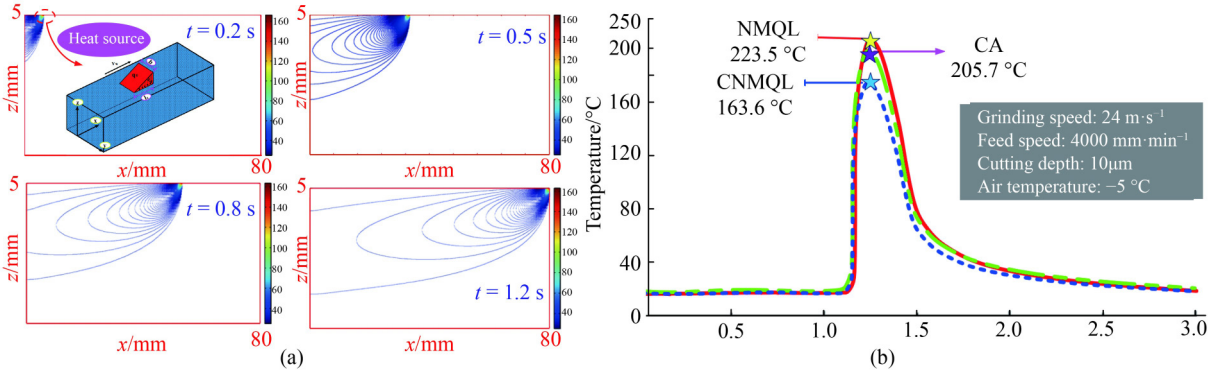

Fig. 50 Heat source movement law and comparison of cooling effect under different methods: (a) simulation grinding phase diagram, and (b) theoretical result of grinding temperature. Reproduced from Ref. [219] with permission from Springer Nature.

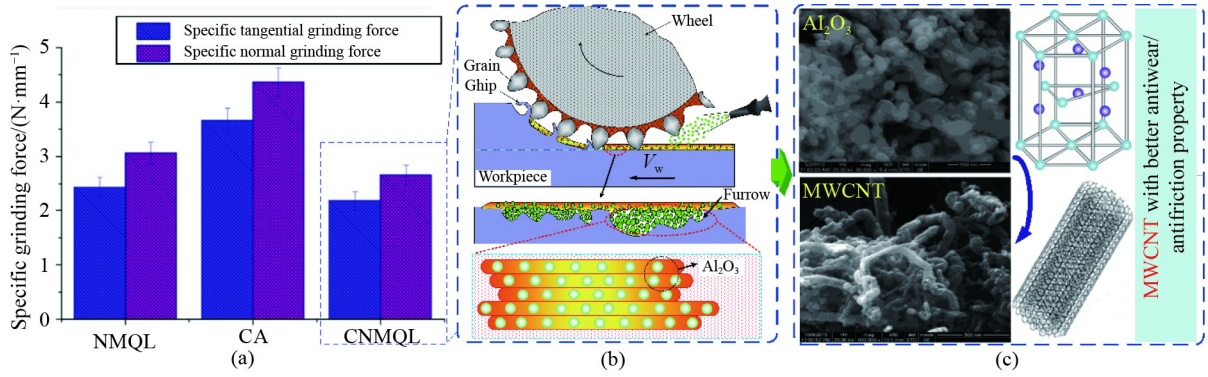

Fig. 51 Effect of nanoparticles on specific grinding forces: (a) specific grinding force under different cooling conditions, (b) nanoparticle distribution in the grinding zone, and (c) different micro structures of Al_2O_3 and MWCNT. Reproduced from Ref. [219] with permission from Springer Nature.

tangential and normal grinding forces are 2.17 and 2.66 N/mm, respectively.

Paul et al. [93] compared the effects of Al_2O_3 and multiwalled carbon nanotube (MWCNT) on grinding force. The structural characteristics of the two nanoparticles are shown in Fig. 51(c). The results reveal that MWCNT has the lowest specific tangential and normal grinding forces due to the stable structure, high specific strength, and high thermal conductivity of MWCNT [221]. MWCNT not only considerably improves heat transfer capacity but can also effectively reduce friction, demonstrating an enhanced cooling–lubrication effect. The sharpness and cutting performance of abrasive grains are also maintained [222].

6.3 Specific grinding energy

Energy consumption varies with different material removal methods. Specific grinding energy refers to the energy required to remove the unit volume of material, which can characterize the lubrication effect of the grinding wheel/workpiece interface [223]. A small specific grinding energy produces an improved lubrication effect and grinding performance.

Zhang et al. [224] compared and analyzed the effects of NMQL, CA, and CA + NMQL on grinding energy. The results show that the specific grinding energy of CA + NMQL is the smallest under similar process parameters. This similarity is due to the cooling–lubricating capability of CA + NMQL, which maintains a sharp abrasive cutting edge for a long time. This condition not only improves material removal rate but also effectively maintains a low grinding force. Compared with CA + NMQL, the grinding energy obtained by NMQL and CA can be increased by 12.3% and 33.1%, respectively.

The research of Garcia et al. [106] shows that compared with the traditional cooling–lubrication method, grinding specific energy can be markedly reduced by using LCO_2 + MQL. The specific energy of grinding depends on the intensity of friction between grinding wheel and workpiece. LCO_2 + MQL can form a solidified oil film on the surface of the grinding wheel, which can play a role in continuous cooling and lubrication, as shown in Fig. 52(a). In addition, the flow rate Q of LCO_2 + MQL has a direct effect on grinding specific energy, as shown in Fig. 52(b). When Q = 3 mL/min, the thickness of oil film on the grinding wheel surface is insufficient, which leads to high passivation speed of abrasive particles and a decrease in cutting capability. When Q = 15 mL/min, grinding specific energy substantially decreases, which

indicates that the solidified oil film can play a continuous lubrication role. The grinding wheel can maintain high material removal capability with a low energy consumption.

6.4 Surface quality

Stachurski et al. [225] studied the influence of MQL, CA, and CA + MQL on surface quality in grinding hob. Figure 53 shows that the surface roughness Rz of CA is substantially higher than that of other cooling–lubrication methods. CA can inhibit thermal softening of workpiece; however, it has no lubrication effect, and the improvement of surface quality is limited. MQL can reduce severe friction between grinding wheel and workpiece, and then decrease Rz effectively. CA + MQL can further improve surface quality. The Rz value decreases by 30.5% compared with MQL when cutting depth is 0.03 mm due to the superposition effect of the cooling–lubricating capability of CA and MQL [226].

Zhang et al. [227] compared the effects of dry, flood, CA + MQL, and CA + NMQL (MoS_2) on surface profile and workpiece roughness when grinding GCr15. Figure 54 shows that the surface morphology of CA + NMQL is the best. The surface profile curve, texture density, wave crest, and valley are the most uniform, indicating that the degree of material accumulation and adhesion is low. This finding is consistent with the results of SEM. The binding force between Mo and S atoms is strong for MoS_2, whereas that between molecular layers is weak. The molecular layer breaks and forms a slip surface when subjected to shear force, which determines that MoS_2 has certain looseness and ductility [228]. Part of MoS_2 reacts chemically and then spreads into the composite film under the action of grinding force. Furthermore, MoS_2 with a good surface activity is continuously adsorbed on the composite film, which not only effectively reduces the wear but also plays a role in repair. Therefore, CA +

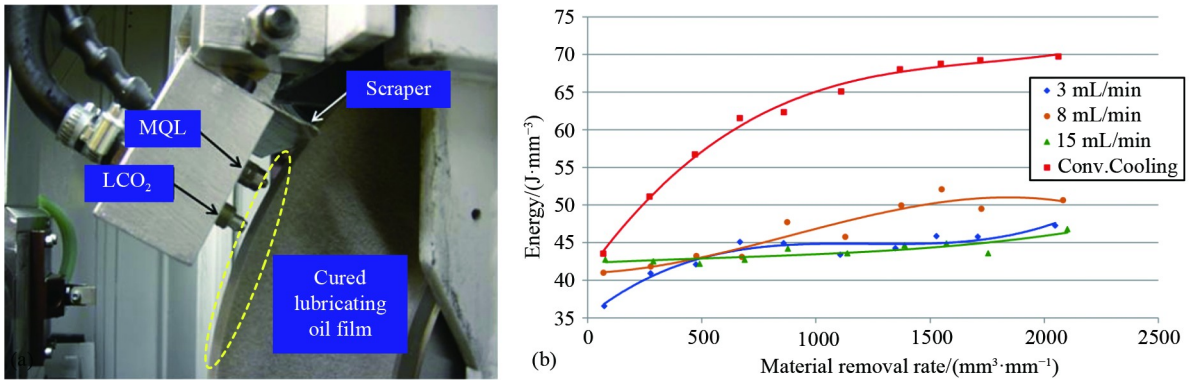

Fig. 52 Influence of LCO_2 + MQL and its flow rate on grinding specific energy: (a) setup of tooling for efficient application of LCO_2 + MQL, and (b) relation between pressure and CO_2 flow rate. Reproduced from Ref. [106] with permission from Elsevier.

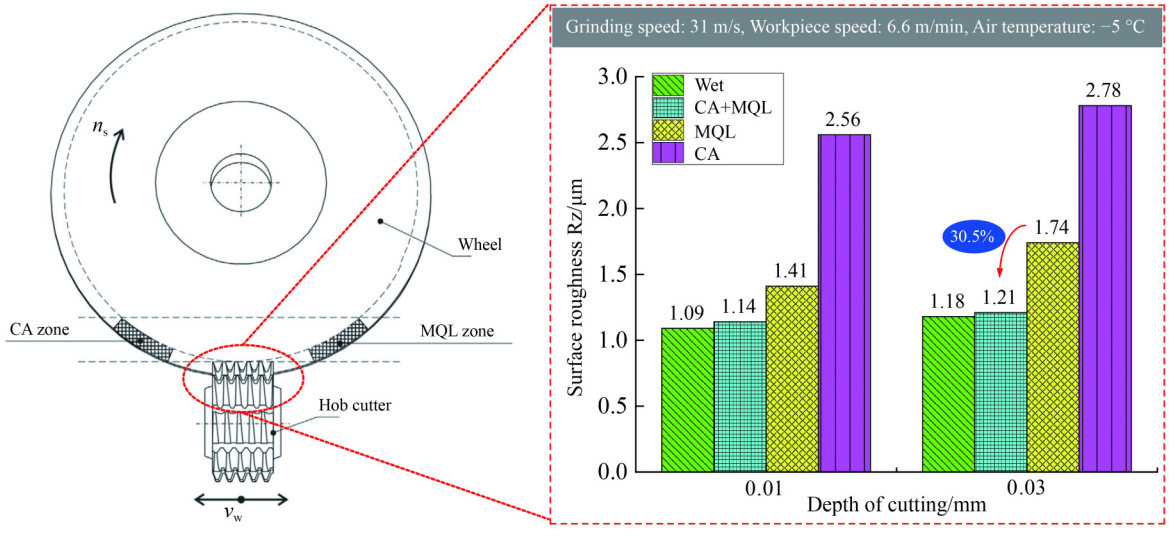

Fig. 53 Surface roughness parameter Rz of rake face with different methods of cutting fluid delivery. Reproduced from Ref. [225] with permission from Elsevier.

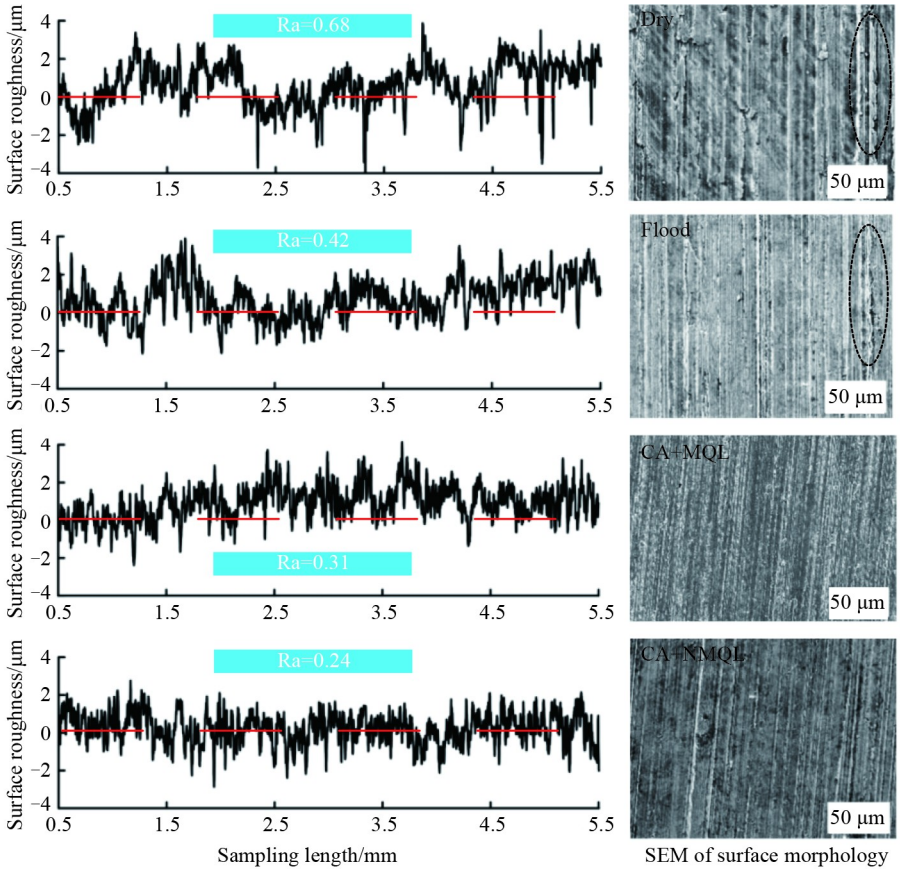

Fig. 54 Surface morphologies of workpiece under different lubrication conditions. Reproduced from Ref. [227] with permission from China Mechanical Engineering.

NMQL can improve surface quality.

6.5 Application effect of CMQL

To date, CMQL is seldom used in grinding. CA is the main cryogenic medium, whereas LN_2 and LCO_2 are seldom used. For several types of grinding wheel, such as corundum or silicon carbide wheel, the low temperature of LN_2 or LCO_2 produces excessively hard and brittle abrasive grains, resulting in batch fracture under the action of grinding force. This phenomenon seriously affects grinding accuracy. This situation is weakened for diamond or cubic boron nitride grinding wheel. The cooling–lubrication effect of CA + MQL is similar to that of turning and milling in grinding. However, heat generated by the same workpiece material is far more than turning and milling due to the particularity of the grinding wheel. Moreover, the temperature of CA is limited, and CA + MQL may cause insufficient cooling when grinding difficult-to-cut materials. Therefore, adding nanoparticles into micro lubricating oil will become an effective way to improve grinding performance based on high thermal conductivity and antiwear properties of nanoparticles with different structures. However, effectively matching grinding parameters with the type of nanoparticles is also necessary to achieve the best effect.

7 Conclusions

Aiming at the problem of high thermal–mechanical coupling damage in the cutting of titanium alloy, nickel-based alloy, and other difficult-to-cut materials, the application forms of CMQL device in different machining methods and the mechanism of CMQL are systematically introduced in this paper. The research progress of application performance of CMQL in turning, milling, and grinding in recent years is reviewed. The main findings are as follows.

(1) For turning, the external spray type is a common supply form of the cooling–lubrication medium based on the block structure of the turning tool. Increasing the number of nozzles and improving their position help increase the coverage area of the medium on the turning tool surface. The cooling medium can be directly transported to the rake and flank face through the internal channel by improving the structure of the tool holder. This condition can further improve coverage and permeability. For milling, the cooling–lubrication

medium is supplied through the inner channel of the milling cutter based on the cylindrical structure and rotary motion characteristics of the milling cutter and tool holder. This condition is conducive to direct spraying into the cutting zone and effectively avoids the obstruction of a high-speed rotary airflow field. Furthermore, the solubility of LCO_2 (or $scCO_2$) to lubricating oil is conducive to the internal jet mode after mixing, which is especially suitable for milling. For grinding, the cooling–lubrication medium is sprayed on the surface of the grinding wheel to form a solid lubricating oil film due to the special structure and geometric relationship of the grinding wheel and workpiece. This medium is then carried into the friction interface by the high-speed rotating wheel.

(2) The cooling–lubrication mechanism of CMQL is complex and different. Compared with MQL, CMQL can effectively reduce cutting temperature. Simultaneously, CMQL can increase viscosity of lubricating oil, and the thickness of oil film can maintain the complete separation of the tool−workpiece interface. Carrying capacity is also improved. Compared with cryogenic technology, CMQL has an excellent lubricating capability. The cooling and lubrication capabilities of CMQL are coupled and synergetic, which can effectively reduce cutting force by restraining thermal softening to provide suitable workpiece hardness for material removal. The decrease in thermal–mechanical level not only slows down tool wear but also helps obtain the ideal surface quality of the workpiece.

(3) The machining of difficult-to-cut materials is facing severe challenges of high thermal–mechanical damage. The application of CMQL in turning, milling, and grinding can reduce cutting temperature, cutting force, and tool wear, and improve the surface quality of the workpiece. The application of cooling or lubricating medium alone under different cutting parameters may produce either an increasing or decreasing effect on cutting performance. However, at the same parameter level, the application effect of CMQL is remarkably better than that of cryogenic technology or MQL based on the synergetic-superposed effect, which plays a positive role in restraining tool failure and surface burn. Therefore, the surface quality of the workpiece is considerably improved.

The promotion of engineering application and development of CMQL technology requires joint efforts of the entire world. Thus, this paper aims to provide theoretical basis and technical support for researchers to study the green, clean processing of aerospace refractory materials.

8 Prospects

In recent years, the key technology of CMQL has achieved remarkable results in the cutting field of aerospace difficult-to-cut materials, and the number of literature on the application of CMQL is increasing. However, several limitations still exist. The previous systematic review indicates that future research directions may focus on the following topics.

(1) Design and improvement of lubricating oil suitable for cryogenic environment

Biodegradability is necessary for the preparation of lubricating oil based on clean environmental protection and sustainable resource acquisition. The viscosity of lubricating oil increases at low temperatures, which leads to a decrease in fluidity, spreadability, and wettability. Gradually modifying the molecular structure of lubricating oil is necessary to achieve the balance between viscosity–temperature characteristics and wettability under different processing conditions. Combined with the synergistic effect of CMQL under different thermal and mechanical conditions, the preparation scheme of lubricant should be studied. Designing an intelligent matching system or database is necessary to realize the intelligent selection of lubricating oil type and its parameters (such as concentration and volume fraction) under different working conditions.

(2) Matching performance between cutting parameters and types of cryogenic medium (or nanoparticles)

Different machining methods set specific cutting parameters for certain types of difficult-to-cut materials and target requirements. Therefore, reasonable matching between cutting parameters and cryogenic medium types is a problem. If matching is unreasonable, then such a phenomenon can cause poor processing quality or excessive consumption of resources.

The quantitative corresponding relationship between evaluation index level and cooling medium level (including its flow parameters) is established in accordance with specific machining target and cutting parameters, which help improve machining quality. Therefore, the type of nanoparticles should be selected reasonably according to the processing effect to realize synergy between CMQL and nanoparticles.

(3) Introduction of a new auxiliary method of electrostatic atomization to suppress CMQL droplet dispersion

The existing high-pressure gas atomization may lead to droplet diffusion and floating, thus complicating the control of transport and harming the health of workers. The electrostatic atomization method aims to charge the atomized droplets by a high-voltage electric field. Driven by the electrostatic field, the charged droplets precisely enter the cutting zone according to the predetermined trajectory, which can effectively suppress droplet dispersion in atomization and transportation. This kind of technology is expected to become a new auxiliary mode of CMQL application in the future.

(4) Design of intelligent nozzle for precise supply of

CMQL medium

Transporting the cooling–lubrication medium into the cutting zone accurately is difficult for the external spray nozzle with a traditional fixed position based on the constraint geometry and motion law of the tool and workpiece. Therefore, building an adaptive optimization scheme of jet parameters (liquid flow rate, gas–liquid mass ratio) with cutting parameters and designing an intelligent nozzle that can automatically adjust its spatial posture with machining surface (plane, outer circumference, inner hole, and cavity) is crucial.

(5) Processing technology solution considering multiple factors

The application of CMQL in aerospace machining of difficult-to-cut materials must consider several factors, including processing form, workpiece material, tool type, cooling lubrication medium type, energy consumption, and other process parameters. The amount of data cited in this paper is insufficient to support the establishment of a database. Further research can focus on the multiparameter coordinated control of the specific process system and establish the quantitative characterization mathematical model of optimal processing performance to guide production practice.

Nomenclature

Abbreviations

BUE	Build-up edge
BUL	Build-up layer
CA	Cryogenic air
CMQL	Cryogenic minimum quantity lubrication
CNMQL	Cryogenic nanoparticle minimum quantity lubrication
DHC	Double-helix channel
DL	Dissolved lubricant in $scCO_2$
DSC	Double straight channel
hBN	Hexagonal boron nitride
HRE	Heat removal efficiency
HRP	Heat removal potential
LCO_2	Liquid carbon dioxide
LN_2	Liquid nitrogen
MQL	Minimum quantity lubrication
MWCNT	Multiwalled carbon nanotube
NDL	No dissolved lubricant
NMQL	Nanoparticle minimum quantity lubrication
Oow	Oil-on-water
$scCO_2$	Supercritical carbon dioxide
SEM	Scanning electron microscope
SSC	Single straight channel
XL	Lubricant expanded with $scCO_2$

Variables

a_e	Milling width, mm
a_p	Depth of cutting, mm
A	Heat transfer area, m^2
d	Diameter of channel, mm
f	Feed rate, mm
f_z	Milling feed rate, mm/tooth
F_1	Surface tension under CMQL, N
F_2	Surface tension under MQL, N
h	Heat transfer coefficient, $W/(m^2 \cdot K)$
h_1	Oil film thickness under CMQL, mm
h_2	Oil film thickness under MQL, mm
P_c	Pressure of MQL, MPa
P_0	Surface pressure, MPa
P_∞	External environment pressure, MPa
q	Heat flux, W/m
Q	Flow rate, mL/min
r	Radius of a curved surface, mm
R	Diameter of droplets, mm
S_1	Spreading length under CMQL, mm
S_2	Spreading length under MQL, mm
t	Time, s
t_h	Thickness of the outlet section, mm
T_0	Temperature, °C
T_1	Temperature under CMQL, °C
T_2	Temperature under MQL, °C
u	Velocity at a tangent, m/s
v_c	Cutting speed, m/min
v_f	Feed speed, mm/rev
V_1	Viscosity at T_1, Pa·s
V_2	Viscosity at T_2, Pa·s
ΔT	Temperature difference, °C
θ_1	Contact angle under CMQL, (°)
θ_2	Contact angle under MQL, (°)
ρ	Fluid density, kg/m^3

Acknowledgements This paper was financially supported by the National Natural Science Foundation of China (Grant Nos. 51975305 and 51905289), the Key Project of Shandong Province, China (Grant No. ZR2020KE027), the Major Research Project of Shandong Province, China (Grant Nos. 2019GGX104040 and 2019GSF108236), the Natural Science Foundation of Shandong Province, China (Grant No. ZR2020ME158), and the Applied Basic Research Youth Project of Qingdao Science and Technology Plan, China (Grant No. 19-6-2-63-cg).

References

1. Kim J H, Kim E J, Lee C M. A study on the heat affected zone and machining characteristics of difficult-to-cut materials in laser and induction assisted machining. Journal of Manufacturing Processes, 2020, 57: 499–508
2. Gupta K, Laubscher R F. Sustainable machining of titanium alloys: a critical review. Proceedings of the Institution of Mechanical Engineers. Part B, Journal of Engineering Manufacture, 2017, 231(14): 2543–2560
3. Zoya Z A, Krishnamurthy R. The performance of CBN tools in the machining of titanium alloys. Journal of Materials Processing Technology, 2000, 100(1–3): 80–86
4. Gao X X, Zeng W D, Ma H Y, et al. The origin of coarse macrograin during thermo-mechanical processing in a high temperature titanium alloy. Journal of Alloys and Compounds, 2019, 775: 589–600
5. Thakur A, Gangopadhyay S. State-of-the-art in surface integrity in machining of nickel-based super alloys. International Journal of Machine Tools and Manufacture, 2016, 100: 25–54
6. Al-Nehari A M, Liang G X, Ming L, et al. Grinding mechanism of high-temperature nickel-based alloy using FEM-FBM technique. International Journal of Advanced Manufacturing Technology, 2021, 112(1–2): 87–105
7. Ajaja J, Jomaa W, Bocher P, et al. Hard turning multi-performance optimization for improving the surface integrity of 300M ultra-high strength steel. International Journal of Advanced Manufacturing Technology, 2019, 104(1–4): 141–157
8. Putz M, Cardone M, Dix M, et al. Analysis of workpiece thermal behaviour in cut-off grinding of high-strength steel bars to control quality and efficiency. CIRP Annals-Manufacturing Technology, 2019, 68(1): 325–328
9. Abdelrazek A H, Choudhury I A, Nukman Y, et al. Metal cutting lubricants and cutting tools: a review on the performance improvement and sustainability assessment. International Journal of Advanced Manufacturing Technology, 2020, 106(9–10): 4221–4245
10. Gajrani K K, Suvin P S, Kailas S V, et al. Hard machining performance of indigenously developed green cutting fluid using flood cooling and minimum quantity cutting fluid. Journal of Cleaner Production, 2019, 206: 108–123
11. Mao C, Zou H F, Huang Y, et al. Analysis of heat transfer coefficient on workpiece surface during minimum quantity lubricant grinding. International Journal of Advanced Manufacturing Technology, 2013, 66(1–4): 363–370
12. Shokrani A, Dhokia V, Newman S T. Environmentally conscious machining of difficult-to-machine materials with regard to cutting fluids. International Journal of Machine Tools and Manufacture, 2012, 57: 83–101
13. Chetan N, Ghosh S, Rao P V. Application of sustainable techniques in metal cutting for enhanced machinability: a review. Journal of Cleaner Production, 2015, 100: 17–34
14. Araújo Junior A S, Sales W F, da Silva R B, et al. Lubri-cooling and tribological behavior of vegetable oils during milling of AISI 1045 steel focusing on sustainable manufacturing. Journal of Cleaner Production, 2017, 156: 635–647
15. Deng Z H, Zhang H, Fu Y H, et al. Research on intelligent expert system of green cutting process and its application. Journal of Cleaner Production, 2018, 185: 904–911
16. Mia M, Gupta M K, Singh G, et al. An approach to cleaner production for machining hardened steel using different cooling-lubrication conditions. Journal of Cleaner Production, 2018, 187: 1069–1081
17. Li H N, Wang J P, Wu C Q, et al. Damage behaviors of unidirectional CFRP in orthogonal cutting: a comparison between single- and multiple-pass strategies. Composites. Part B, Engineering, 2020, 185: 107774
18. Gao T, Li C H, Yang M, et al. Mechanics analysis and predictive force models for the single-diamond grain grinding of carbon fiber reinforced polymers using CNT nano-lubricant. Journal of Materials Processing Technology, 2021, 290: 116976
19. Debnath S, Reddy M M, Yi Q S. Environmental friendly cutting fluids and cooling techniques in machining: a review. Journal of Cleaner Production, 2014, 83: 33–47
20. Dong L, Li C H, Zhou F M, et al. Temperature of the 45 steel in the minimum quantity lubricant milling with different biolubricants. International Journal of Advanced Manufacturing Technology, 2021, 113(9–10): 2779–2790
21. Hamran N N N, Ghani J A, Ramli R, et al. A review on recent development of minimum quantity lubrication for sustainable machining. Journal of Cleaner Production, 2020, 268: 122165
22. Wang Y G, Li C H, Zhang Y B, et al. Experimental evaluation of the lubrication properties of the wheel/workpiece interface in minimum quantity lubrication (MQL) grinding using different types of vegetable oils. Journal of Cleaner Production, 2016, 127: 487–499
23. Beheshti A, Huang Y, Ohno K, et al. Improving tribological properties of oil-based lubricants using hybrid colloidal additives. Tribology International, 2020, 144: 106130
24. Sharma A K, Tiwari A K, Dixit A R. Effects of minimum quantity lubrication (MQL) in machining processes using conventional and nanofluid based cutting fluids: a comprehensive review. Journal of Cleaner Production, 2016, 127: 1–18
25. Gunan F, Kivak T, Yildirim C V, et al. Performance evaluation of MQL with Al_2O_3 mixed nanofluids prepared at different concentrations in milling of Hastelloy C276 alloy. Journal of Materials Research and Technology, 2020, 9(5): 10386–10400
26. Şirin S, Sarikaya M, Yildirim C V, et al. Machinability performance of nickel alloy X-750 with SiAlON ceramic cutting tool under dry, MQL and hBN mixed nanofluid-MQL. Tribology International, 2021, 153: 106673

27. Cui X, Li C H, Ding W F, et al. Minimum quantity lubrication machining of aeronautical materials using carbon group nanolubricant: from mechanisms to application. Chinese Journal of Aeronautics, 2021 (in press)
28. Said Z, Gupta M, Hegab H, et al. A comprehensive review on minimum quantity lubrication (MQL) in machining processes using nano-cutting fluids. International Journal of Advanced Manufacturing Technology, 2019, 105(5–6): 2057–2086
29. Çakır A, Yagmur S, Kavak N, et al. The effect of minimum quantity lubrication under different parameters in the turning of AA7075 and AA2024 aluminium alloys. International Journal of Advanced Manufacturing Technology, 2016, 84(9–12): 2515–2521
30. Mishra S K, Ghosh S, Aravindan S. Machining performance evaluation of Ti-6Al-4V alloy with laser textured tools under MQL and nano-MQL environments. Journal of Manufacturing Processes, 2020, 53: 174–189
31. Agrawal C, Khanna N, Pruncu C I, et al. Tool wear progression and its effects on energy consumption and surface roughness in cryogenic assisted turning of Ti-6Al-4V. International Journal of Advanced Manufacturing Technology, 2020, 111(5–6): 1319–1331
32. Fernández D, Sandá A, Bengoetxea I. Cryogenic milling: study of the effect of CO_2 cooling on tool wear when machining Inconel 718, Grade EA1N steel and Gamma TiAl. Lubricants (Basel, Switzerland), 2019, 7(1): 10
33. Mulyana T, Rahim E A, Md Yahaya S N. The influence of cryogenic supercritical carbon dioxide cooling on tool wear during machining high thermal conductivity steel. Journal of Cleaner Production, 2017, 164: 950–962
34. Zhang H P, Zhang Z S, Zheng Z Y, et al. Tool wear in high-speed turning ultra-high strength steel under dry and CMQL conditions. Integrated Ferroelectrics, 2020, 206(1): 122–131
35. Ali Khan M, Jaffery S H I, Khan M, et al. Statistical analysis of energy consumption, tool wear and surface roughness in machining of titanium alloy (Ti-6Al-4V) under dry, wet and cryogenic conditions. Mechanical Sciences, 2019, 10(2): 561–573
36. Khan A M, Anwar S, Jamil M, et al. Energy, environmental, economic, and technological analysis of Al-GnP nanofluid- and cryogenic LN_2-assisted sustainable machining of Ti-6Al-4V alloy. Metals, 2021, 11(1): 88
37. Albertelli P, Monno M. Energy assessment of different cooling technologies in Ti-6Al-4V milling. International Journal of Advanced Manufacturing Technology, 2021, 112(11–12): 3279–3306
38. Khan A M, Zhao W, Li L, et al. Assessment of cumulative energy demand, production cost, and CO_2 emission from hybrid CryoMQL assisted machining. Journal of Cleaner Production, 2021, 292: 125952
39. Damir A, Shi B, Attia M H. Flow characteristics of optimized hybrid cryogenic-minimum quantity lubrication cooling in machining of aerospace materials. CIRP Annals-Manufacturing Technology, 2019, 68(1): 77–80
40. Yin X L, Chen H T, Deng W J. Effects of machining velocity on ultra-fine grained Al 7075 alloy produced by cryogenic temperature large strain extrusion machining. Materials (Basel), 2019, 12(10): 1656
41. Dinesh S, Senthilkumar V, Asokan P, et al. Effect of cryogenic cooling on machinability and surface quality of bio-degradable ZK60 Mg alloy. Materials & Design, 2015, 87: 1030–1036
42. Jerold B D, Kumar M P. The influence of cryogenic coolants in machining of Ti-6Al-4V. Journal of Manufacturing Science and Engineering, 2013, 135(3): 031005
43. Jadhav P S, Mohanty C P, Hotta T K, et al. An optimal approach for improving the machinability of Nimonic C-263 superalloy during cryogenic assisted turning. Journal of Manufacturing Processes, 2020, 58: 693–705
44. Tazehkandi A H, Shabgard M, Pilehvarian F. Application of liquid nitrogen and spray mode of biodegradable vegetable cutting fluid with compressed air in order to reduce cutting fluid consumption in turning Inconel 740. Journal of Cleaner Production, 2015, 108: 90–103
45. Jawahir I S, Attia H, Biermann D, et al. Cryogenic manufacturing processes. CIRP Annals-Manufacturing Technology, 2016, 65(2): 713–736
46. Yildiz Y, Sundaram M M. Cryogenic machining of composites. Machining Technology for Composite Materials, 2012, 8: 365–393
47. Hollis W S. The application and effect of controlled atmospheres in the machining of metals. International Journal of Machine Tool Design and Research, 1961, 1(1–2): 59–78
48. Jamil M, Khan A M, Hegab H, et al. Effects of hybrid Al_2O_3-CNT nanofluids and cryogenic cooling on machining of Ti-6Al-4V. International Journal of Advanced Manufacturing Technology, 2019, 102(9–12): 3895–3909
49. Chaabani S, Rodriguez I, Cuesta M, et al. Tool wear and cutting forces when machining Inconel 718 under cryogenic conditions: liquid nitrogen and carbon dioxide. AIP Conference Proceedings, 2019, 2113(1): 080002
50. Zhang X, Li L F, Du Z F, et al. Discovery of supercritical carbon dioxide in a hydrothermal system. Science Bulletin, 2020, 65(11): 958–964
51. Putra N R, Che Yunus M A, Machmudah S. Solubility model of arachis hypogea skin oil by modified supercritical carbon dioxide. Separation Science and Technology, 2019, 54(5): 731–740
52. An Q L, Cai C Y, Zou F, et al. Tool wear and machined surface characteristics in side milling Ti-6Al-4V under dry and supercritical CO_2 with MQL conditions. Tribology International, 2020, 151: 106511
53. Lopes J C, Fragoso K M, Garcia M V, et al. Behavior of hardened steel grinding using MQL under cold air and MQL CBN wheel cleaning. International Journal of Advanced Manufacturing Technology, 2019, 105(10): 4373–4387
54. Garcia M V, Lopes J C, Diniz A E, et al. Grinding performance of bearing steel using MQL under different dilutions and wheel cleaning for green manufacture. Journal of Cleaner Production, 2020, 257: 120376
55. Saberi A, Rahimi A R, Parsa H, et al. Improvement of surface grinding process performance of CK45 soft steel by minimum quantity lubrication (MQL) technique using compressed cold air jet from vortex tube. Journal of Cleaner Production, 2016, 131: 728–738

56. Zhang J C, Wu W T, Li C H, et al. Convective heat transfer coefficient model under nanofluid minimum quantity lubrication coupled with cryogenic air grinding Ti-6Al-4V. International Journal of Precision Engineering and Manufacturing-Green Technology, 2021, 8(4): 1113–1135
57. Shokrani D V, Dhokia V, Newman S T, et al. An initial study of the effect of using liquid nitrogen coolant on the surface roughness of Inconel 718 nickel-based alloy in CNC milling. Procedia CIRP, 2012, 3: 121–125
58. Susanne C, Fabian H, Thomas S. Next generation high performance cutting by use of carbon dioxide as cryogenics. Procedia CIRP, 2014, 14: 401–405
59. He A D, Ye B Y, Wang Z Y. Experimental study on effect of cryogenic MQL cutting by tool with internal cooling structure. Tool Engineering, 2015, 49(503): 21–24 (in Chinese)
60. Busch K, Hochmuth C, Pause B, et al. Investigation of cooling and lubrication strategies for machining high-temperature alloys. Procedia CIRP, 2016, 41: 835–840
61. Pušavec F, Grguras D, Koch M, et al. Cooling capability of liquid nitrogen and carbon dioxide in cryogenic milling. CIRP Annals-Manufacturing Technology, 2019, 68(1): 73–76
62. Guo S M, Li C H, Zhang Y B, et al. Analysis of volume ratio of castor/soybean oil mixture on minimum quantity lubrication grinding performance and microstructure evaluation by fractal dimension. Industrial Crops and Products, 2018, 111: 494–505
63. Zhang Y B, Li H N, Li C H, et al. Nano-enhanced biolubricant in sustainable manufacturing: from processability to mechanisms. Friction, 2021 (in press)
64. Seyedzavvar M, Abbasi H, Kiyasatfar M, et al. Investigation on tribological performance of CuO vegetable-oil based nanofluids for grinding operations. Advances in Manufacturing, 2020, 8(3): 344–360
65. Chetan N, Ghosh S, Rao P V. Comparison between sustainable cryogenic techniques and nano-MQL cooling mode in turning of nickel-based alloy. Journal of Cleaner Production, 2019, 231: 1036–1049
66. Gajrani K K. Assessment of cryo-MQL environment for machining of Ti-6Al-4V. Journal of Manufacturing Processes, 2020, 60: 494–502
67. Pusavec F, Deshpande A, Yang S, et al. Sustainable machining of high temperature nickel alloy-Inconel 718: part 1-predictive performance models. Journal of Cleaner Production, 2014, 81: 255–269
68. Mia M, Gupta M K, Lozano J A, et al. Multi-objective optimization and life cycle assessment of eco-friendly cryogenic N-2 assisted turning of Ti-6Al-4V. Journal of Cleaner Production, 2019, 210: 121–133
69. Hegab H, Damir A, Attia H. Sustainable machining of Ti-6Al-4V using cryogenic cooling: an optimized approach. Procedia CIRP, 2021, 101: 346–349
70. Mia M, Dhar N R. Influence of single and dual cryogenic jets on machinability characteristics in turning of Ti-6Al-4V. Proceedings of the Institution of Mechanical Engineers. Part B, Journal of Engineering Manufacture, 2019, 233(3): 711–726
71. Bermingham M J, Palanisamy S, Kent D, et al. A comparison of cryogenic and high pressure emulsion cooling technologies on tool life and chip morphology in Ti-6Al-4V cutting. Journal of Materials Processing Technology, 2012, 212(4): 752–765
72. Pereira O, Català P, Rodríguez A, et al. The use of hybrid CO_2+MQL in machining operations. Procedia Engineering, 2015, 132: 492–499
73. Pereira O, Rodriguez A, Barreiro J, et al. Nozzle design for combined use of MQL and cryogenic gas in machining. International Journal of Precision Engineering and Manufacturing-Green Technology, 2017, 4(1): 87–95
74. Biermann D, Abrahams H, Metzger M. Experimental investigation of tool wear and chip formation in cryogenic machining of titanium alloys. Advances in Manufacturing, 2015, 3(4): 292–299
75. Zou L, Huang Y, Zhou M, et al. Effect of cryogenic minimum quantity lubrication on machinability of diamond tool in ultraprecision turning of 3Cr2NiMo steel. Materials and Manufacturing Processes, 2018, 33(9): 943–949
76. Su Y S, Li L, Wang G, et al. Cutting mechanism and performance of high-speed machining of a titanium alloy using a super-hard textured tool. Journal of Manufacturing Processes, 2018, 34: 706–712
77. Jebaraj M, Kumar M P, Anburaj R. Effect of LN_2 and CO_2 coolants in milling of 55NiCrMoV7 steel. Journal of Manufacturing Processes, 2020, 53: 318–327
78. Sheikh-Ahmad J, He Y, Qin L. Cutting force prediction in milling CFRPs with complex cutter geometries. Journal of Manufacturing Processes, 2019, 45: 720–731
79. Shokrani A, Al-Samarrai I, Newman S T. Hybrid cryogenic MQL for improving tool life in machining of Ti-6Al-4V titanium alloy. Journal of Manufacturing Processes, 2019, 43: 229–243
80. Park K H, Suhaimi M A, Yang G D, et al. Milling of titanium alloy with cryogenic cooling and minimum quantity lubrication (MQL). International Journal of Precision Engineering and Manufacturing, 2017, 18(1): 5–14
81. Zhu G Y, Yuan S M, Chen B C. Numerical and experimental optimizations of nozzle distance in minimum quantity lubrication (MQL) milling process. International Journal of Advanced Manufacturing Technology, 2019, 101(1–4): 565–578
82. Islam A, Mia M, Dhar N R. Effects of internal cooling by cryogenic on the machinability of hardened steel. International Journal of Advanced Manufacturing Technology, 2017, 90(1–4): 11–20
83. Suhaimi M A, Yang G D, Park K H, et al. Effect of cryogenic machining for titanium alloy based on indirect, internal and external spray system. Procedia Manufacturing, 2018, 17: 158–165
84. Lu T, Kudaravalli R, Georgiou G. Cryogenic machining through the spindle and tool for improved machining process performance and sustainability: Pt. I, system design. Procedia Manufacturing, 2018, 21: 266–272
85. Grguraš D, Sterle L, Krajnik P, et al. A novel cryogenic machining concept based on a lubricated liquid carbon dioxide. International Journal of Machine Tools and Manufacture, 2019, 145: 103456
86. Duchosal A, Werda S, Serra R, et al. Numerical modeling and experimental measurement of MQL impingement over an insert

in a milling tool with inner channels. International Journal of Machine Tools and Manufacture, 2015, 94: 37–47
87. Bergs T, Pušavec F, Koch M, et al. Investigation of the solubility of liquid CO_2 and liquid oil to realize an internal single channel supply in milling of Ti-6Al-4V. Procedia Manufacturing, 2019, 33: 200–207
88. Yuan S M, Yan L T, Liu W D, et al. Effects of cooling air temperature on cryogenic machining of Ti-6Al-4V alloy. Journal of Materials Processing Technology, 2011, 211(3): 356–362
89. Song K H, Lim D W, Park J Y, et al. Investigation on influence of hybrid nozzle of CryoMQL on tool wear, cutting force, and cutting temperature in milling of titanium alloys. International Journal of Advanced Manufacturing Technology, 2020, 110(7–8): 2093–2103
90. Zhang C L, Zhang S, Yan X F, et al. Effects of internal cooling channel structures on cutting forces and tool life in side milling of H13 steel under cryogenic minimum quantity lubrication condition. International Journal of Advanced Manufacturing Technology, 2016, 83(5–8): 975–984
91. Shokrani A, Dhokia V, Munoz-Escalona P, et al. State-of-the-art cryogenic machining and processing. International Journal of Computer Integrated Manufacturing, 2013, 26(7): 616–648
92. Manimaran G, Kumar M P, Venkatasamy R. Surface modifcations in grinding AISI D3 steel using cryogenic. Journal of the Brazilian Society of Mechanical Sciences, 2015, 37: 1357–1363
93. Paul S, Singh A K, Ghosh A. Grinding of Ti-6Al-4V under small quantity cooling lubrication environment using alumina and MWCNT nanofluids. Materials and Manufacturing Processes, 2017, 32(6): 608–615
94. Mao C, Zhou X, Yin L R, et al. Investigation of the flow field for a double-outlet nozzle during minimum quantity lubrication grinding. International Journal of Advanced Manufacturing Technology, 2016, 85(1–4): 291–298
95. Sanchez J A, Pombo I, Alberdi R, et al. Machining evaluation of a hybrid MQL-CO_2 grinding technology. Journal of Cleaner Production, 2010, 18(18): 1840–1849
96. Ribeiro F S F, Lopes J C, Garcia M V, et al. New knowledge about grinding using MQL simultaneous to cooled air and MQL combined to wheel cleaning jet technique. International Journal of Advanced Manufacturing Technology, 2020, 109(3–4): 905–917
97. Nguyen T, Liu M, Zhang L C. Cooling by sub-zero cold air jet in the grinding of a cylindrical component. International Journal of Advanced Manufacturing Technology, 2014, 73(1–4): 341–352
98. Şirin E, Kivak T, Yildirim C V. Effects of mono/hybrid nanofluid strategies and surfactants on machining performance in the drilling of Hastelloy X. Tribology International, 2021, 157: 106894
99. Jia B H, Feng Y, Wang X Y, et al. Research on the drilling micromechanical properties of TiBW/TC_4 composites based on drilling force and temperature analysis. International Journal of Advanced Manufacturing Technology, 2019, 104(1–4): 931–941
100. Ahmed L S, Kumar M P. Cryogenic drilling of Ti-6Al-4V alloy under liquid nitrogen cooling. Materials and Manufacturing Processes, 2016, 31(7): 951–959
101. Dix M, Wertheim R, Schmidt G, et al. Modeling of drilling assisted by cryogenic cooling for higher efficiency. CIRP Annals-Manufacturing Technology, 2014, 63(1): 73–76
102. Hanenkamp N, Amon S, Gross D. Hybrid supply system for conventional and CO_2/MQL-based cryogenic cooling. Procedia CIRP, 2018, 77: 219–222
103. Park K H, Yang G D, Suhaimi M A, et al. The effect of cryogenic cooling and minimum quantity lubrication on end milling of titanium alloy Ti-6Al-4V. Journal of Mechanical Science and Technology, 2015, 29(12): 5121–5126
104. Tahmasebi E, Albertelli P, Lucchini T, et al. CFD and experimental analysis of the coolant flow in cryogenic milling. International Journal of Machine Tools and Manufacture, 2019, 140: 20–33
105. Manimaran G, Pradeep kumar M, Venkatasamy R. Influence of cryogenic cooling on surface grinding of stainless steel 316. Cryogenics, 2014, 59: 76–83
106. Garcia E, Pombo I, Sanchez J A, et al. Reduction of oil and gas consumption in grinding technology using high pour-point lubricants. Journal of Cleaner Production, 2013, 51: 99–108
107. Awale A S, Vashista M, Khan Yusufzai M Z. Multi-objective optimization of MQL mist parameters for eco-friendly grinding. Journal of Manufacturing Processes, 2020, 56: 75–86
108. Rahim E A, Ibrahim M R, Rahim A A, et al. Experimental investigation of minimum quantity lubrication (MQL) as a sustainable cooling technique. Procedia CIRP, 2015, 26: 351–354
109. Sadik M I, Isakson S, Malakizadi A, et al. Influence of coolant flow rate on tool life and wear development in cryogenic and wet milling of Ti-6Al-4V. Procedia CIRP, 2016, 46: 91–94
110. Maruda R W, Krolczyk G M, Feldshtein E, et al. A study on droplets sizes, their distribution and heat exchange for minimum quantity cooling lubrication (MQCL). International Journal of Machine Tools and Manufacture, 2016, 100: 81–92
111. Josyula S K, Narala S K R. Performance enhancement of cryogenic machining and its effect on tool wear during turning of Al-Tic_p composites. Machining Science and Technology, 2018, 22(2): 225–248
112. Zou L T, Zhang S, Zhang Q. Computer fluid dynamics analysis of cryogenic oil mist and structural optimization of spraying nozzle. Applied Mechanics and Materials, 2013, 241–244: 1310–1315
113. Li B, Wong C H. Molecular dynamics study of ultrathin lubricant films with functional end groups: thermal-induced desorption and decomposition. Computational Materials Science, 2014, 93: 11–14
114. Rusanov A I. Temperature dependence of liquid contact angle at a deformable solid surface. Colloid Journal, 2020, 82(5): 567–572
115. Shi B, Elsayed A, Damir A, et al. A hybrid modeling approach for characterization and simulation of cryogenic machining of Ti-6Al-4V alloy. Journal of Manufacturing Science and Engineering, 2019, 141(2): 021021
116. Liu N M, Chiang K T, Hung C M. Modeling and analyzing the effects of air-cooled turning on the machinability of Ti-6Al-4V titanium alloy using the cold air gun coolant system. International Journal of Advanced Manufacturing Technology, 2013, 67(5–8): 1053–1066
117. Wang Z Y, Rajurkar K P. Cryogenic machining of hard-to-cut materials. Wear, 2000, 239(2): 168–175

118. Pradeep A V, Dumpala L, Ramakrishna S. Effect of MQL on roughness, white layer and microhardness in hard turning of AISI 52100. Emerging Materials Research, 2019, 8(1): 29–43
119. Umbrello D, Bordin A, Imbrogno S, et al. 3D finite element modelling of surface modification in dry and cryogenic machining of EBM Ti-6Al-4V alloy. CIRP Journal of Manufacturing Science and Technology, 2017, 18: 92–100
120. Rotella G, Dillon O W Jr, Umbrello D, et al. The effects of cooling conditions on surface integrity in machining of Ti-6Al-4V alloy. International Journal of Advanced Manufacturing Technology, 2014, 71(1–4): 47–55
121. Pusavec F, Hamdi H, Kopac J, et al. Surface integrity in cryogenic machining of nickel based alloy-Inconel 718. Journal of Materials Processing Technology, 2011, 211(4): 773–783
122. Chaabani S, Arrazola P J, Ayed Y, et al. Surface integrity when machining Inconel 718 using conventional lubrication and carbon dioxide coolant. Procedia Manufacturing, 2020, 47: 530–534
123. Nimel Sworna Ross K, Manimaran G. Effect of cryogenic coolant on machinability of difficult-to-machine Ni–Cr alloy using PVD-TiAlN coated WC tool. Journal of the Brazilian Society of Mechanical Sciences, 2019, 41(1): 44
124. Jamil M, Khan A M, Gupta M K, et al. Influence of CO_2-snow and subzero MQL on thermal aspects in the machining of Ti-6Al-4V. Applied Thermal Engineering, 2020, 177: 115480
125. Sivaiah P, Chakradhar D. Influence of cryogenic coolant on turning performance characteristics: a comparison with wet machining. Materials and Manufacturing Processes, 2017, 32(13): 1475–1485
126. Zhao Y J, Xu W H, Xi C Z, et al. Automatic and accurate measurement of microhardness profile based on image processing. IEEE Transactions on Instrumentation and Measurement, 2021, 70: 6006009
127. Kaynak Y, Gharibi A, Ozkutuk M. Experimental and numerical study of chip formation in orthogonal cutting of Ti-5553 alloy: the influence of cryogenic, MQL, and high pressure coolant supply. International Journal of Advanced Manufacturing Technology, 2018, 94(1–4): 1411–1428
128. Huang P, Li H C, Zhu W L, et al. Effects of eco-friendly cooling strategy on machining performance in micro-scale diamond turning of Ti-6Al-4V. Journal of Cleaner Production, 2020, 243: 118526
129. Pu Z, Outeiro J C, Batista A C, et al. Enhanced surface integrity of AZ31B Mg alloy by cryogenic machining towards improved functional performance of machined components. International Journal of Machine Tools and Manufacture, 2012, 56: 17–27
130. Leksycki K, Feldshtein E, Lisowicz J, et al. Cutting forces and chip shaping when finish turning of 17-4 PH stainless steel under dry, wet, and MQL machining conditions. Metals, 2020, 10(9): 1187
131. Nouioua M, Yallese M, Khettabi R, et al. Investigation of the performance of the MQL, dry, and wet turning by response surface methodology (RSM) and artificial neural network (ANN). International Journal of Advanced Manufacturing Technology, 2017, 93(5–8): 2485–2504
132. Darshan C, Jain S, Dogra M, et al. Influence of dry and solid lubricant-assisted MQL cooling conditions on the machinability of Inconel 718 alloy with textured tool. International Journal of Advanced Manufacturing Technology, 2019, 105(5–6): 1835–1849
133. Zhang Y B, Li C H, Jia D Z, et al. Experimental evaluation of MoS_2 nanoparticles in jet MQL grinding with different types of vegetable oil as base oil. Journal of Cleaner Production, 2015, 87: 930–940
134. Tascioglu E, Gharibi A, Kaynak Y. High speed machining of near-beta titanium Ti-5553 alloy under various cooling and lubrication conditions. International Journal of Advanced Manufacturing Technology, 2019, 102(9–12): 4257–4271
135. Ross K N S, Manimaran G. Machining investigation of Nimonic-80A superalloy under cryogenic CO_2 as coolant using PVD-TiAlN/TiN coated tool at 45º degrees nozzle angle. Arabian Journal for Science and Engineering, 2020, 45(11): 9267–9281
136. Hong S Y. Lubrication mechanisms of LN_2 in ecological cryogenic machining. Machining Science and Technology, 2006, 10(1): 133–155
137. Wstawska I, Ślimak K. The influence of cooling techniques on cutting forces and surface roughness during cryogenic machining of titanium alloys. Archives of Mechanical Technology and Materials, 2016, 36(1): 12–17
138. Hong S Y, Ding Y C, Jeong J. Experimental evaluation of friction coefficient and liquid nitrogen lubrication effect in cryogenic machining. Machining Science and Technology, 2002, 6(2): 235–250
139. Sivaiah P, Chakradhar D. Comparative evaluations of machining performance during turning of 17-4 PH stainless steel under cryogenic and wet machining conditions. Machining Science and Technology, 2018, 22(1): 147–162
140. Bermingham M J, Kirsch J, Sun S, et al. New observations on tool life, cutting forces and chip morphology in cryogenic machining Ti-6Al-4V. International Journal of Machine Tools and Manufacture, 2011, 51(6): 500–511
141. Kim D Y, Kim D M, Park H W. Predictive cutting force model for a cryogenic machining process incorporating the phase transformation of Ti-6Al-4V. International Journal of Advanced Manufacturing Technology, 2018, 96(1–4): 1293–1304
142. Hong S Y, Ding Y C, Jeong W C. Friction and cutting forces in cryogenic machining of Ti–6Al–4V. International Journal of Machine Tools and Manufacture, 2001, 41(15): 2271–2285
143. Paula Oliveira G, Fonseca M C, Araujo A C. Residual stresses and cutting forces in cryogenic milling of Inconel 718. Procedia CIRP, 2018, 77: 211–214
144. Gong L, Zhao W, Ren F, et al. Experimental study on surface integrity in cryogenic milling of 35CrMnSiA high-strength steel. International Journal of Advanced Manufacturing Technology, 2019, 103(1–4): 605–615
145. Patel T, Khanna N, Yadav S, et al. Machinability analysis of nickel-based superalloy Nimonic 90: a comparison between wet and LCO_2 as a cryogenic coolant. International Journal of Advanced Manufacturing Technology, 2021, 113(11–12): 3613–3628
146. Elanchezhian J, Kumar M P. Effect of nozzle angle and depth of cut on grinding titanium under cryogenic CO_2. Materials and Manufacturing Processes, 2018, 33(13): 1466–1470

147. Sun S, Brandt M, Dargusch M S. Machining Ti-6Al-4V alloy with cryogenic compressed air cooling. International Journal of Machine Tools and Manufacture, 2010, 50(11): 933–942
148. Rahman M, Kumar A S, Salam M U, et al. Effect of chilled air on machining performance in end milling. International Journal of Advanced Manufacturing Technology, 2003, 21(10–11): 787–795
149. Yıldırım C V, Kivak T, Sarikaya M, et al. Evaluation of tool wear, surface roughness/topography and chip morphology when machining of Ni-based alloy 625 under MQL, cryogenic cooling and CryoMQL. Journal of Materials Research and Technology, 2020, 9(2): 2079–2092
150. Bordin A, Bruschi S, Ghiotti A, et al. Analysis of tool wear in cryogenic machining of additive manufactured Ti-6Al-4V alloy. Wear, 2015, 328: 328–329
151. Li L, He N, Wang M, et al. High speed cutting of Inconel 718 with coated carbide and ceramic inserts. Journal of Materials Processing Technology, 2002, 129(1–3): 127–130
152. Dutta S, Kanwat A, Pal S K, et al. Correlation study of tool flank wear with machined surface texture in end milling. Measurement, 2013, 46(10): 4249–4260
153. Sartori S, Ghiotti A, Bruschi S. Hybrid lubricating/cooling strategies to reduce the tool wear in finishing turning of difficult-to-cut alloys. Wear, 2017, 376–377: 107–114
154. Sivalingam V, Sun J, Yang B, et al. Machining performance and tool wear analysis on cryogenic treated insert during end milling of Ti-6Al-4V alloy. Journal of Manufacturing Processes, 2018, 36: 188–196
155. Kaynak Y. Evaluation of machining performance in cryogenic machining of Inconel 718 and comparison with dry and MQL machining. International Journal of Advanced Manufacturing Technology, 2014, 72(5–8): 919–933
156. Jamil M, Khan A M, He N, et al. Evaluation of machinability and economic performance in cryogenic-assisted hard turning of alpha-beta titanium: a step towards sustainable manufacturing. Machining Science and Technology, 2019, 23(6): 1022–1046
157. Sivaiah P, Chakradhar D. Machinability studies on 17-4 PH stainless steel under cryogenic cooling environment. Materials and Manufacturing Processes, 2017, 32(15): 1775–1788
158. Gupta M K, Song Q H, Liu Z Q, et al. Ecological, economical and technological perspectives based sustainability assessment in hybrid-cooling assisted machining of Ti-6Al-4V alloy. Sustainable Materials and Technologies, 2020, 26: e00218
159. Zhou H Y, Shi X L, Lu G C, et al. Friction and wear behaviors of TC4 alloy with surface microporous channels filled by Sn-Ag-Cu and Al_2O_3 nanoparticles. Surface and Coatings Technology, 2020, 387: 125552
160. Yıldırım C V. Investigation of hard turning performance of eco-friendly cooling strategies: cryogenic cooling and nanofluid based MQL. Tribology International, 2020, 144: 106127
161. Khanna N, Shah P, Chetan. Comparative analysis of dry, flood, MQL and cryogenic CO_2 techniques during the machining of 15-5-PH SS alloy. Tribology International, 2020, 146: 106196
162. Iturbe A, Hormaetxe E, Garay A, et al. Surface integrity analysis when machining Inconel 718 with conventional and cryogenic cooling. Procedia CIRP, 2016, 45: 67–70
163. Artozoul J, Lescalier C, Dudzinski D. Experimental and analytical combined thermal approach for local tribological understanding in metal cutting. Applied Thermal Engineering, 2015, 89: 394–404
164. Cheng Y, Liu L, Lu Z, et al. Research on temperature distribution mathematical model of cutting tool during heavy cutting difficult-to-machine materials. International Journal of Nanomanufacturing, 2019, 15(4): 381–393
165. Rech J. Influence of cutting tool coatings on the tribological phenomena at the tool–chip interface in orthogonal dry turning. Surface and Coatings Technology, 2006, 200(16–17): 5132–5139
166. Yıldırım C V. Experimental comparison of the performance of nanofluids, cryogenic and hybrid cooling in turning of Inconel 625. Tribology International, 2019, 137: 366–378
167. Yıldırım C V, Sarikaya M, Kivak T, et al. The effect of addition of hBN nanoparticles to nanofluid-MQL on tool wear patterns, tool life, roughness and temperature in turning of Ni-based Inconel 625. Tribology International, 2019, 134: 443–456
168. Sarıkaya M, Şirin Ş, Yıldırım Ç V, et al. Performance evaluation of whisker-reinforced ceramic tools under nano-sized solid lubricants assisted MQL turning of Co-based Haynes 25 superalloy. Ceramics International, 2021, 47(11): 15542–15560
169. Kumar A S, Deb S, Paul S. Tribological characteristics and micromilling performance of nanoparticle enhanced water based cutting fluids in minimum quantity lubrication. Journal of Manufacturing Processes, 2020, 56: 766–776
170. Bagherzadeh A, Budak E. Investigation of machinability in turning of difficult-to-cut materials using a new cryogenic cooling approach. Tribology International, 2018, 119: 510–520
171. Supekar S D, Clarens A F, Stephenson D A, et al. Performance of supercritical carbon dioxide sprays as coolants and lubricants in representative metalworking operations. Journal of Materials Processing Technology, 2012, 212(12): 2652–2658
172. Qu S S, Gong Y D, Yang Y Y, et al. An investigation of carbon nanofluid minimum quantity lubrication for grinding unidirectional carbon fibre-reinforced ceramic matrix composites. Journal of Cleaner Production, 2020, 249: 119353
173. Cui X, Li C H, Zhang Y B, et al. Tribological properties under the grinding wheel and workpiece interface by using graphene nanofluid lubricant. International Journal of Advanced Manufacturing Technology, 2019, 104(9–12): 3943–3958
174. Fodor G, Sykora H T, Bachrathy D. Stochastic modeling of the cutting force in turning processes. International Journal of Advanced Manufacturing Technology, 2020, 111(1–2): 213–226
175. Çetindağ H A, Çiçek A, Uçak N. The effects of CryoMQL conditions on tool wear and surface integrity in hard turning of AISI 52100 bearing steel. Journal of Manufacturing Processes, 2020, 56: 463–473
176. Liu L, Wu M Y, Li L B, et al. FEM simulation and experiment of high-pressure cooling effect on cutting force and machined surface quality during turning Inconel 718. Integrated Ferroelectrics, 2020, 206(1): 160–172
177. Mehta A, Hemakumar S, Patil A, et al. Influence of sustainable cutting environments on cutting forces, surface roughness and tool wear in turning of Inconel 718. Materials Today: Proceedings, 2018, 5(2): 6746–6754
178. Klocke F, Krämer A, Sangermann H, et al. Thermo-mechanical

tool load during high performance cutting of hard-to-cut materials. Procedia CIRP, 2012, 1: 295–300

179. Hong S Y, Ding Y C. Cooling approaches and cutting temperatures in cryogenic machining of Ti-6Al-4V. International Journal of Machine Tools and Manufacture, 2001, 41(10): 1417–1437
180. Kalyan Kumar K V B S, Choudhury S K. Investigation of tool wear and cutting force in cryogenic machining using design of experiments. Journal of Materials Processing Technology, 2008, 203(1–3): 95–101
181. Musfirah A H, Ghani J A, Haron C H C. Tool wear and surface integrity of Inconel 718 in dry and cryogenic coolant at high cutting speed. Wear, 2017, 376–277: 125–133
182. Chaabani S, Arrazola P J, Ayed Y, et al. Comparison between cryogenic coolants effect on tool wear and surface integrity in finishing turning of Inconel 718. Journal of Materials Processing Technology, 2020, 285: 116780
183. Iqbal A, Suhaimi H, Zhao W, et al. Sustainable milling of Ti-6Al-4V: investigating the effects of milling orientation, cutter's helix angle, and type of cryogenic coolant. Metals, 2020, 10(2): 258
184. Sivaiah P, Chakradhar D. Effect of cryogenic coolant on turning performance characteristics during machining of 17-4 PH stainless steel: a comparison with MQL, wet, dry machining. CIRP Journal of Manufacturing Science and Technology, 2018, 21: 86–96
185. Kaynak Y, Gharibi A. Cryogenic machining of titanium Ti-5553 alloy. Journal of Manufacturing Science and Engineering, 2019, 141(4): 041012
186. Iqbal A, Zhao W, Zaini J, et al. Comparative analyses of multi-pass face-turning of a titanium alloy under various cryogenic cooling and micro-lubrication conditions. International Journal of Lightweight Materials and Manufacture, 2019, 2(4): 388–396
187. Su Y, He N, Li L, et al. Refrigerated cooling air cutting of difficult-to-cut materials. International Journal of Machine Tools and Manufacture, 2007, 47(6): 927–933
188. Sales W F, Schoop J, Jawahir I S. Tribological behavior of PCD tools during superfinishing turning of the Ti-6Al-4V alloy using cryogenic, hybrid and flood as lubri-coolant environments. Tribology International, 2017, 114: 109–120
189. Lin H S, Wang C Y, Yuan Y H, et al. Tool wear in Ti-6Al-4V alloy turning under oils on water cooling comparing with cryogenic air mixed with minimal quantity lubrication. International Journal of Advanced Manufacturing Technology, 2015, 81(1–4): 87–101
190. Kaynak Y, Gharibi A. Progressive tool wear in cryogenic machining: the effect of liquid nitrogen and carbon dioxide. Journal of Manufacturing and Materials Processing, 2018, 2(2): 31
191. Pereira O, Rodriguez A, Fernandez-Abia A I, et al. Cryogenic and minimum quantity lubrication for an eco-efficiency turning of AISI 304. Journal of Cleaner Production, 2016, 139: 440–449
192. Courbon C, Sterle L, Cici M, et al. Tribological effect of lubricated liquid carbon dioxide on Ti-6Al-4V and AISI1045 under extreme contact conditions. Procedia Manufacturing, 2020, 47: 511–516
193. An Q L, Fu Y C, Xu J H. The application of cryogenic pneumatic mist jet impinging in high-speed milling of Ti-6Al-4V. Key Engineering Materials, 2006, 315–316: 244–248
194. Park K H, Yang G D, Lee M G, et al. Eco-friendly face milling of titanium alloy. International Journal of Precision Engineering and Manufacturing, 2014, 15(6): 1159–1164
195. Pereira O, Celaya A, Urbikain G, et al. CO_2 cryogenic milling of Inconel 718: cutting forces and tool wear. Journal of Materials Research and Technology, 2020, 9(4): 8459–8468
196. Shokrani A, Newman S T. Hybrid cooling and lubricating technology for CNC milling of Inconel 718 nickel alloy. Procedia CIRP, 2018, 77: 215–218
197. Zhuang K J, Zhu D H, Zhang X M, et al. Notch wear prediction model in turning of Inconel 718 with ceramic tools considering the influence of work hardened layer. Wear, 2014, 313(1–2): 63–74
198. Wika K K, Gurdal O, Litwa P, et al. Influence of supercritical CO_2 cooling on tool wear and cutting forces in the milling of Ti-6Al-4V. Procedia CIRP, 2019, 82: 89–94
199. Yuan Y H, Wang C Y, Yang J Z, et al. Performance of supercritical carbon dioxide ($scCO_2$) mixed with oil-on-water (OoW) cooling in high-speed milling of 316L stainless steel. Procedia CIRP, 2018, 77: 391–396
200. Pušavec F, Sterle L, Kalin M, et al. Tribology of solid-lubricated liquid carbon dioxide assisted machining. CIRP Annals-Manufacturing Technology, 2020, 69(1): 69–72
201. Sterle L, Mallipeddi D, Krajnik P, et al. The influence of single-channel liquid CO_2 and MQL delivery on surface integrity in machining of Inconel 718. Procedia CIRP, 2020, 87: 164–169
202. Lai Z W, Wang C Y, Zheng L J, et al. Effect of cryogenic oils-on-water compared with cryogenic minimum quantity lubrication in finishing turning of 17-4PH stainless steel. Machining Science and Technology, 2020, 24(6): 1016–1036
203. Bagherzadeh A, Kuram E, Budak E. Experimental evaluation of eco-friendly hybrid cooling methods in slot milling of titanium alloy. Journal of Cleaner Production, 2021, 289: 125817
204. Zhang S, Li J F, Wang Y W. Tool life and cutting forces in end milling Inconel 718 under dry and minimum quantity cooling lubrication cutting conditions. Journal of Cleaner Production, 2012, 32: 81–87
205. Wika K K, Litwa P, Hitchens C. Impact of supercritical carbon dioxide cooling with minimum quantity lubrication on tool wear and surface integrity in the milling of AISI 304L stainless steel. Wear, 2019, 426–427: 1691–1701
206. Ross K N S, Manimaran G, Anwar S, et al. Investigation of surface modifcation and tool wear on milling Nimonic 80A under hybrid lubrication. Tribology International, 2021, 155: 106762
207. Cai C Y, Liang X, An Q L, et al. Cooling/Lubrication performance of dry and supercritical CO_2-based minimum quantity lubrication in peripheral milling Ti-6Al-4V. International Journal of Precision Engineering and Manufacturing-Green Technology, 2021, 8(2): 405–421
208. Yang M, Li C H, Zhang Y B, et al. Predictive model for minimum chip thickness and size effect in single diamond grain grinding of zirconia ceramics under different lubricating conditions. Ceramics International, 2019, 45(12): 14908–14920
209. Yang M, Li C H, Luo L, et al. Predictive model of convective

heat transfer coeffcient in bone micro-grinding using nanofluid aerosol cooling. International Communications in Heat and Mass Transfer, 2021, 125: 105317

210. Hadad M, Hadi M. An investigation on surface grinding of hardened stainless steel S34700 and aluminum alloy AA6061 using minimum quantity of lubrication (MQL) technique. International Journal of Advanced Manufacturing Technology, 2013, 68(9–12): 2145–2158
211. Lopes J C, Garcia M V, Valentim M, et al. Grinding performance using variants of the MQL technique: MQL with cooled air and MQL simultaneous to the wheel cleaning jet. International Journal of Advanced Manufacturing Technology, 2019, 105(10): 4429–4442
212. Zhou L, Huang S T, Yu X L. Machining characteristics in cryogenic grinding of SiCp/Al composites. Acta Metallurgica Sinica (English Letters), 2014, 27(5): 869–874
213. Paul S, Bandyopadhyay P P, Chattopadhyay A B. Effects of cryo-cooling in grinding steels. Journal of Materials Processing Technology, 1993, 37(1–4): 791–800
214. Ben Fredj N, Sidhom H. Effects of the cryogenic cooling on the fatigue strength of the AISI 304 stainless steel ground components. Cryogenics, 2006, 46(6): 439–448
215. Ben Fredj N, Sidhom H, Braham C. Ground surface improvement of the austenitic stainless steel AISI 304 using cryogenic cooling. Surface and Coatings Technology, 2005, 200(16–17): 4846–4860
216. Reddy P P, Ghosh A. Some critical issues in cryo-grinding by a vitrified bonded alumina wheel using liquid nitrogen jet. Journal of Materials Processing Technology, 2016, 229: 329–337
217. Kumar S S, Vijayender S, Kumar S A, et al. Improvement in grinding of composite ceramic by using cryogenic cooling technique. International Journal of Manufacturing Technology and Management, 2012, 25(1–3): 60–77
218. An Q L, Fu Y C, Xu J H. Research on cryogenic pneumatic mist jet impinging cooling and lubricating of grinding processes. Key Engineering Materials, 2008, 359–360: 460–464
219. Zhang J C, Li C H, Zhang Y B, et al. Temperature field model and experimental verification on cryogenic air nanofluid minimum quantity lubrication grinding. International Journal of Advanced Manufacturing Technology, 2018, 97(1–4): 209–228
220. Wang Y G, Li C H, Zhang Y B, et al. Experimental evaluation on tribological performance of the wheel/workpiece interface in minimum quantity lubrication grinding with different concentrations of Al_2O_3 nanofluids. Journal of Cleaner Production, 2017, 142: 3571–3583
221. Kıvak T, Sarıkaya M, Yıldırım Ç V, et al. Study on turning performance of PVD TiN coated Al_2O_3+TiCN ceramic tool under cutting fluid reinforced by nano-sized solid particles. Journal of Manufacturing Processes, 2020, 56: 522–539
222. Öndin O, Kıvak T, Sarıkaya M, et al. Investigation of the influence of MWCNTs mixed nanofluid on the machinability characteristics of PH 13-8 Mo stainless steel. Tribology International, 2020, 148: 106323
223. Sinha M K, Ghosh S, Paruchuri V R. Modelling of specific grinding energy for Inconel 718 superalloy. Proceedings of the Institution of Mechanical Engineers. Part B, Journal of Engineering Manufacture, 2019, 233(2): 443–460
224. Zhang J C, Li C H, Zhang Y B, et al. Experimental assessment of an environmentally friendly grinding process using nanofluid minimum quantity lubrication with cryogenic air. Journal of Cleaner Production, 2018, 193: 236–248
225. Stachurski W, Sawicki J, Wojcik R, et al. Influence of application of hybrid MQL-CCA method of applying coolant during hob cutter sharpening on cutting blade surface condition. Journal of Cleaner Production, 2018, 171: 892–910
226. Inoue S, Aoyama T. Application of air cooling technology and minimum quantity lubrication to relief grinding of cutting tools. Key Engineering Materials, 2004, 257–258: 345–352
227. Zhang G F, Li J T, Wang Z G, et al. Experimental study on nano-CMQL grinding of bearing steels. China Mechanical Engineering, 2019, 30(19): 2342–2348 (in Chinese)
228. Zhang Y B, Li C H, Jia D Z, et al. Experimental study on the effect of nanoparticle concentration on the lubricating property of nanofluids for MQL grinding of Ni-based alloy. Journal of Materials Processing Technology, 2016, 232: 100–115